# CHARACTERISATION OF THE HUMAN CYTOMEGALOVIRUS IMMUNOMODULATORY GENE UL141

**Thesis submitted in candidature for the degree of**

**DOCTOR OF PHILOSOPHY**

**By**

**Daniel Cochrane**

**September 2009**





ProQuest LLC
789 East Eisenhower Parkway
P.O. Box 1346
Ann Arbor, MI 48106-1346

**ACKNOWLEDGEMENTS**

I would firstly like to thank my supervisors Professor Gavin Wilkinson and Dr Eddie Wang, whose constant advice, encouragement, guidance and hard work have made this project possible, and is greatly appreciated.

I would also like to thank my colleagues in the medical Microbiology and Medical biochemistry department for their invaluable help, support and advice throughout this project. Special thanks to Dr Peter Tomasec, and Dr Virginie Prod'homme for their work on UL141 and, Dr Mel Armstrong for her work on UL14 and Dr Richard Stanton for his work producing the AdZ system. Thanks also to Dr Brian McSharry, Dr James Davies, Dr Becky Aichler, Dr Carole Rickards and Sian Llewellyn-Lacey for all their advice and support throughout this study and I would like to thank the MRC and IR3G for funding me.

I would also like to that my family and Elise for their understanding and support.

**ABSTRACT**

Human cytomegalovirus (HCMV) UL141 is a potent modulator of natural killer (NK) cell function that acts by suppressing cell surface expression of CD155, a recognised ligand for the ubiquitous NK cell activating receptors DNAM-1 and CD96. CD155, also known as nectin-like molecule 5 (necl-5) or poliovirus receptor (PVR), is an important adhesion molecule that impacts on cell motility, proliferation and cellular signalling complexes. The focus of this study is to characterise UL141 expression, interactions and biological properties.

Consistent with the role of CD155 as a cell adhesion molecule, UL141 expression was associated with reduced cellular adhesion whether expressed in continuous cell lines or by adenovirus vector. UL14 and UL141 exhibit significant amino acid sequence homology and are members of the same HCMV gene family. Interestingly, UL14 also impaired cell adhesion. Consistent with HCMV downregulating multiple adhesion molecules, productive infection was associated with greatly reduced cell adhesion. Against this background, deletion of UL141 from the virus had no overt effect in adhesion assays. When co-expressed with C-terminal fluorescent tags, gpUL141 and CD155 co-localise with each other and endoplasmic reticulum marker. When over-expressed CD155 and gpUL141 co-localised in inclusion bodies along with calnexin; implying gpUL141 may hold CD155 in a partially destabilised form.

gpUL141 was identified as a component of the envelope of mature HCMV virus particles, whilst CD155 and gpUL14 were excluded. gpUL141 is predominantly an endoglycosidaseH (Endo-H)-sensitive, ER-resident glycoprotein in HCMV infected cell that is subject to post-translational modification, consistent with proteolytic cleavage, during the later stages of infection. However, the protein incorporated into virions is full length and had acquired Endo-H resistance, consistent with transit through the Golgi apparatus. As CD155 is recognised to be a cellular receptor for poliovirus and other herpesviruses, the identification of UL141 as a virion protein may have implications for virus entry.

**TABLE OF CONTENTS**

## LIST OF TABLES

## LIST OF FIGURES

## SUPPLIERS AND COMPANY ADDRESSES

**Abcam**, Cambridge, UK
**Adobe**, California, USA
**Alpha Diagnostics**, USA
**Applied Biosystems**, Foster City, USA
**BD**, New Jersey, USA
**BDH ltd**. Poole, UK
**Beckman Coulter**, California, USA
**BioRad**, California, USA
**Calbiochem**, California, USA
**Chemicon**, Massachusetts, USA
**Clontech**, California, USA
**EdgeBio**, Maryland, USA
**Eurogentec**, Southampton, UK
**Fisher Scientific**, Loughborough, UK
**GE healthcare**, Buckinghamshire, UK
**Graphpad**, California, USA
**Improvision**, Coventry, UK
**Invitrogen**, Paisley, UK
**Leica**, Germany
**Lonza**, Cologne, Germany
**Melford**, Ipswich, UK
**Merck**, West Drayton, UK
**NEB**, Massachusetts, USA
**Oxoid**, Hampshire, UK
**PerkinElmer**, Boston, USA
**Pierce**, Rockford, USA
**Promega**, Wisconsin, USA
**Qiagen**, Sussex, UK
**R&D**, Abingdon, UK
**Roche**, Mannheim, Germany
**Sigma-Aldrich**, Poole, UK
**Thermo Scientific**, Massachusetts, USA
**UVP Bioimaging systems**, Cambridge, UK

## ABBREVIATIONS

| | |
|---|---|
| °C | Degrees Centigrade |
| µg | Micrograms |
| µl | Microlitre |
| µm | Micrometre |

**A**

| | |
|---|---|
| Ad | Adenovirus |
| Ad5 | Adenovirus serotype 5 |
| AF488 | Alexa Fluor 488 |
| AF594 | Alexa Fluor 594 |
| AF647 | Alexa Fluor 647 |
| AJ | Adherin junction |
| AP | Assembly Protein |

**B**

| | |
|---|---|
| BAC | Bacterial artificial chromosome |
| bp | Base pairs |

**C**

| | |
|---|---|
| CCMV | Chimpanzee cytomegalovirus |
| CD | Cluster determinant |
| cDNA | Complementary Deoxyribonucleic acid |
| CFP | Cyan florescent protein |
| CREB | cAMP response element binding |
| CRTAM | Class-I MHC-restricted T-cell-associated molecule |
| $CO_2$ | Carbon dioxide |
| cpe | Cytopathic effect |
| *crs* | *cis* repression signal |

**D**

| | |
|---|---|
| DABCO | 1,4-Diazabicyclo[2,2,2]octane |
| DC | Dendritic cell |
| DMEM | Dulbeccos modified eagle's medium |
| DMSO | Dimethyl sulphoxide |
| DNA | Deoxyribonucleic acid |
| DNAM | DNAX accessory molecule |
| dNTP | Deoxynucleotide triphosphate |
| DTT | Dithiothreitol |

**E**

| | |
|---|---|
| EBV | Epstein-Barr virus |
| ECM | Extracellular matrix |
| *E.coli* | *Escherichia coli* |
| EDTA | Ethylenediaminetetraactic acid |
| EGF | Epidermal growth factor |
| EGFR | Epidermal growth factor receptor |
| Endo H | Endoglycosidase H |
| ER | Endoplasmic reticulum |
| ERGIC | Endoplasmic reticulum-Golgi intermediate compartment |

**F**

| | |
|---|---|
| Fab | Fragment antigen-binding |
| FACS | Fluorescence activated cell sorter |
| FAK | Focal adhesion kinase |
| Fc | Fragment crystallisable |
| FCS | Foetal calf serum |
| FSC | Forward scatter |

**G**

| | |
|---|---|
| g | Grams |
| gB | Glycoprotein B |
| gCI | Glycoprotein complex I |
| gCII | Glycoprotein complex II |
| gCIII | Glycoprotein complex III |
| GFP | Enhanced Green Fluorescent protein |
| gH | Glycoprotein H |
| gL | Glycoprotein L |
| gM | Glycoprotein M |
| gN | Glycoprotein N |
| gO | Glycoprotein O |
| gp | Glycoprotein |

**H**

| | |
|---|---|
| h | Hours |
| HCMV | Human Cytomegalovirus |
| hCAR | Human cocksackie and adenovirus receptor |
| HFFF | Human foetal foreskin fibroblast |
| HHV | Human Herpesvirus |
| HLA | Human leukocyte antigen |
| HPC | haematopoietic cell |
| h.p.i | Hours post infection |
| HRP | Horse radish peroxidase |
| HSV | Herpes simplex virus |

**I**

| | |
|---|---|
| IE | Immediate early |
| IE1 | Immediate early gene 1 |
| IE2 | Immediate early gene 2 |
| Ig | Immunoglobulin |

| | |
|---|---|
| IL | Interleukin |
| IRS | Internal repeat short |
| IRL | Internal repeat long |
| ITIM | Intracellular tyrosine-based inhibitory motif |

**K**

| | |
|---|---|
| kbp | Kilobasepairs |
| kDa | kilodaltons |
| KSHV | Kaposi's sarcoma-associated herpesvirus |

**L**

| | |
|---|---|
| l | Litre |
| LB | Luria Bertani Agar |
| LTP | Largest tegument protein |

**M**

| | |
|---|---|
| M | Molar |
| mM | millimolar |
| mAb | Monoclonal antibody |
| mCh | mCherry |
| MCMV | Murine cytomegalovirus |
| MCP | Major capsid protein |
| mCP | Minor capsid protein |
| mCPbp | Minor capsid binding protein |
| mg | milligrams |
| MHC | Major histocompatibility complex |
| MICA | MHC class I chain related gene A |
| MICB | MHC class I chain related gene B |
| MIE | Major immediate early |
| MIEP | Major immediate early promoter |
| miRNA | Micro ribonucleic acid |

| | |
|---|---|
| ml | Millilitres |
| MOI | Multiplicity of infection |

**N**

| | |
|---|---|
| ND-10 | Nuclear domain 10 |
| Necl | Nectin-like molecule |
| NFAT | Nuclear factor of activated T-cells |
| NIEP | Non-infectious enveloped particle |
| NK | Natural killer |
| NP40 | Nonidet p-40 |
| NRE | Negative response element |

**O**

| | |
|---|---|
| ORF | Open reading frame |

**P**

| | |
|---|---|
| p | protein |
| PAGE | Polyacrylamide gel electrophoresis |
| PDGF | Platelet derived growth factor |
| PDGFR | Platelet derived growth factor receptor |
| PBS | Phosphate buffered saline |
| PBST | Phosphate buffered saline 0.1% Tween 20 |
| PCR | Polymerase chain reaction |
| pfu | Plaque forming units |
| p.i. | Post infection |
| PI3K | Phosphoinositide 3-kinase |
| PKR | Protein kinase R |
| pmol | Picomole |
| PML | Promyelocitic Leukaemia |
| PNGase | Peptide N-glycosidase |
| pp | phosphoprotein |

| | |
|---|---|
| PRE | Positive response element |
| PRR | Poliovirus receptor-related |
| PVR | Poliovirus receptor |

**R**

| | |
|---|---|
| RAd | Recombinant adenovirus |
| RANTES | Regulated upon activation, normal T cell expressed and secreted |
| RNA | Ribonucleic acid |
| RNAi | Ribonucleic acid interference |

**S**

| | |
|---|---|
| SCP | Smallest capsid protein |
| SDS | Sodium dodecyl sulphate |
| SHH | Sonic Hedgehog |
| shRNA | Short hairpin Ribonucleic acid |
| SSC | Side scatter |

**T**

| | |
|---|---|
| TAE | Tris acetic acid EDTA |
| Tactile | T cell-activated increased late expression |
| TAP | Transporter associated with antigen presentation |
| TBq | Terra Becquerel |
| $TCID_{50}$ | Tissue culture infectious dose |
| TGN | Trans Golgi network |
| TJ | Tight junction |
| Tris | Tris(hydroxymethyl)aminomethan |
| TRL | Terminal repeat long |
| TRS | Terminal repeat short |

**U**

| | |
|---|---|
| UL | Unique long |

| | |
|---|---|
| ULBP | UL16 binding protein |
| US | Unique short |

**V, W, X,** Y

| | |
|---|---|
| V | Volts |
| v/v | volume to volume ratio |
| vICA | Viral inhibitor of caspase-8 activation |
| vMIA | Viral inhibitor of apoptosis targeting mitochondria |
| VZV | Varicella zoster virus |
| w/v | Weight to volume ratio |
| x-gal | 5-bromo-4-chloro-3-indoyl-β-D-galactopyranoside |
| YFP | Yellow fluorescent protein |

# 1 INTRODUCTION

## 1.1 HUMAN CYTOMEGALOVIRUS

Human Cytomegalovirus (HCMV) is a ubiquitous virus associated with opportunistic disease. Serious pathology can be caused by congenital infection or infection of immunosuppressed individuals. The virus was first isolated by Wallace Rowe in the 1950s from human adenoids (Rowe et al. 1956). It was later recognised to be the causative agent of cytomegalic inclusion disease, a severe congenital disease associated with a characteristic owl's eye cytopathology.

HCMV is a member of the herpesvirus family, betaherpesvirus subfamily. It is one of eight herpesviruses that infect humans (table 1.1). HCMV shares virion structure with other herpesviruses and, like other herpesviruses, has the ability to establish long term persistent and latent infection. Like other betaherpesviruses, HCMV infection is limited to its natural host. HCMV-associated disease remains an important medical issue as a prominent opportunistic infection of immunocompromised hosts. Congenital infection of newborns can cause severe disease leading to prolonged hospitalisation and death in 10% of symptomatic infants. HCMV infection of transplant recipients can cause a systemic febrile illness and will often causes dysfunction of the transplanted organ increasing the risk of organ rejection.

HCMV biology, especially *in vivo*, is complex and our understanding is incomplete. However modern techniques have advanced our understanding.

**Table 1.1. Human Herpesvirus (HHV) classification**

| Name | | Subfamily |
|---|---|---|
| HHV 1 | Herpes simplex virus 1 (HSV 1) | Alpha |
| HHV 2 | Herpes simplex virus 2 (HSV 2) | Alpha |
| HHV 3 | Varicella zoster virus (VZV) | Alpha |
| HHV 4 | Epstein-Barr virus (EBV) | Gamma |
| HHV 5 | Human cytomegalovirus (HCMV) | Beta |
| HHV 6 | Human herpes virus 6 | Beta |
| HHV 7 | Human herpes virus 7 | Beta |
| HHV-8 | Kaposi's sarcoma-asssociated herpesvirus (KSHV) | Gamma |

## 1.2 VIRUS STRUCTURE

### 1.2.1 Genome

HCMV has the largest genome of a human virus at 236kb and is predicted to encode ~167 open reading frames, ~10 miRNAs and additional non-protein coding transcripts (Davison et al. 2003; Grey and Nelson 2008). The virus has a class E genome (Karlin et al. 1994) consisting of a unique long region ($U_L$) and a unique short region ($U_S$), each flanked by inverted internal and terminal repeats (terminal repeat long (TRL), internal repeat long (IRL), terminal repeat short (TRS) and internal repeat short (IRS) (fig 1.1). The length of the repeats varies between strains and passage history. A directly repeated sequence, termed *a*, is present at the termini and between the $U_L$ and $U_S$ regions (fig 1.1). The arrangement of the terminal and internal *a* sequences encourage genome isomerisation producing four isomers of the genome which are equally packaged into mature virions (Weststrate et al. 1980). The *a* repeats contain the herpesvirus conserved *pac1* and *pac2* elements (Spaete and Mocarski 1985a). These sequences act as a signal for the packaging of the genome into the capsid.

Most studies on HCMV have been performed using the laboratory strains AD169 and Towne. Strain AD169 was originally isolated during culture of adenoid tissue from a 7 year old girl and cultured 14 times in human fibroblasts and a defined stock was generated (Rowe et al. 1956). This stock was passaged another 56-64 times in fibroblasts

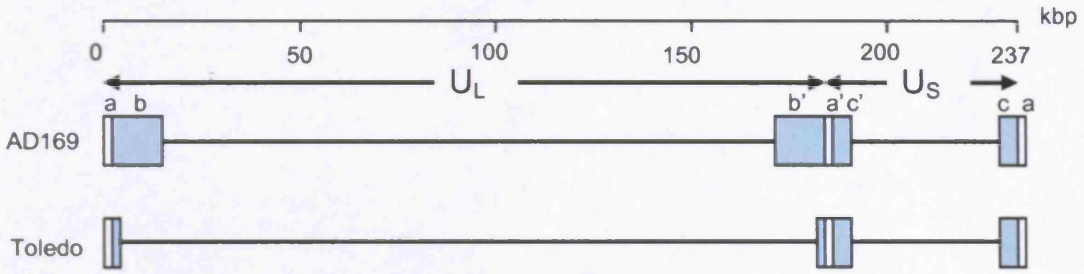


**Figure 1.1. HCMV strain AD169 and Toledo genome structures.**
The HCMV genome is split into two main regions $U_L$ (unique long) and $U_S$ (unique short). These regions are flanked by terminal and inverted terminal repeats. The b and b' repeats are also termed terminal repeat long (TRL) and internal repeat long (IRL). The c and c' repeats are also termed internal repeat short (IRS) and internal repeat long (IRL). The *a* sequence is directly repeated sequence and the number of copies can vary between strains. The top line is a scale in kilobasepairs. Adapted from (Mocarski et al. 2007).

at St Georges Hospital (London) before being used to produce batches of an attenuated *in vitro* for use in vaccination (Bradley et al. 2009; Elek and Stern 1974). The genome of this virus (strain AD169varUK) was cloned (Oram et al. 1982), and then these clones used to generate the first complete sequence of the HCMV genome (Chee et al. 1990a). The attenuation of strain AD169 can be attributed to the multiple mutations that accumulated during extensive passage *in vitro*. Most significantly, 13 and 15Kb respectively have been deleted from high passage strains of Towne and AD169 (Bradley et al. 2009; Cha et al. 1996). This region, termed UL/b', is located at the right end of the $U_L$ region of the genome. In AD169 the UL/b' region has been replaced with an inverted duplication of 10Kb from the left end of the UL region. In addition to other minor defects, some variants of strain AD169 have also suffered a 929 base pair deletion affecting UL42 and UL43 (Dargan et al. 1997; Mocarski et al. 1997). HCMV clinical isolates rapidly acquire mutations when propagated *in vitro* (Akter et al. 2003a; Davison et al. 2003; Dolan et al. 2004). These mutations allow the virus to adapt to growth in fibroblasts. Merlin strain HCMV is currently the best characterised clinical isolate (fig 1.2), has been designated the prototype HCMV clinical isolate by GenBank and will be the preferred virus strain used in this study.

HCMV open reading frames (ORFs) were classified originally in strain AD169 based on which sequence element encoded it and their relative order on the genome (fig 1.2). For example, UL44 was the forty-fourth ORF of the $U_L$ region and US8 is the eighth ORF of the $U_S$ region. Following the sequencing of the UL/b' region in strain Toledo (Cha et al. 1996), the closely-related of chimpanzee CMV (CCMV), and the low passage strain

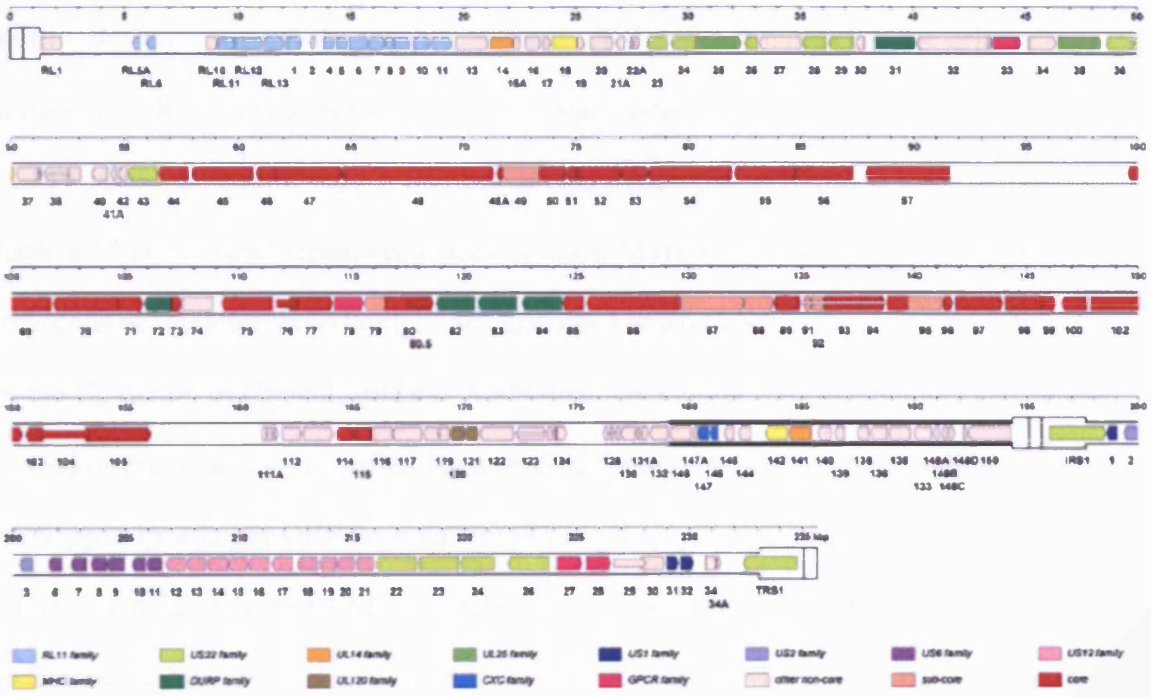

**Figure 1.2. Genomic map of Merlin strain HCMV.**
Annotation of the wild type genome of Merlin strain HCMV. Protein coding regions are indicated by arrows with ORF nomenclature below. Reproduced from (Wilkinson et al. 2008) adapted from (Dolan et al. 2004).

Merlin, the annotation of the genome evolved. A significant number of the originally designated ORFs lacked credible translation start codons and were not conserved in CCMV; these were removed. A number of ORFs (designated RL1-13) were artificially duplicated in extended repeat sequences in strain AD169 (and Towne) still retain their erroneous designation even though they are now known to be single copy genes encoded by the $U_L$ region of clinical isolates. Additional letters after the ORF number can denote revised or previously unidentified open reading frames. When a protein coding region is overlapped by a larger ORF the smaller ORF is given a .5 suffix (Davison et al. 2003). Further modifications to HCMV gene designation can be anticipated as our understanding develops. The most current GenBank strain Merlin gene designation will be used throughout this thesis (fig 1.2).

### 1.2.2 Capsid

The HCMV and HSV-1 capsids have a similar structure and appearance, although the HCMV capsid has a 17% greater volume and packages a genome ~50% larger (Bhella et al. 2000; Chee et al. 1989; Dittmer and Bogner 2005; Gibson 1983; Gibson et al. 1996a; Gibson et al. 1996b; Irmiere and Gibson 1985a). The HCMV capsid displays T=16 icosahedral symmetry which consists of five herpesvirus core proteins arranged in hexons, pentons and triplexes (fig 1.3). The 5 proteins are major capsid protein (MCP, UL86), minor capsid protein (mCP, UL85), minor capsid-binding protein (mCPBp, UL46), smallest capsid protein (SCP, UL48.5) and PORT (portal protein, UL104)

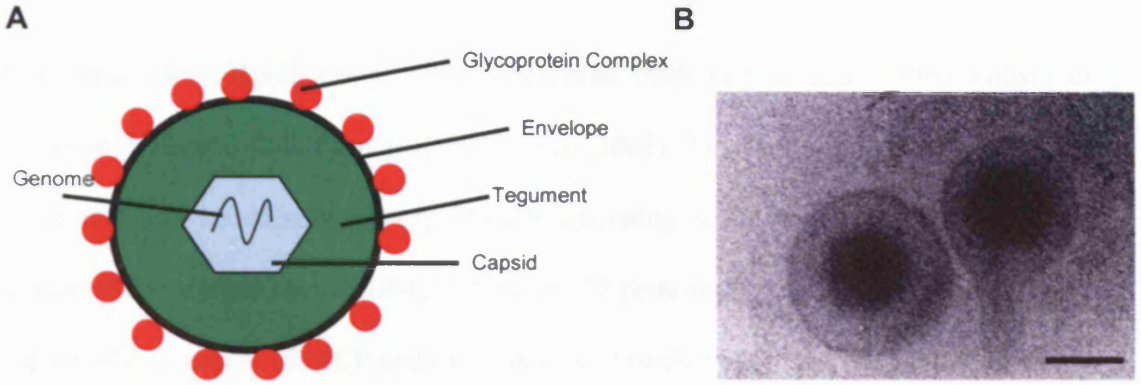


**Figure 1.3. HCMV virus particle**
A) Cartoon of the HCMV virion (not to scale). The genome is enclosed in an icosahedral capsid which is surrounded by the tegument. The virion is surrounded by a host-derived membrane envelope. B) electron micrograph of two HCMV virions. Capsid, tegument and envelope are visible. Scale bar is 100nm. Reproduced from (Bhella et al. 2000).

(Booy et al. 1991; Butcher et al. 1998; Chen et al. 1999; Gibson et al. 1996a; Gibson et al. 1996b; Irmiere and Gibson 1985b; Yu et al. 2005). Hexons are the most abundant capsomer, with 150 hexons per capsid each consisting of six copies of MCP (Irmiere and Gibson 1983; Varnum et al. 2004). There are 12 pentons present in each capsid; eleven consist of five copies of MCP and one consists of twelve copies of the portal protein pUL104 (Sarcinella et al. 2004; Varnum et al. 2004). The triplexes consist of a 2:1 ratio of mCP to mCPBp (Munger et al. 2006). SCP binds to the tip of MCP in hexons, but not to MCP in pentons (Chen et al. 1999; Irmiere and Gibson 1983).

Within infected cells three different forms of capsids are observed. These are termed A, B and C capsids. C capsids are the fully mature nucleocapsids and are the only form with DNA incorporated into the capsid (Baxter and Gibson 2001). A capsids consist of only the protein shell with no DNA in the cavity (Irmiere and Gibson 1983). B capsids are an intermediate in the assembly of the fully mature nucleocapsid consisting of the capsid shell containing Assembly protein (AP, UL80) (Bechtel and Shenk 2002; Munger et al. 2006; Sanchez et al. 2000b; Silva et al. 2003). All three capsid forms are capable of acquiring envelopes, but only C capsids go on to produce mature infectious virus. Enveloped A and B capsids are found in cytoplasmic and cell-free preparations of virus particles. They are classified as non-infectious enveloped particles (NIEP) and can be purified free of infectious virions by density gradient centrifugation; the absence of DNA alters their density (Chevillotte et al. 2009).

### 1.2.3 Tegument

Surrounding the nucleocapsid is the tegument which appears in electron micrographs as an amorphous region between the capsid and the envelope (fig 1.3). More than half of all recognised virion proteins are believed to be located within the tegument, 22 in total (Varnum et al. 2004). Tegument proteins have a tendency to be both phosphorylated and highly immunogenic (Varnum et al. 2004). The most abundant tegument protein is the UL83 gene product pp65 (lower matrix protein) which accounts for 15% of HCMV virion protein (Varnum et al. 2004). Other tegument proteins which are present at high levels include pp71 (Virus Transactivator, VTA, ppUL82), pp150 (Large matrix protein, pUL32) and the largest tegument protein (LTP, pUL48) (Baxter and Gibson 2001; Bechtel and Shenk 2002; Benko et al. 1988; Liu and Stinski 1992). Several proteins encoded by members of the US22 family are also components of the tegument, including UL23, UL24, IRS1 and TRS1 (Adair et al. 2002; Romanowski et al. 1997). The tegument also contains a sampling of cellular and viral mRNAs (Baldick et al. 1997).

Although the tegument appears amorphous, it is known to participate in highly structured ordered interactions with both the capsid and the envelope (Liu and Stinski 1992). Distinct interactions between the capsid and tegument have been observed by comparing capsids with various levels of tegumentation by cryo-electron microscopy (Romanowski et al. 1997; Trus et al. 1999; Winkler and Stamminger 1996). pp150 binds to the capsid via a conserved amino-terminus region (Baxter and Gibson 2001), while pUL47 (a tegument protein) co-precipitates with the capsid protein MCP (Baldick and Shenk 1996); the latter interaction being implicated in the unpackaging of the viral DNA

following infection. The tegument protein pp28 (ppUL99) interacts with the virion envelope membrane via a myristylated domain (Silva et al. 2003). This interaction is important for the accumulation of tegument proteins prior to envelopment (Sanchez et al. 2000a).

Tegumentation occurs in two separate cellular locations during the assembly of the virus particle. Initial components of the tegument, including pp65 (Sanchez et al. 1998) and UL97 kinase (Wolf et al. 2001), initiate interactions with the nucleocapsid in the nucleus. These tegument components have both functional and structural roles important for the efficient assembly of the virion; UL97 kinase is involved in DNA replication and capsid assembly (Wolf et al. 2001), while the major tegument protein pp65 is required for the recruitment of other tegument proteins, including pUL25 and pUL69, into the virion (Chevillotte et al. 2009; Zini et al. 1999). Following nuclear egress, a second round of tegumentation occurs in the cytoplasm. The tegument protein pp28, which is added in the cytoplasm (Sanchez et al. 2000b) is required for the final envelopment of the virion (Silva et al. 2003).

In addition to their structural roles in assembling the virus, the virion tegument proteins play important roles in the initiation of productive infection. The tegument proteins are present in productively infected cells prior to immediate early (IE) gene expression. pp71 plays a critical role in the initiation of infection by relieving hDaxx repression of virus replication by promoting its proteasome-mediated degradation (Baldick et al. 1997; Cantrell and Bresnahan 2006; Lukashchuk et al. 2008; Woodhall et al. 2006). pUL69 is a viral transactivator which is incorporated into the tegument (Winkler et al. 1994; Winkler

and Stamminger 1996). It is expressed as three differentially phosphorylated forms, however, only one of these forms is incorporated into the tegument (Winkler and Stamminger 1996).

### 1.2.4 Envelope

The processes involved in virus envelopment are the object of intensive ongoing research (fig 1.3). The virus nucleocapsid and tegument are known to be enclosed in a membrane derived from the host cell endoplasmic reticulum (ER)-Golgi intermediate compartment (ERGIC) membrane (Sanchez et al. 2000a). HCMV encodes many putative glycoproteins or transmembrane proteins, many of which potentially could be incorporated into the virus envelope. There were originally believed to be three major glycoprotein complexes present on the envelope: gCI (gB), gCII (gM:gN) and gCIII (gH:gL) (Gretch et al. 1988). These glycoproteins are members of the herpesvirus core set and are essential for virus replication. gCI consists of a disulphide-linked gB (gpUL55) homodimer (Cranage et al. 1986; Kari et al. 1990). gB is translated as a 160kDa monomer, which is then processed by a host protease to generate 116kDa and 55kDa polypeptides. The 55kDa species on the outside of the envelope remains in complex with the 116kDa transmembrane component by disulphide bonding (Britt and Auger 1986; Spaete et al. 1988). Proteolytic cleavage of gB is dispensable for virus growth (Strive et al. 2002b). gB is involved in the initial virion:cell attachment through its reaction with cellular heparan sulphate (Boyle and Compton 1998; Compton et al. 1993), after which the glycoprotein also promotes specific interactions with EGFR, and $\alpha_v\beta_3$ integrin (Wang et al. 2005). The glycoprotein is a major target of human

neutralising antibodies (Marshall et al. 1992); neutralising antibodies prevent both attachment and fusion of the virus (Gicklhorn et al. 2003).

The gCII complex is comprised of gM (gpUL100) and gN (gpUL73), the two components also being covalently linked by a disulphide bond (Mach et al. 2000). gCII complex will form in the absence of disulphide bonding (Mach et al. 2005). Most of the multiple trans-membrane spanning gM is dispensable for the interaction with gN, only the initial 118 amino acids are essential (Mach et al. 2005). Complex formation occurs within the ER, and is required for the transport of gM:gN to the secretory system. gM:gN has also been reported to interact with heparan sulphate proteoglycans on entry (Kari and Gehrz 1992; Mach et al. 2000). As with gCI, gCII is also a target for neutralizing antibodies in human serum (Mach et al. 2000; Shimamura et al. 2006).

gCIII, consist of gH (gpUL75), gL (gpUL115) and gO (gpUL74) in virions purified from laboratory-adapted HCMV strains (Huber and Compton 1997, 1998; Kaye et al. 1992; Li et al. 1997) and has been implicated in viral fusion; antibodies against gH or gO will inhibit viral fusion (Milne et al. 1998; Paterson et al. 2002). gH is linked to gL by disulphide bonds which form in the ER (Huber and Compton 1999). gL is required for the transport of gH to the cell surface (Spaete et al. 1993). The gH:gL complex binds to a gO precursor forming a 220kDa gCIII precursor (Theiler and Compton 2001), before gO is post-translationally modified in a post-ER compartment for the formation the fully mature gCIII complex. It has been reported that gH binds EGFR and $\alpha_v\beta_3$ integrin (Baldwin et al. 2000; Wang et al. 2005), although antibodies to gH block viral fusion but do not inhibit attachment (Keay and Baldwin 1991).

A second envelope glycoprotein complex involving gH and gL has been described (Wang and Shenk 2005b). gH:gL:pUL131A/pUL130/128 comprises of gH, gL and the products of UL128, UL130 and UL131A. The co-expression of UL128, UL130 and UL131A increases the transport of gH:gL from the ER, suggesting that the complex forms in the ER (Ryckman et al. 2008b). The gH:gL:UL131A-128 complex is required for epithelial and endothelial cell tropism (Adler et al. 2006; Patrone et al. 2007; Ryckman et al. 2008a; Wang and Shenk 2005a). HCMV cells lacking this complex can internalise in epithelial cells but do not express immediate early genes (Sinzger et al. 2000). When HCMV is passaged in fibroblasts mutations tend to be selected rapidly in one of UL128, UL130 or UL131 that leads to an inability to productively infect epithelial cells (Akter et al. 2003b; Dolan et al. 2004).

In addition to the major glycoprotein complexes there are also other virus-encoded glycoproteins present in the virion envelope. HCMV encodes four G coupled protein-receptor homologues UL33, US27, US28 and UL74 (Chee et al. 1990b; Wang et al. 2004b). Two of these proteins, UL33 and UL76, have been described as components of the virion (Fraile-Ramos et al. 2001; Wang et al. 2004b) and it has been suggested that one, US28, is also present on the virion (Fraile-Ramos et al. 2001). US28 is a functional chemokine receptor (discussed in section 1.5.4) but its role in the virion envelope is still unclear (Gao and Murphy 1994).

Varnum and colleagues (Varnum et al. 2004) identified seventeen virus encoded glycoproteins in HCMV virion envelopes. The most abundant envelope glycoproteins are the glycoprotein complexes discussed above; however, they detected approximately

twelve HCMV glycoproteins that are minor envelope constituents including RL10, UL33 and UL5.

### 1.2.5 Other Components

In addition to the viral encoded proteins present in the HCMV virion over 70 host encoded proteins have been identified in the virion including actin, clatharin, and translation elongation factors (Varnum et al. 2004). The presence of many of these host proteins in the virion is controversial as cellular contamination may occur during the purification of the virus particles (Hudecz et al. 1985). However, support for the active incorporation of cellular protein come from electron microscopy or functional studies (Grundy et al. 1987; Spear et al. 1995; Stannard 1989). For example, the host cell phospholipase cPLA2α was detected in virions (Allal et al. 2004), and inhibition of cPLA2α activity in the virion correlated with a decrease of immediate early (IE) virus gene expression. Over 1000 annexin II molecules are present per virus particle (Wright et al. 1995), and HCMV infectivity could be inhibited by treating the virus with annexin II-specific monoclonal antibodies.

There have also been several reports of viral and host RNA being present in the virion (Greijer et al. 2000; Sarcinella et al. 2004; Terhune et al. 2004). IE, early and late transcripts have all been detected in the tegument (Greijer et al. 2000; Sarcinella et al. 2004). Initial reports identified a selective concentration of specific transcripts implying a biological function (Sarcinella et al. 2004). However, later studies have shown that

RNA molecules are incorporated into the virion in proportion to their cellular concentration (Terhune et al. 2004). Incorporation is most likely via non-specific interactions with RNA-binding virion proteins such as pp28 (Terhune et al. 2004). RNA is also present within the capsid (Prichard et al. 1998). Viral RNA molecules bind to the genome at the oriLyt region forming a persistent DNA-RNA hybrid structure.

Investigation into HCMV virion components have been performed predominantly using laboratory adapted stains. There is strong selection against members of the UL128-UL131A complex during fibroblast growth. It remains possible that further HCMV encoded virion protein may be identified (or lost) when more detailed studies are performed with wild type HCMV.

## 1.3 VIRUS GROWTH AND LIFE CYCLE

### 1.3.1 Infection And Entry

HCMV infection can be detected in a wide range of cell types *in vivo*, including fibroblasts, endothelial cells, epithelial cells, smooth muscle cells, macrophages, dendritic cells and neuronal cells (Gerna et al. 2005; Luo et al. 2008; Sinzger et al. 2008; Sinzger et al. 1995; Wang et al. 2008). The replication cycle in all cell types that support productive infection consists of several stages; attachment, entry, DNA replication, capsid assembly, DNA encapsidation, nuclear egress, secondary envelopment and release (fig 1.4).

HCMV virions initially bind heparan sulphate proteoglycans on the cell surface (Compton et al. 1993; Nowlin et al. 1991). The envelope glycoprotein gB is crucial for this interaction, however, gM:gN and gH:gL are also involved (Boyle and Compton 1998). Following the initial interaction with heparan sulphate it is thought that a series of subsequent interactions with receptors and co-receptors occur to facilitate virus entry. Integrins, including $\alpha_V\beta_3$ integrin and $\beta_1$ integrins, have been implicated in the entry process (Feire et al. 2004). The wide range of cellular targets implies the primary receptor should be a ubiquitous host protein, yet it is also possible that the virus exploits multiple cell type-specific receptors to expand its tropism. Infection is not controlled entirely by entry; HCMV can enter cell lines yet fail to replicate efficiently, e.g. African green monkey kidney cells (Ellsmore et al. 2003). Following the interaction with the host cell receptors the virion enters the cell by fusing directly with the plasma membrane

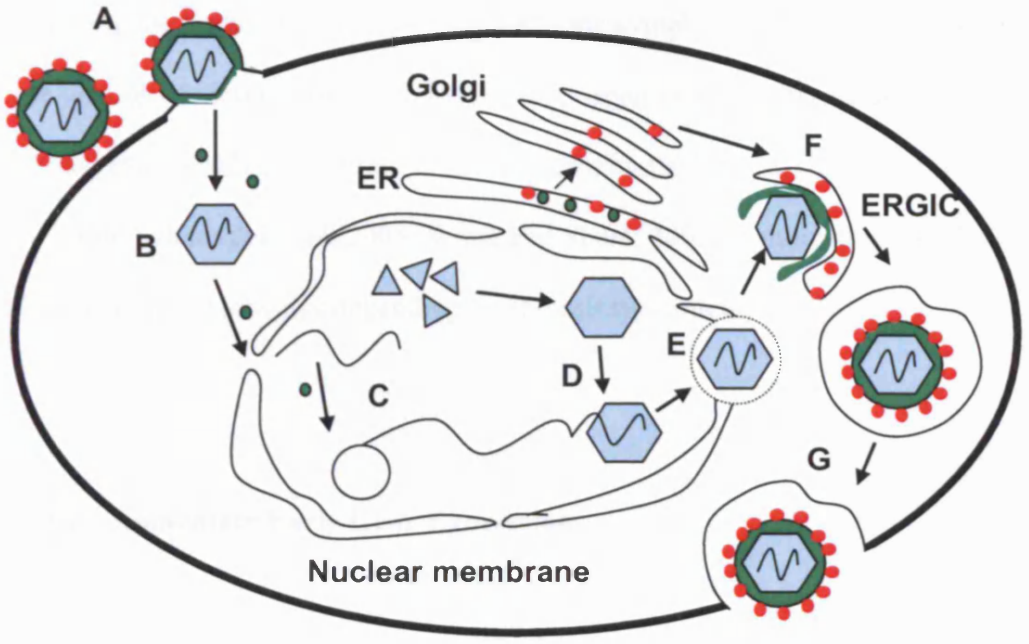


**Figure 1.4. Lifecycle of HCMV.**
A) Attachment and entry. B) Uncoating and transport to nucleus. C) DNA Replication. D) Capsid assembly. E) Nuclear egress consisting of primary envelopment and de-envelopment F) Tegumentation and secondary envelopment. G) Release. Adapted from (Mocarski et al. 2007).

releasing the tegument and nucleocapsid to the cytoplasm. However, in endothelial cells the viruses can internalise by endocytosis (Sinzger et al. 2000) as well as by direct fusion (Wang et al. 2007). This process is dependent on the UL128-UL131A complex (Adler et al. 2006; Schuessler et al. 2008; Wang and Shenk 2005a), indicating HCMV can utilise different entry pathways depending on the cell type infected.

### 1.3.2 Immediate Early Gene Expression

IE genes are defined as those transcribed in the presence of an inhibitor of protein synthesis, and thus their expression is independent of *de novo* virus encoded gene expression. Four regions of IE gene expression have been mapped on the HCMV genome: the major IE gene region encodes IE1 (UL123), IE2 (UL122) and additional less abundant products via differential splicing, UL36 and UL37, TRS1 IRS1 and US3. By definition, IE genes expression is required to progress productive infection. Although IE genes are primarily associated with their key functions as transcriptional trans-activators, the majority of characterised HCMV IE gene functions have been attributed to evading intrinsic, innate and adaptive host immunity to infection.

The expression of IE1 and IE2 genes are under the control of the major immediate early promoter (MIE) and is purported to contain the strongest enhancer element identified to date (Boshart et al. 1985). The core sequence element that regulate the MIEP are located between -580 and -40 relative to the start of transcription and contains a remarkable array of 16, 18, 19 and 21 base-pair repeats (Akrigg et al. 1985; Boshart et al. 1985; Thomsen

et al. 1984). However, transcription has also been shown to be modulated by sequences lying both upstream and downstream of the core promoter (reviewed in(Sinclair and Sissons 2006). The MIEP also contains binding sites for a remarkable array of transcription factors, which include NF-κB and CREB (Sambucetti et al, 1987). As well as being activated by a range of host transcription factors, the MIEP is also regulated by viral proteins. The tegument proteins pp71 and ppUL35 can stimulate expression from the MIEP (Spaete and Mocarski 1985b). Virion transactivators ensure IE gene expression without relying on *de novo* viral gene expression or host factors.

Transcription from the MIEP produces differentially spliced and polyadenylated transcripts encoding two major proteins, IE1p72 and IE2p86 (Stenberg et al. 1985; Wilkinson et al. 1984). These proteins contain the same N-terminal 85 amino acid (exons 2 and 3) but following differential splicing IE1 fuses with exon 4 and IE2 with exon 5. Three less abundant products are also produced; IE1p38, IE2p55 and IE2p18. These proteins play an important role in initiating and maintaining gene regulation during infection.

IE1 stimulates expression from its own promoter, but by itself tends to be a relatively weak activator of heterologous promoters. However, by interacting with other factors, including IE2, it can influence gene expression.

The IE1 gene product (IE-72K) initially traffics to and induces the disruption of PML-bodies (also known as ND10 or PODs). PML-bodies are punctuated intranuclear domains defined by their association with the tumour suppressor protein PML. The

expression of PML and additional PML-body associated protein (notably hDaxx and Sp100) are enhanced by interferon. PML-bodies are believed to constitute an intrinsic barrier to DNA virus infection; knock down of PML or hDaxx using RNAi technology will significantly enhance the efficiency of HCMV infection (Tavalai et al. 2008). IE1 traffics to PML-bodies and induces disruption PML bodies during the first 6 h p.i. (Ahn et al. 1998a; Ahn and Hayward 1997; Kelly et al. 1995; Lafemina et al. 1989; Wilkinson et al. 1998). While pp71 also promotes proteolysis of hDaxx, IE1 induces its dislocation from PML-bodies; the site HCMV transcription and DNA replication. The interaction of hDaxx with histones (H2A, H2B, H3 and H4) and chromatin-associated proteins are related to its capacity to recruit histone deacetylase to sites of transcription. HCMV replicates by altering the chromatin structure of the MIEP (Woodhall et al. 2006). By preventing the recruitment of Daxx-dependant histone deacetylase to the site of transcription, IE1 and pp71 together act to counter an intrinsic barrier to HCMV infection (Hollenbach et al. 2002; Murphy et al. 2002). IE1-72K remains in a complex with PML and can be seen to induce its association with metaphase chromatin. Interestingly, IE1 also has a similar effect on STAT-2; IE1 thereby contributes to suppression of one aspect of the interferon response (Huh et al. 2008).

IE2p86 functions as a promiscuous transactivator of viral and host promoter (Pizzorno et al. 1988) while efficiently negatively autoregulates transcription from the MIEP (Cherrington et al. 1991; Liu et al. 1991). IE2-86K does not localise exactly with PML-bodies, but is found in discrete domains adjacent to them, in close association with input HCMV genomic DNA (Ahn and Hayward 1997; Ishov et al. 1997). IE2 binds the 15 base-pair *cis* repression signal (*crs*) immediately upstream of the transcription initiation

site (Ahn et al. 1998b; Cherrington et al. 1991; Lang and Stamminger 1993) negatively regulating expression (Liu et al. 1991). Through its function as a transcriptional trans-activator, IE2 mediates the switch from the IE to early phase of gene expression. At early and late times in infection two addition proteins are expressed from the IE2 gene, IE2p40 and IE2p60 (Jenkins et al. 1994). While IE2p40 represses the MIEP, the other two proteins are required for efficient early and late gene expression by maintaining IE2 functions throughout infection (White et al. 2007).

UL36 and UL37 are both IE inhibitors of apoptosis. They are individually dispensable but the presence of one is essential for HCMV growth (Colberg-Poley 1996; Patterson and Shenk 1999). pUL36 codes for a protein termed vICA which blocks Fas-mediated apoptosis by binding to caspase 8 (Skaletskaya et al. 2001). UL37 encodes a protein termed vMIA, which functions downstream of caspase 8 to inhibit apoptosis (Goldmacher et al. 1999). While vMIA is functionally similar to the human anti-apoptotic factor Bcl2, there is no sequence similarity. IE1 and IE2 also have anti-apoptotic functions as they both inhibit TNFα-induced apoptosis (Zhu et al. 1995).

In addition to being IE proteins, pTRS1 and pIRS1 are both present in the virion and are thus introduced into cells prior to IE gene expression. pTRS1 and pIRS1 prevents the shut-off of host cell protein synthesis by interacting directly with and sequestering the inducible Protein Kinase R (PKR), preventing the phosphorylation of EIF-2α (Child et al. 2004; Hakki et al. 2006), thereby preventing interferon-induced inhibition of protein synthesis.

US3 encodes an ER-resident membrane glycoprotein that inhibits antigen presentation by MHC class I by retaining the antigen-MHC class I complex in the ER (Jones et al. 1996). By preventing egress of MHC class I complexes to the cell surface, pUS3 suppresses MHC-1-restricted antigen presentation of antigen. This is this first stage in a multistep process of countermeasures against MHC class I antigen presentation that continue throughout infection (as discussed in section 1.5.2).

### 1.3.3 Early And Late Gene Expression And Regulation

Early phase gene expression is defined as that which precedes the initiation of viral DNA synthesis. Operationally, this can readily be achieved by infecting and harvesting RNA in the presence of an inhibitor of the HCMV DNA polymerase. Many early genes continue to express at the same level or greater during the late phase. True late gene expression is characterised by a dependency on viral DNA replication. The regulation of early and late phase gene expression is incompletely understood with detailed studies being based primarily on the study of a small number of genes; β2.7, UL112-113, UL54 and UL34 for early gene expression and UL99, UL94 and UL44 for late gene expression (Biegalke et al. 2004; Isomura et al. 2008).

The most abundant early transcript, β2.7, which accounts for more than 20% of viral transcripts, does not appear to produce a translated protein (Greenaway and Wilkinson 1987; McSharry et al. 2003). Rather, the 2.7Kbp RNA molecule interacts with the mitochondrial enzyme complex 1 (Reeves et al. 2007), to preserve mitochondrial

membrane integrity while suppressing apoptosis. UL112-113 encodes four nuclear phosphoproteins which are involved in the initiation of viral DNA synthesis (Penfold and Mocarski 1997; Wright et al. 1988). The proteins are detectable in the nucleus of infected cells 8 h post infection (p.i.) and increase in abundance through late time points; transcription is controlled by promoter containing ATF/CREB and IE2p86 binding sites (Rodems et al. 1998). The ATF/CREB binding site is required for early expression; mutation of this binding site prevents early phase expression. The IE2p86 site modulates early expression and may be required for activating late transcription (Rodems et al. 1998). Early genes are also involved in gene regulation. pUL34 represses the expression of the immediate early gene US3 (Biegalke et al. 2004; LaPierre and Biegalke 2001) by binding a transcriptional repression element in the genes promoter comparable with the *crs* of MIEP (LaPierre and Biegalke 2001).

Few HCMV genes are considered true late genes; transcription of true late genes are observed only after onset of HCMV DNA synthesis. The UL94 gene product is a tegument protein that associates with pp28 (ppUL99) (Liu et al. 2009). UL94 is a true late gene which is controlled by a promoter with a negative response element (NRE) and a positive response element (PRE) (Wing et al. 1998; Wing et al. 1996). During the early phase of infection, IE2p86 and cellular p53 interact with the NRE to prevent expression (Wing et al. 1998). At late times the PRE is dominant driving expression of the gene. Another true late gene, UL99, also contains repressor elements which modulate gene expression (Kerry et al. 1997).

UL44, a DNA polymerase processivity factor, has three distinct transcription start sites which produce three functionally different proteins with differing kinetics (Isomura et al. 2007). The proximal and distal start sites produce proteins with early kinetics which are essential for viral DNA replication (Iwayama et al. 1994). Expression of the proximal and distal gene products are under control of TATA elements (Isomura et al. 2008), the middle start site produces a protein with true late kinetics (Isomura et al. 2007). This gene product does not influence DNA synthesis but instead increases viral protein synthesis. The middle start site is controlled by a non-canonical TATA element (Isomura et al. 2008).

### 1.3.4 Genome Maturation And Virion Morphogenesis

Viral DNA synthesis begins as early as 15 h p.i. with progeny virus released 48 h after DNA synthesis (Wang et al. 2008). HCMV utilises six core herpesvirus genes for DNA replication; UL54, UL44, UL57, UL105, UL70 and UL102 (reviewed in (Pari 2008)). The replication machinery forms at sub-nuclear locations defined by UL112-113 gene products producing linear genomes linked together in concatemers (McVoy et al. 1998). Concurrent with DNA replication the capsid is assembled. The 5 capsid components form around the assembly protein precursor (pAP) creating the procapsid (Gibson et al. 1990). pAP is then digested by the maturational protease PR to form the mature form of the assembly protein (AP) (Baum et al. 1993). pAP is sufficient to provide for the formation of procapsids, but PR is required for the incorporation of the viral genome into the nucleocapsid (Baum et al. 1993). In addition, the nuclear localisation of pAP and PR

is essential for virus production (Nguyen et al. 2008). The encapsidation machinery, which consists of ten core proteins, recognises the concatemeric template via conserved *pac1* and *pac2* elements within the terminal *a* sequence (Bogner et al. 1998; Penfold and Mocarski 1997). The terminase complex threads the genome into the capsid by interacting with the portal protein pUL104, and then cleaves at the *pac* sequence at the end of the genome (Dittmer et al. 2005).

Following the encapsidation of the genome, the nucleocapsid then buds from the nucleus. Nuclear egress is not completely understood but is thought to consist of envelopment step and de-envelopment steps (Azzeh et al. 2006; Camozzi et al. 2008). Primary envelopment delivers the nucleocapsid through a remodelled nuclear lamina (Camozzi et al. 2008) to the perinuclear space which is then followed by a de-envelopment step which releases the nucleocapsid to the cytoplasm. The nucleocapsid is then transported to the cytoplasmic assembly site (Das et al. 2007). The cytoplasmic assembly site is a structure consisting of Golgi apparatus, Trans-Golgi network and early endosomes where final tegumentation and secondary envelopment occurs (Das et al. 2007; Homman-Loudiyi et al. 2003; Sanchez et al. 2000b). While some tegument proteins associate with the nucleocapsid in the nucleus, a majority of them associate in the cytoplasm (Azzeh et al. 2006; Liu et al. 2009; Sanchez et al. 2000a). Final envelopment occurs in an assembly complex comprised of concentric rings of Golgi, trans-Golgi network (TGN) and early endosomes organelles (Das et al. 2007). The tegument proteins pp28 and pp150 and the membrane glycoprotein gO are involved in promoting the envelopment process (Jiang et al. 2008; Sanchez et al. 2000a; Sanchez et al. 2000b). Following envelopment, the virus particle is released from the cell by exocytosis.

NIEPs follow the same method of tegumentation and envelopment (Irmiere and Gibson 1983). However, instead of mature nucleocapsids leaving the nucleus procapsids, still with pAP associated, leave the nucleus and are subsequently enveloped (Irmiere and Gibson 1985b). In addition to infectious virions and NIEPs, dense bodies are also released from the cells (Craighead et al. 1972). Dense bodies are accumulations of tegument proteins, which are enveloped in the cytoplasm and released.

A majority of the experiments studying the maturation of the virus have been performed in human fibroblasts. The situation is likely to be far more dynamic in vivo; substantial differences are likely to be seen as studies are performed on other cell types.

## 1.4 PATHOGENESIS, LATENCY AND REACTIVATION

### 1.4.1 Pathogenesis

Initial infection occurs in the mucosal epithelial following direct contact with virus from infectious secretions from another individual (Gerna et al. 2004). Infected individuals secrete virus in saliva, urine, breast milk, cervical secretions and semen (Zanghellini et al. 1999). Following infection, a systemic phase which distributes virus in the host can last for several months (Revello et al. 1998). HCMV replicates in a wide range of host cells including epithelial, endothelial and haematopoietic cells (HPC) (Sinzger et al. 1995; Wang et al. 2008) with myeloid-lineage haematopoietic cells important for life-long persistence (Hahn et al. 1998). Dissemination through the host is thought to be mediated by HPC and more differentiated myeloid cell type (Sinzger et al. 1995). Epithelial cells are the site of virus production and shedding into secretions (Sinzger et al. 1995), replication in the salivary glands and kidney tubule ductal epithelial respectively results in the shedding in saliva and urine (Heieren et al. 1988).

### 1.4.2 Latency And Reactivation

Following the primary phase of infection, a lifelong latent infection is established. Classically, latency has been characterised as the maintenance of the viral genome without the production of cell free virus. However, in HCMV lifelong infection is associated with frequent reactivation of virus replication (Zanghellini et al. 1999). While

long-term low-level persistent replication may be involved, it is likely that a latent HCMV reservoir is constantly reactivating lytic replication. Reactivation is quickly controlled by the cellular immune response in immunocompetent individuals but causes disease in immunocompromised individuals. Haematopoietic cells (HPC) have been identified as a major latent reservoir of HCMV (Hahn et al. 1998; Taylor-Wiedeman et al. 1991). $CD34^+$ HPC, resident in the bone marrow constantly renew the short-lived monocyte population (Katz et al. 1985; Metcalf 1989). HCMV DNA can be detected in myeloid precursor cells from healthy seropositive individuals indicating that they are an important latent reservoir of virus *in vivo* (Hahn et al. 1998; Mendelson et al. 1996).

Little is known about the initiation of latent infection of HPC. However, recently Goodrum and colleagues (2007) identified the UL138 ORF as promoting latent infection of HPCs. They discovered that while low-passage clinical isolates of HCMV would establish latent infection of HPC *in vitro*, laboratory-adapted HCMV strains, which lack the UL/b' region, would establish productive infections. By using recombinant viruses UL138 was identified as required for HCMV to establish latent infection.

During latency the HCMV genome is maintained as a circular plasmid (Bolovan-Fritts et al. 1999). Repression of immediate early gene expression is controlled by the transcriptional repression of the MIEP by chromatin (Reeves et al. 2005a; Reeves et al. 2005b). It has been problematic to detect expression from latent genomes, several putative latency-associated transcripts has been identified only for them to later be detected during productive infection of fibroblasts (Kondo et al. 1996; Lunetta and Wiedeman 2000). The only true latency associated transcript identified so far is an anti-

sense transcript from the UL81-82 region of the genome (UL81-82ast) (Bego et al. 2005). This transcript and its protein (pUL82as) can be detected in bone marrow from seropositive healthy donors in the absence of immediate early gene expression(Bego et al. 2005). As this transcript runs anti-sense to the UL82 ORF, which encodes the viral transactivator pp71, it is postulated that either UL81-82ast or pUL82as may affect the expression of pp71 thus affecting immediate early expression. This function may have a role in the control of latent infection.

Reactivation from latent infection causes disease. Reactivation occurs in mature cells but not in the BM resident or peripheral blood circulating progenitors. Maturation of $CD34^+$ HPC to mature dendritic cells (DC) or monocyte-derived macrophages leads to the acetylation of histones bound to the MIEP allowing transcription and expression of immediate early genes (Reeves et al. 2005b). Allogenic stimulation of naturally infected PBMCs leads to viral replication and production of virus from monocyte-derived macrophages (Soderberg-Naucler et al. 1997). These studies suggest that virus reactivation is the result of chromatin remodelling of the MIEP during cell differentiation which results in the induction of immediate early gene expression

## 1.5 IMMUNE RESPONSE AND MODULATION

### 1.5.1 Immune Response

HCMV infection is controlled by a combination of the innate and adaptive arms of the immune response working together. However, Natural killer (NK) cells are clearly crucial in controlling cytomegalovirus infections in mouse and man. Individuals with defects in their NK response are rare, but do exhibit greatly enhanced sensitivity to HCMV (Biron et al. 1989; Guma et al. 2004). Deletion of NK cells renders mice vulnerable to MCMV pathology, while deletion of NK resistance functions compromises its virulence (Bukowski et al. 1984; Jonjic et al. 2008). In allogeneic bone marrow transplant recipients, the rapid expansion of functional NK cells can be detected within days following HCMV infection (Hokland et al. 1988). The protective potential of the adaptive immune response has primarily focussed on cytotoxic T cells, yet HCMV-specific antibody can also elicit therapeutic benefit (Lilleri et al. 2009; Reusser et al. 1991; Stone et al. 2006; Tu et al. 2006). $CD4^+$ and $CD8^+$ T cell response develop simultaneously, generally 10 days following detection of HCMV DNA in the individuals blood (Gamadia et al. 2003; Lilleri et al. 2009). Adoptive transfer of HCMV-specific $CD8^+$ T-cells transplant recipients is associated with therapeutic benefit (Cobbold et al. 2005; Hakki et al. 2003; Manley et al. 2004; Peggs et al. 2002; Walter et al. 1995). HCMV-specific $CD8^+$ T-cell responses to the tegument protein pp65 and the major immediate early protein, IE-1, are immunodominant, however, responses to these epitopes are not present in all infected individuals (Borysiewicz et al. 1988; Kern et al. 2000; Kondo et al. 2004). The HCMV-specific $CD4^+$ T-cell response is also important

for the control of infection (Harari et al. 2004a; Harari et al. 2002; Tamarit et al. 2004). IFN-γ secreting $CD4^+$ T-cells are protective and prevent horizontal transmission from mother to foetus (Lilleri et al. 2007). Over 150 HCMV ORF have been identified as $CD4^+$ or $CD8^+$ targets (Sylwester et al. 2005).

As HCMV is cell-associated in the host and only cell-free in secretions, the antibody response may be important for the control of transmission. Sera from seropositive individuals has antibodies specific for envelope glycoproteins and tegument proteins, including neutralising antibodies against gB, gM:gN and gH:gL (Mach et al. 2000; Marshall et al. 1992; Shimamura et al. 2006; Stinski 1976). The administration of high-titre hyperimmune globulin specific to HCMV reduced the risk of transplacental transmission (Nigro et al. 2005).

The immune response controls infection but has never been documented as being capable of clearing the virus. HCMV has an array of immune modulating and subverting gene functions which have co-evolved with the immune response (Harari et al. 2004b). These immune modulation functions are required to provide for long term survival of the virus.

### 1.5.2 Downregulation Of MHC Class I

T cells recognise antigens via an interaction between their T cell receptor and the antigen-MHC class I complex on the target cell (reviewed in Smith-Garvin et al. 2009). HCMV infection induced the downregulation of MHC I on the cell surface and thereby inhibits $CD8^+$ MHC-I-restricted cytotoxic T lymphocytes (Hengel et al. 1996; Warren et al.

1994a). The accelerated downregulation of MHC class I is independent of ß2-microglobulin (Beersma et al. 1993). Four gene products are responsible for downregulating antigen presentation by MHC-I during HCMV infection; US2, US3, US6 and US11 (Noriega and Tortorella 2009). HCMV US2-11 deletion mutants do not downregulate MHC class I during infection, indeed MHC-1 is upregulated, yet expression of only one of the four genes will successfully downregulate MHC class I, indicating a redundancy of function (Hewitt et al. 2001; Jones and Sun 1997; Jones et al. 1996; Noriega and Tortorella 2009; Wiertz et al. 1996).

US3 is a spliced IE gene that encodes an ER resident glycoprotein (Ahn et al. 1996; Misaghi et al. 2004) that binds directly to the MHC class I heavy chain immediately following synthesis preventing its egress to the Golgi apparatus (Jones et al. 1996). gpUS3 directly binds tapasin and inhibits tapasin-mediated peptide loading (Park et al. 2004). gpUS3 is an IE protein that is expressed only transiently during the early stages of infection.

Starting at early times continuing throughout infection US2 and US11 inhibit surface expression of MHC class I by degrading newly synthesised MHC class I heavy chains (Jones and Sun 1997; Story et al. 1999; Wiertz et al. 1996). US2 and US11 both target newly synthesised MHC class I to ubiquitination-dependant proteasome-mediated degradation (Shamu et al. 2001; Shamu et al. 1999; Story et al. 1999). The newly synthesised MHC class I heavy chains are dislocated from the ER to the cytosol, where they are degraded by the proteasome. US11 recruits Derlin-1, a protein which is involved in the degradation of misfolded ER proteins, to MHC class I (Lilley and Ploegh 2004). In

contrast, gpUS6 binds to the transporter associated with antigen processing (TAP) in the lumen of the ER and inhibits the import of peptides epitopes into the ER (Ahn et al. 1997). gpUS6 binds to TAP and prevents ATP binding and the conformational rearrangement induced by peptide binding (Hewitt et al. 2001). Inhibition of antigen presentation by MHC class I is likely to allow the virus to escape clearance by cytotoxic T cells.

### 1.5.3 Downregulation Of MHC Class II

Antigen presenting cells, including DCs and macrophages present antigens to $CD4^+$ T cells via MHC class II. HCMV also downregulates MHC class II expression in antigen presenting cells (Lee et al. 2006). Two HCMV genes target both MHC-I and MHC–II: gpUS2 binds to HLA-DRα and HLA-DMα and promotes their degradation in the ER (Hegde and Johnson 2003; Tomazin et al. 1999) while gpUS3 binding to class II α/β complexes preventing their association with the invariant chain (Hegde et al. 2002). The gpUS3-MHC-II complex moves from the ER to the Golgi apparatus bypassing the class II loading compartment, resulting in a reduction of peptide-loaded MHC class II complexes on the cell surface. MHC-II transcription is also suppressed by HCMV infection causing the degradation of the cellular kinase JAK, which in turn inhibits a key transcription factor (CTIIA) (Miller et al. 1998). cmvIL10 has also been shown to downregulate MHC class II expression on macrophages(Kotenko et al. 2000; Redpath et al. 1999).

### 1.5.4 Natural Killer Cell Evasion

Natural Killer cell function is regulated by a balance of activating and inhibitory signals received from potential targets (fig 1.5). The default situation is clearly for the NK cells not to be activated. In line with Klaus Karre's missing self hypothesis, NK cells receive a strong inhibitory signal from receptor recognition of self MHC-1 molecules. HCMV downregulation of endogenous MHC-1 has the potential to render HCMV-infected cells vulnerable to NK attack (table 1.2). The sequence of HCMV strain AD169 revealed that an ORF (later designated UL18) was a MHC-I homologue gpUL18 (Beck and Barrell 1988). The gpUL18 is expressed on the cell surface in complex with β2-microglobulin and endogenous peptide (Browne et al. 1990; Fahnestock et al. 1995). Two differentially glycosylated forms of gpUL18 have been described; an Endo H sensitive form and a highly-glycosylated Endo H resistant form (Griffin et al. 2005). An early study supported the hypothesis that gpUL18 was an NK cell evasion function, albeit by an erroneous mechanism (Reyburn et al. 1997). Its role became more contentious when UL18 was reported to stimulate NK cell-mediated cytolysis (Leong et al. 1998). gpUL18 has been shown to bind the NK cell receptor LIR-1 (Chapman et al. 1999; Cosman et al. 1997); LIR-1 is an inhibitory NK receptor which normally binds MHC class I NK cells; LIR-1 binds gpUL18 with 1000 fold higher affinity than to MHC class I (Chapman et al. 1999). The conflict with respect to UL18 function was resolved when it was shown to inhibit cytotoxicity mediated by LIR-1$^+$ NK cells while activating LIR-1$^-$ populations (Prod'homme et al. 2007). The activation of LIR-1$^+$ NK cell cytotoxicity implies that gpUL18 interacts with an unidentified NK cell activating receptor.

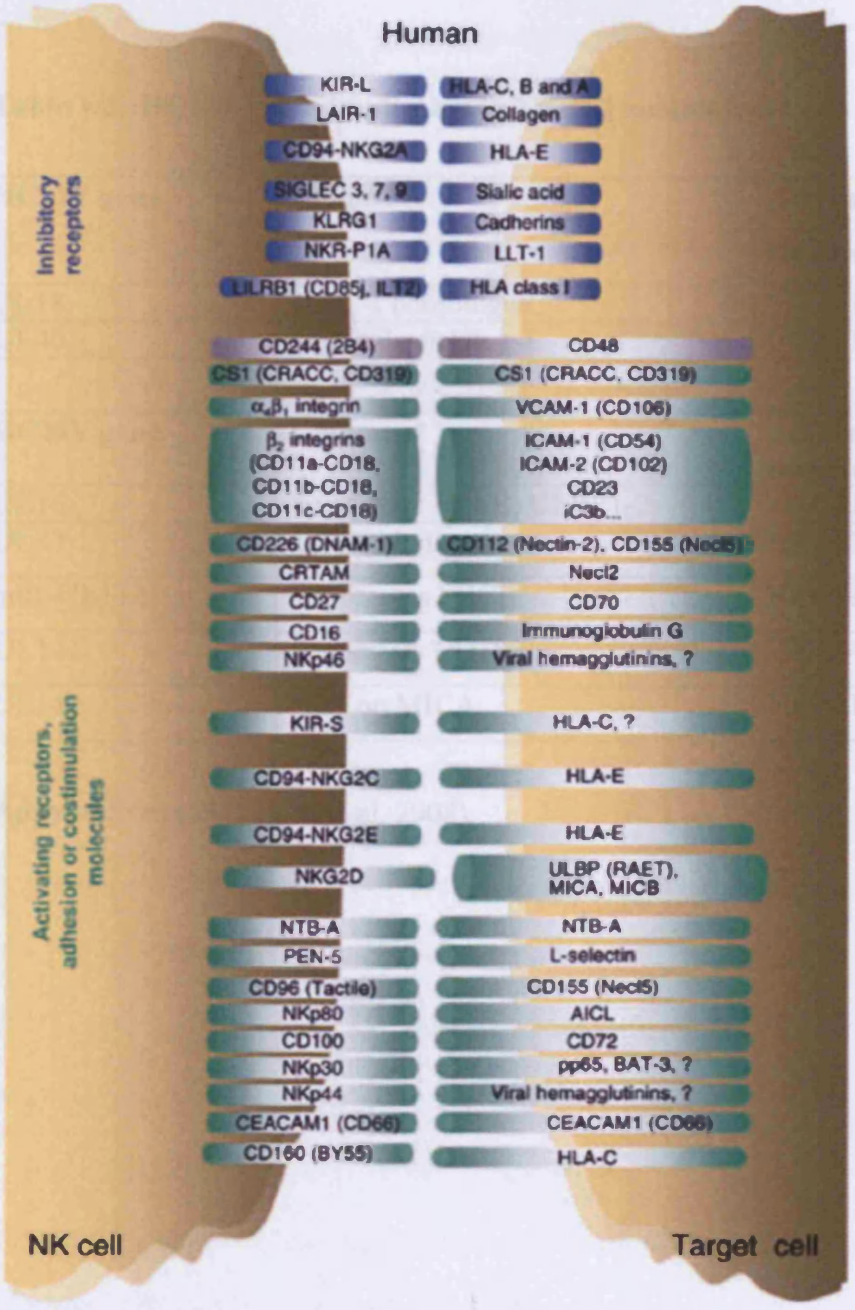


**Figure 1.5. Activating and inhibitory interactions between NK cells and target cells** The interaction between NK cell receptors and their ligands on target cells. Activating ligands are in green and inhibitory receptors are shown in blue. Reproduced from (Vivier et al. 2008).

**Table 1.2. HCMV genes implicated in NK cell modulation**

| **HCMV gene** | **Comment** | **Acts on inhibitory receptor** |
|---|---|---|
| UL18 | MHC-I homologue | LIR1 (ILT2) |
| UL40 | Upregulates HLA-E | CD94/NKG2A |
| | | |
| **HCMV gene** | **Comment** | **Acts on activating receptor** |
| UL16 | Sequesters MICB, ULBP1-2 | NKG2D |
| UL83 | Direct binding | NKp30 |
| miR-UL112 | Suppresses MICB | NKG2D |
| UL141 | Sequesters CD155 | DNAM-1, CD96 |
| UL142 | Acts on MICA | NKG2D |

Adapted from (Wilkinson et al. 2008).

The first HCMV gene unequivocally demonstrated to elicit protection against NK cell recognition was UL40. HLA-E is a non-classical MHC molecule which is also expressed a trimeric complex with ß-2m and a restricted group of peptides, normally derived from the leader sequences of classical MHC-I molecules. Maturation and cell surface expression is dependent on acquisition of this endogenous peptide in a TAP-dependent manner. When expressed on the cell surface, HLA-E is then available to be recognised by the NK cell inhibitory NK receptor CD94/NKG2A (Braud et al. 1998). With the inhibition of TAP by US6, surface expression of HLA-E is downregulated (Tomasec et al. 2000). A peptide derived from the leader sequence of UL40 is secreted into the ER independently of TAP to both rescue and enhance surface expression of HLA-E, and to elicit protection against NK cells (Tomasec et al. 2000; Wang et al. 2002).

The ligands for the activating receptor NKG2D are upregulated in response to stress (Groh et al. 1996). CD94/NKG2D recognises seven ligands; MICA, MICB, ULBP (UL16 binding protein) 1-5 (Bacon et al. 2004; Groh et al. 1996; Kubin et al. 2001). HCMV infection, notably IE1 and IE2 functions, activate the expression of NKG2D ligands (NKG2DLs) during the early phase of infection (Venkataraman et al. 2007). UL16 encodes a protein expressed at early times, accumulates during infection and binds to MICB, ULBP-1 and ULBP-2 retaining them in the ER (Cosman et al. 2001; Dunn et al. 2003; Welte et al. 2003). By sequestering NKG2DLs in the ER, gpUL16 prevents their expression on the cell surface. In support of UL16, UL142 acts to suppress expression of full length alleles of MICA and ULBP3 (Wills et al. 2005, Wills personal communication).

The major tegument protein pp65 (ppUL83) inhibits the NK cell activating receptor NKp30 by binding directly with the receptor (Arnon et al. 2005). This interaction leads to disruption of NKp30-induced signalling by disrupting the interaction between NKp30 and CD3ζ. The dissociation of CD3ζ leads to reduced killing by the NK cell.

It is expected that more NK evasion functions will be discovered as research into HCMV progresses. The use of clinical isolates and different cell types will likely provide novel NK modulatory genes.

### 1.5.5 The UL141 ORF Of HCMV

UL141 was identified as a potent NK evasion gene by Tomasec and colleagues (Tomasec et al. 2005) and is the object of this study. It was identified as a NK evasion gene during a systematic screen of the UL/b' region of Toledo strain HCMV. UL141 expression protected target cells from lysis by 67% of NK cell clones tested (Tomasec et al. 2005). It was determined that gpUL141 was downregulating the cell surface expression of CD155, a ligand for the NK cell activating receptor DNAM-1 (see fig 1.6) (as described in section 1.6.6). gpUL141 specifically downregulates CD155, it does not downregulate cell surface expression of the other identified DNAM-1 ligand, nectin-2. gpUL141 prevents the maturation of the fully-matured cell surface form of CD155, retaining it within the cell in an immature form (Tomasec et al. 2005). The immature intracellular form of CD155 has different glycosylation than the mature cell surface form (Bernhardt

et al. 1994). Soluble CD155 is able to block the interaction between CD155-specific monoclonal antibodies and CD155 implying that there is direct interaction between CD155 and gpUL141.

The UL141 ORF was first described during the identification of the 15 kb UL/b' region in the low passage clinical isolate Toledo HCMV (Cha et al. 1996). It was predicted to encode an immunoglobulin-like protein (Novotny et al. 2001), however, the originally described sequence contained a frame shift (Dolan et al. 2004). The updated sequence encoded for an immunoglobulin-like protein predicted to contain a signal peptide, hydrophobic transmembrane domain and an immunoglobulin-like β-sandwich domain (fig 1.7). While absent in laboratory strain of HCMV, the sequence of UL141 is highly conserved between clinical isolates with between 97-100% identity at both the nucleotide and amino acid level (Ma et al. 2006). The UL141 protein has 50% homology to another HCMV ORF, UL14 (Davison et al. 2003), which, together, comprise the UL14 gene family (fig 1.2). The function of UL14 protein is currently unknown, but it does not downregulate CD155 (Tomasec et al. 2005).

UL141 protein (gpUL141) is detected 24 hour post infection with protein levels increasing during infection (Tomasec et al. 2005). gpUL141 is a glycoprotein with three predicted glycosylation sites which is detected as a doublet with apparent molecular masses of 37 and 40 kDa. Digestion with Endo H or PNGase produced a 34 kDa product, similar to the predicted molecular mass (Tomasec et al. 2005). The sensitivity to digestion by Endo H implies that gpUL141 is resident in the endoplasmic reticulum.

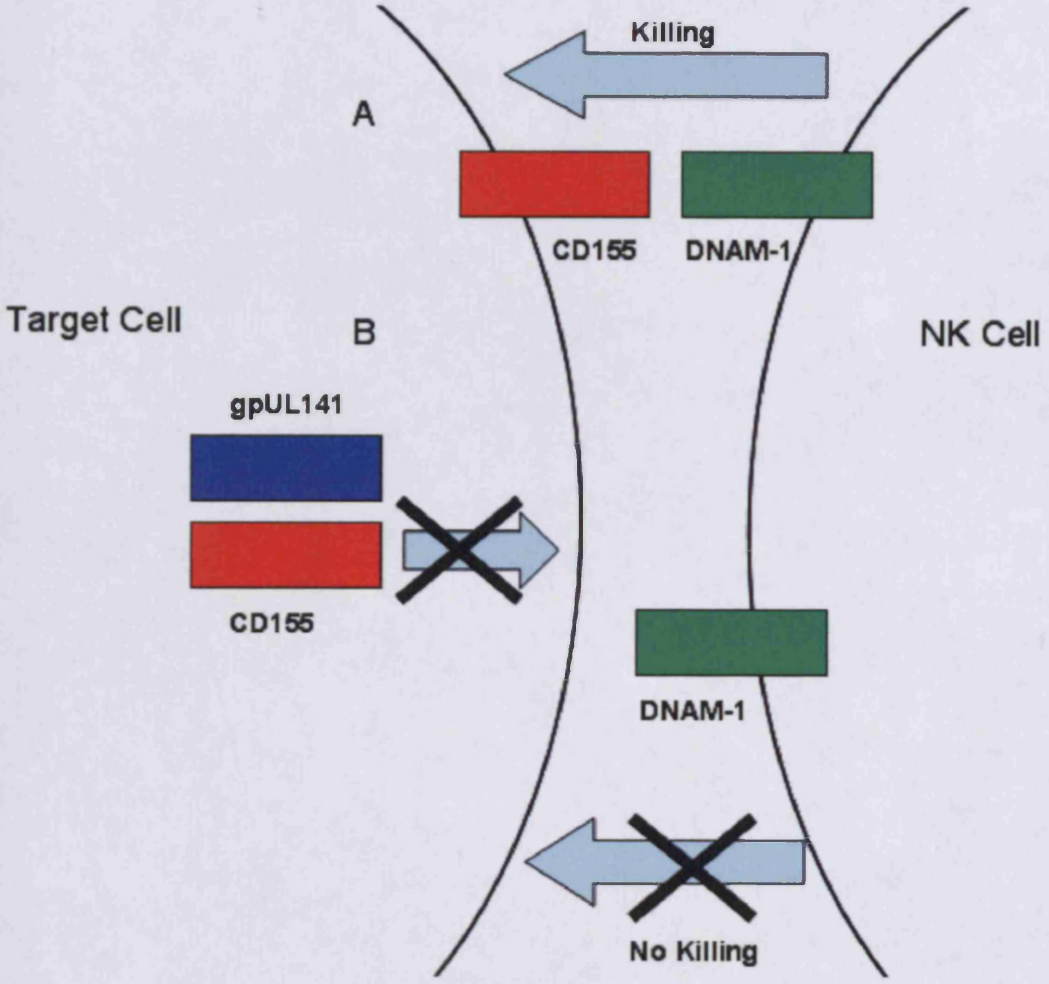


**Figure 1.6. Downregulation of cell surface CD155 protects cells from NK cell mediated lysis**

A) In the absence of gpUL141 expression, fully mature CD155 is expressed on the cell surface where it can interact with DNAM-1 on NK cells. This interaction triggers NK cell to lyse the target cell. B) When gpUL141 is expressed, it retains CD155 within the cell preventing the surface expression of CD155 and the interaction with DNAM-1. This protects the cell from NK cell-mediated lysis.

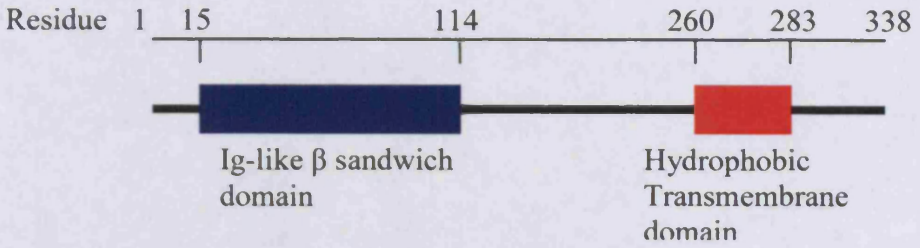


**Figure 1.7. Predicted structure of gpUL141**
gpUL141 is predicted to contain a Ig-like β sandwich domain at residue 15-114 in the luminal domain, a hydrophobic transmembrane domain and a short cytoplasmic domain. Adapted from Tomasec (2005).

At the beginning of this study it was unknown if gpUL141 had any additional role during HCMV infection. In addition to being a NK ligand, CD155 is involved in a wide range of cellular function (as discussed in section 1.6) and it is possible that gpUL141 may modulate these as well. As a result of technical limitation it has previously not been possible to directly or indirectly visualise the interaction and localisation of CD155 and gpUL141. These issues will be addressed in this study.

### 1.5.6 Other Methods Of Immune Evasion

HCMV expresses three G protein-coupled receptor homologues, one of which is a functional chemokine receptor (Chee et al. 1990b). gpUS28 binds multiple CC chemokines, it has highest affinity for fractalkine yet is able to bind RANTES (Released upon Activation, Normal T-cell Expressed and Secreted), MCP-1 (Monocyte Chemoattractant Protein 1) and MIP-1α and β (macrophage inflammatory protein) (Gao and Murphy 1994; Kledal et al. 1998; Kuhn et al. 1995). Following interaction with chemokines, gpUS28 signals by modulating the activity of the transcription factors NFAT (nuclear factor of activated T-cells) and CREB (cAMP response element) (Billstrom et al. 1998; McLean et al. 2004). While gpUS28 signalling has been implicated in cell migration (Streblow et al. 1999), continuous internalisation of chemokines by gpUS28 has also been demonstrated to result in a reduction of extracellular chemokine concentration (Bodaghi et al. 1998). HCMV also a small soluble secreted RANTES binding protein, pUL21A, which acts as a decoy receptor (Wang et al. 2004a). pUL21A and pUS28 may work in harness to suppress chemokine function.

UL146 is a highly variable ORF (Bradley et al. 2008) which encodes for a potent α chemokine, termed vCXC-1 (Penfold et al. 1999). This is a fully functional chemokine which can induce chemotaxis and degranulation of neutrophils. HCMV also encodes a homologue of interleukin 10 (IL-10), termed cmvIL-10 (Kotenko et al. 2000; Lockridge et al. 2000). cmvIL-10 functions in a similar manner as its human homologue and has been shown to inhibit interferon release by dendritic cells and cytokine release by monocytes (Chang et al. 2009; Nachtwey and Spencer 2008; Spencer et al. 2002).

HCMV encode two immunoglobulin G Fc receptors, RL11 and UL119, which are present on the plasma membrane of infected cells and on the envelope of the virions (Atalay et al. 2002; Lilley et al. 2001; Xu et al. 1989). These receptors bind the constant Fc region of IgG molecules. A process called antibody bipolar binding is thought to protect the virus from the complement pathway (Frank and Friedman 1989). Antibody bipolar binding is when the Fc receptor binds the Fc region of an immunoglobulin molecule while the Fab region binds to its antigen on the virion. This process has been shown to resist complement-mediated neutralisation and antibody-mediated cellular cytotoxicity in HSV (Dubin et al. 1991; Frank and Friedman 1989).

HCMV also controls the complement pathway by upregulating the host regulators of complement activation CD55 and CD46 (Spiller et al. 1996). Host regulators of complement activation suppress the activation of C3 convertase on virus-infected cells providing a mechanism to protect HCMV-infected cells from complement mediated lysis. This technique is also utilised in the virions; CD55 and another complement control protein, CD59, are incorporated into the virion envelope (Spear et al. 1995).

pp65 also modulates the interferon response. It inhibits the transcription factors NF-κB and IRF-1 inhibiting pro-inflammatory responses (Browne and Shenk 2003) and downregulating IRF3 (interferon regulatory factor 3) (Abate et al. 2004).

## 1.6 PROPERTIES AND FUNCTIONS OF THE NECTIN AND NECTIN-LIKE FAMILY

### 1.6.1 Nectin And Nectin-Like Family

The nectin and nectin-like (necl) molecules are a family of immunoglobulin-like cell adhesion molecules (Takai et al. 2008b). Members of the family are involved in cell-cell adhesion, polarisation, differentiation, movement and proliferation (Takai et al. 2008a). Nectins are primarily involved in the regulation of various types of cell-cell contacts including Adherin Junctions (AJ) and the formation of tight junctions (TJ) (Kuramitsu et al. 2008; Takahashi et al. 1999) (table 1.3). Necls have more diverse functions including mediating interactions between axons and glial cells, regulation of cell movement and proliferation (see table 1.3) (Boles et al. 2005; Ikeda et al. 2004; Kakunaga et al. 2005; Spiegel et al. 2007). The family consists of four nectins (nectin-1, -2, -3 and -4) and five nectin-like molecules (necl-1, -2, -3, -4 and necl-5/CD155) which are ubiquitously expressed. All members share the same general structure of three extracellular immunoglobulin-like loops, a transmembrane domain and a cytoplasmic domain (Takai et al. 2008a).

The first member of the nectin and necl family to be characterised was CD155; this was due to its important function as the cellular receptor for poliovirus (PVR) although it can also be called necl-5, or Tage4 (Bernhardt et al. 1994; Mendelsohn et al. 1989). Subsequently, nectin-1 and nectin-2 were shown to be related to CD155 (hence their

**Table 1.3. The Nectin and Nectin-like (Necl) Family**

| Name | Alternative Nomenclature | Function | Reference |
|---|---|---|---|
| Nectin-1 | PRR-1, HVEC | Cell-Cell adhesion<br>Receptor for α-herpesviruses entry | (Geraghty et al. 1998) |
| Nectin-2 | PRR-2, HVEC | Cell-Cell adhesion<br>Receptor for α-herpesviruses entry | (Aoki et al. 1997; Warner et al. 1998) |
| Nectin-3 | PRR-3 | Cell-Cell adhesion | (Satoh-Horikawa et al. 2000) |
| Nectin-4 | PRR-4 | Cell-Cell adhesion | (Reymond et al. 2001) |
| Necl-1 | TSLL1, SynCAM3 | Neural tissue-specific cell-cell adhesions. | (Kakunaga et al. 2005; Maurel et al. 2007) |
| Necl-2 | IGSF4, RA175, SgIGSF, TSLC1, SynCAM1 | Cell-Cell adhesion molecule localised to the basolateral membrane in epithelial cells | (Shingai et al. 2003) |
| Necl-3 | SynCAM2 | Neural tissue-specific cell-cell adhesions | (Pellissier et al. 2007) |
| Necl-4 | TSLL2, SynCAM4 | Neural tissue-specific cell-cell adhesions. Mediates myelination. | (Maurel et al. 2007; Spiegel et al. 2007) |
| CD155 | Necl-5, Tage4, PVR | Poliovirus receptor, Ligand for activating NK receptor DNAM-1. | (Ikeda et al. 2003; Mendelsohn et al. 1989) |

initial names poliovirus receptor related (PRR)-1 and -2), and were demonstrated to be co-receptors for alphaherpesviruses (Geraghty et al. 1998; Martinez and Spear 2001). Nectins and necls are predominantly adhesion molecules that form stable interactions with members of the nectin family, although some exceptions interact with other immunoglobulin-like molecules. Characteristically, nectins and necls are expressed as *cis*-homodimers on the plasma membrane (Tachibana et al. 2000), and these homodimers participate in homophilic *trans*-interactions to their partners on an adjacent cell; all nectins, necl-1 and -2 bind in this fashion. Heterophilic *trans*-interactions form when the nectin or necl bind to another family member on another cell, all nectins and necls display limited heterophilic binding capabilities (fig 1.8). The domains of nectins bind uncooperatively in a zipper-like multiply bonded system (Tsukasaki et al. 2007).

The cytoplasmic regions of nectins associate with afadin and tctex-1(Mandai et al. 1997; Mueller et al. 2002). Afadin is an actin filament-binding protein which via the interaction between actin and the cytoplasmic domain of nectins connects AJs to the cytoplasmic cytoskeleton (Mandai et al. 1997). Nectins and necls are differentiated by their ability to bind afadin; nectins interact directly with afadin while necls do not (Ikeda et al. 1999; Mandai et al. 1997). Tctex-1, a component of the dynein microtubule motor complex, interacts with the cytoplasmic domain of CD155 and targets CD155 containing vesicles to the microtubule network (Ohka et al. 2004).

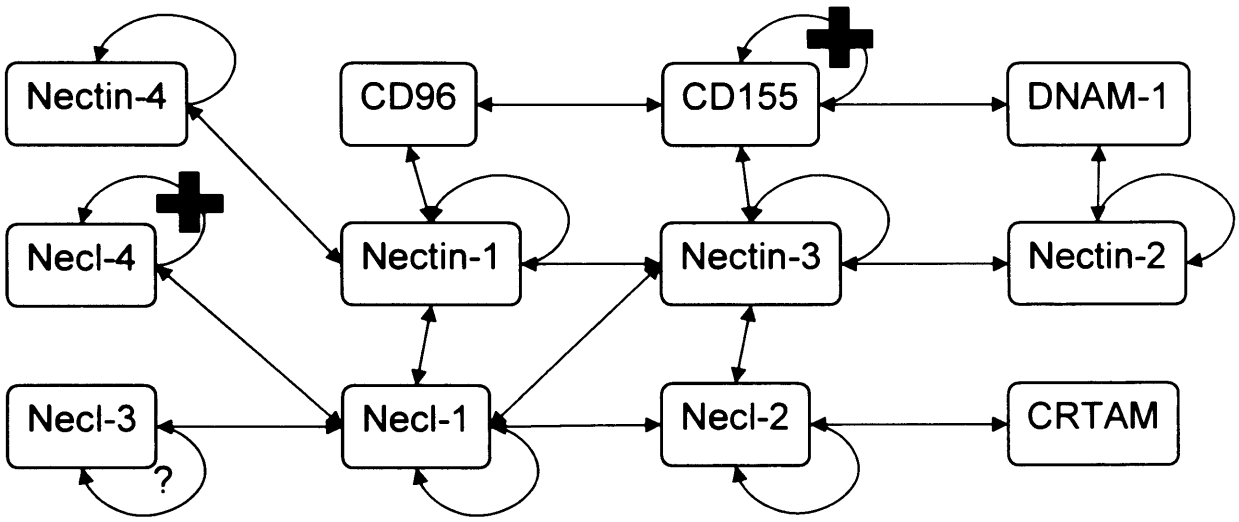


**Figure 1.8. Interactions between Nectins and Necls.**
Nectins, necls and other immunoglobulin family members form heterophilic trans-dimers (straight lines) or Homophilic trans-dimers (curved arrows). Cross denotes no interaction. Question mark denotes interaction not determined. Adapted from (Takai et al. 2008b).

### 1.6.2 Nectins And Cell-Cell Adhesion

Nectins have a major role in the formation of adherens junctions (Takahashi et al. 1999). Together with members of the cadherin family of cell adhesion molecules, nectins form cell-cell contacts connected to the actin cytoskeleton (Tachibana et al. 2000). While nectins and cadherins localise at AJs, necls do not. Nectin-nectin interaction initiates the formation of AJs. Following the nectin interaction, cadherins are recruited to the site of cell-cell contact (Takahashi et al. 1999). Once the cadherins are incorporated into the AJ, the cytoplasmic tail of cadherin binds the F-actin binding proteins α-catenin, α-actinin and vincilin which anchor the cadherins to the actin cytoskeleton (Tachibana et al. 2000).

An important component of the AJ is the integrin $\alpha_V\beta_3$, which modulates the stability of the cell-cell contact (Sakamoto et al. 2006; Sakamoto et al. 2008). Nectin-1 and -2 physically associate with integrin $\alpha_V\beta_3$ in *cis* (Sakamoto et al. 2008). This interaction is essential for AJ formation and for downstream nectin signalling.

A series of signalling reactions occur following nectin *trans*-interactions that result in the dynamic sequential remodelling of the actin cytoskeleton (fig 1.9). Following nectin-nectin interaction the tyrosine kinase Src is recruited and activated in an integrin $\alpha_V\beta_3$-dependant manner (Fukuyama et al. 2005). Src then activates the small G protein Rap1 through the adapter proteins Crk and C3G (the guanine nucleotide exchange factor for Rap1) (Fukuyama et al. 2005). Src also phosphorylates FRG (the guanine nucleotide exchange factor for Cdc42) and Vav2 (the guanine nucleotide exchange factor for Rac)

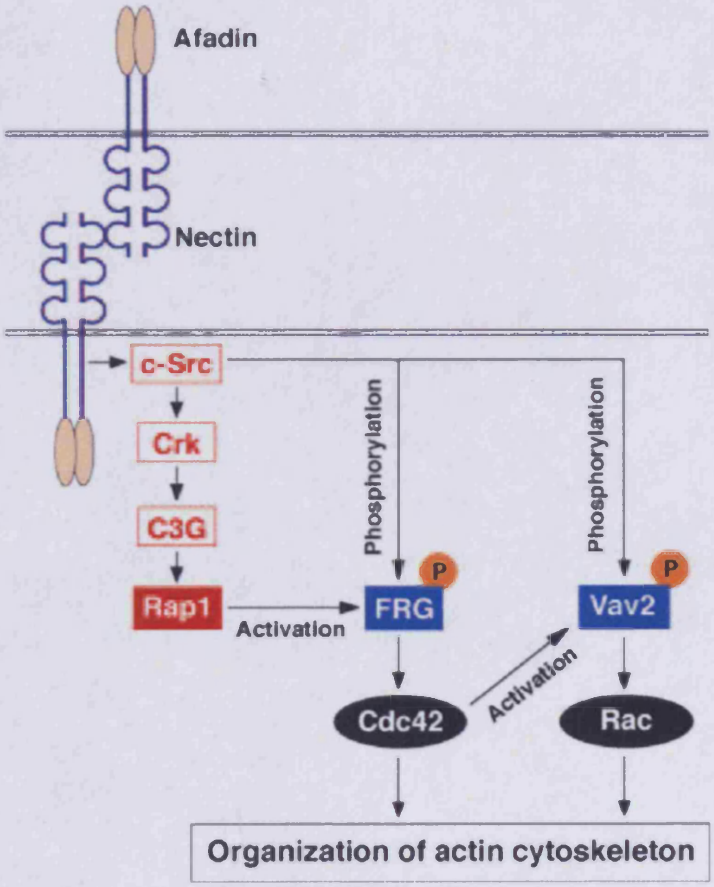


**Figure 1.9. Nectin-dependant intracellular signalling.**
Hetero- or homophilic *trans*-interaction of nectins leads to the reorganisation of the actin cytoskeleton. Reproduced from (Fukuyama et al. 2005).

(Fukuhara et al. 2004; Kawakatsu et al. 2005). Activated Rap1 activates phosphorylated FRG which activates Cdc42. Cdc42 then activates phosphorylated Vav2 which induces activation of Rac (Fukuhara et al. 2004). The activation of Rac and Cdc42 induces the formation of filopodia and lamellipodia (Takahashi et al. 2008). While these protrusions are generally associated with cell movement they increase the number of cell-cell contacts and reduces the intercell distance enhancing cell-cell adhesion (Vasioukhin et al. 2000).

### 1.6.3 CD155

The CD155 gene contains 7 introns (Koike et al. 1990) with alternate splicing producing four recognised variants of CD155; α, β, γ and δ (Koike et al. 1990). CD155α and δ are transmembrane proteins while CD155β and γ are secreted (Baury et al. 2003). Little is known about the function of the alternatively spliced forms of CD155. Soluble CD155 is expressed in that form (not produced by proteolysis), is present in human serum at nanomolar concentrations and can compete with membrane-bound CD155 to inhibit poliovirus entry (Baury et al. 2003). The CD155 core promoter is approximately 280bp long and contains binding sites for Gli1, Gli3, AP2 and nuclear respiratory factor (NRF)-1; these transcription factors have all been shown to bind the promoter to enhance expression (Solecki et al. 2000; Solecki et al. 1999; Solecki et al. 2002). CD155 expression has been shown to be controlled by sonic hedgehog (SHH), SHH is a morphogen that is involved in the development of many structures during development (Solecki et al. 2002). The transcription factors implicated in CD155 expression also have

a role in embryogenesis, consistent with CD155 having an important role during development (Solecki et al. 2002). Indeed, a focussed study has demonstrated CD155 is important in the development of the rat liver (Erickson et al. 2006).

CD155 alone is sufficient to act as the cellular receptor for poliovirus (Koike et al. 1990) (Hogle 2002; Mendelsohn et al. 1989). Following binding, CD155 induction of tyrosine kinases and SHP-2 signalling is required to promote caveola endocytosis (Brandenburg et al. 2007; Coyne et al. 2007). In neuronal cells, the retrograde transport of the endosomes to the nucleus is dependant on CD155 interaction with the dynein-light chain Tctex-1 (Ohka et al. 2004). While the mouse homologue of CD155 (originally termed Tage4, now standardised to necl-5) has a high level of structural and functional identity to human CD155, it does not allow poliovirus entry (Baury et al. 2001; Ravens et al. 2003). The poliovirus binding capabilities of CD155 is restricted to primates (Suzuki 2006). However, the expression of human CD155 in mouse cells is sufficient to confer poliovirus susceptibility (Koike et al. 1990). CD155 also acts as a cellular receptor for viruses other than poliovirus, including porcine psuedorabies virus and bovine herpesvirus 1 (Geraghty et al. 1998).

### 1.6.4 CD155 And Cell Movement.

Unlike nectins, CD155 localises to the leading edge of moving cells where it associates with the platelet-derived growth factor (PDGF) receptor and with integrin $\alpha_V\beta_3$ (Amano et al. 2008; Ikeda et al. 2004; Minami et al. 2007a). CD155 has an important role in the

dynamics of the leading edge. Stimulation of CD155 enhances cell migration (Oda et al. 2004). CD155 enhances PDGF-induced and $\alpha_V\beta_3$-induced signalling (Kakunaga et al. 2004; Minami et al. 2007a). CD155, PDGF receptor and $\alpha_V\beta_3$ integrin can each form heterodimers with either of the other two molecules; CD155:PDGF receptor, CD155: $\alpha_V\beta_3$ integrin and PDGF receptor:$\alpha_V\beta_3$ integrin can all be formed (Amano et al. 2008).

CD155 and $\alpha_V\beta_3$ integrin also co-localise at focal complexes (Amano et al. 2008; Nagamatsu et al. 2008). Focal complexes are immature cell-extracellular matrix adhesion sites that form at the leading edge. As the focal complexes mature into focal adhesions CD155 disassociates leaving $\alpha_V\beta_3$ integrin in the focal adhesion (Ballestrem et al. 2001; Nagamatsu et al. 2008).

Following PDGF-induced cell movement, actin cytoskeleton reorganisation is regulated by Cdc42, Rac and Rho (Nagamatsu et al. 2008; Sato et al. 2005). Cdc42 and Rac induce the formation of cytoplasmic protrusions, while Rho negatively regulates this process. PDGF receptor signalling leads to the downregulation of cell-surface PDGF receptor by endocytosis (Amano et al. 2008). This leads to the inactivation of Rap1 and the activation of Rho kinase, which dissociates CD155 from focal complexes. The PDGF receptor is then re-recruited to the leading edge to start a new cycle of signalling.

An integral part of directional cell movement is the reorganisation of the microtubule network. The association of the cytoplasmic domain of CD155 with the tctex1, a component of the microtubule motor complex dynein, may supply a connection between the leading edge and microtubule network (Mueller et al. 2002).

### 1.6.5 CD155 In Contact Inhibition Of Movement And Proliferation

When cells come into contact with each other movement and proliferation cease. The loss of contact inhibition is frequently associated with cancerous and transformed cells. CD155 has an important function in both contact inhibition and the loss of contact inhibition (Minami et al. 2007b; Sloan et al. 2004; Sloan et al. 2005).

As CD155 is concentrated at the leading edge of moving cells meaning that initial interaction is mediated by CD155 and nectin-3 (Fujito et al. 2005; Ikeda et al. 2003). The initiation of contact also occurs when two independently moving cells meet; afadin in the leading edges recruits nectin-3 to the site of contact (Minami et al. 2007b; Sato et al. 2004). The initial binding of CD155 with nectin-3 is a transient interaction that leads to the downregulation of CD155 in a clatharin dependant manner. Nectin-3 remains at the cell surface forming stable interactions with other nectins initiating the formation of AJs (Sato et al. 2004; Satoh-Horikawa et al. 2000). The downregulation of CD155 disrupts the CD155-PDGF receptor- $\alpha_V\beta_3$ integrin complex resulting in a reduction in cell movement (Amano et al. 2008; Fujito et al. 2005). This together with the initiation of AJ formation causes the cell to arrest.

CD155 is also involved in the inhibition of proliferation following contact (Fujito et al. 2005). CD155 regulates cell proliferation by enhancing growth factor-induced activation of signalling pathways including Ras, Raf and ERK (Kakunaga et al. 2004). Downregulation of CD155 following interaction with nectin-3 prevents the enhancement of these pathways, reducing cell proliferation. The cytoplasmic tail of CD155 interacts with sprouty2, a negative regulator of growth (Kajita et al. 2007). When CD155 is

expressed on the cell surface the interaction between CD155 and sprouty2 prevents the phosphorylation of sprouty2. Following the downregulation of CD155, sprouty2 is released and phosphorylated by Src. Phosphorylated sprouty2 inhibits PDGF-induced Ras which in turn inhibits cell proliferation.

Cancerous cells lose contact inhibition leading to excessive proliferation and invasion. An upregulation of CD155 is a common feature of many primary tumours and transformed cell lines (Masson et al. 2001; Sloan et al. 2004). Upregulation of CD155 can make cell lines metastatic and knock down of CD155 can inhibit cancer development (Sloan et al. 2005). The loss of contact inhibition can partly be explained by the upregulation of CD155 in cancerous cells. The rate of *de novo* CD155 synthesis is greater than the rate of internalisation leading to a net increase of CD155 on the cell surface (Minami et al. 2007b). With the continuous high level cell surface expression of CD155 there is no inhibition of movement or proliferation signals resulting in a loss of contact inhibition.

### 1.6.6 CD155 In Immune Responses

In addition to its other roles, CD155 also interacts with the immune system (Maier et al. 2007). CD155 interacts with DNAM-1 (CD226) (Bottino et al. 2003; Tahara-Hanaoka et al. 2004) and CD96 (Tactile) (Fuchs et al. 2004; Seth et al. 2007) on immune cells triggering responses (Fuchs and Colonna 2006) (fig 1.5).

DNAM-1 is a transmembrane immunoglobulin-like adhesion molecule that was first identified as a T cell-specific activation marker (originally called TLiSA-1) (Burns et al. 1985) then subsequently identified as a marker of platelet activity as well (termed PTA-1) (Scott et al. 1989). DNAM-1 is expressed on NK cells, monocytes, T cells and a sub-set of B cells (Shibuya et al. 1996). The expression of DNAM-1 on monocytes and T cells can be modulated by cytokines via the transcription factors AP-1 and Ets-1 (Jian et al. 2006). DNAM-1 binds CD155 and nectin-2 (Bottino et al. 2003; Pende et al. 2005a; Tahara-Hanaoka et al. 2004) triggering NK cell cytotoxicity and enhances cytotoxic T lymphocytes cytotoxicity (Shibuya et al. 1996). Following ligation, the cytoplasmic tail of DNAM-1 is phosphorylated by the protein kinase C (Shibuya et al. 1998) activating the tyrosine kinase Fyn (Shibuya et al. 1996) and recruiting the actin binding proteins protein 4.1G and human discs large (Ralston et al. 2004). Subsequent downstream DNAM-1 signalling is dependent on the physical association of DNAM-1 with the integrin LFA-1 in lipid rafts (Ralston et al. 2004; Shibuya et al. 2003; Shirakawa et al. 2006).

Many cancerous cell lines and primary tumours constitutively over express CD155 which can be killed by NK cells (Tahara-Hanaoka et al. 2006). NK cells have been show to kill ovarian carcinoma cells, neuroblastoma cells, myeloid leukaemias and lymphoblastic leukaemias mediated CD155-DNAM-1 interaction (Carlsten et al. 2007; Castriconi et al. 2004; Pende et al. 2005b). This interaction is likely part of immunosurveillance for tumours. DNAM-1 is also involved in the differentiation of Th1 T cells (Dardalhon et al. 2005) and may protect against Fas ligand induced apoptosis (Tao et al. 2005).

The CD155-DNAM-1 interaction may also enhance the metastasis of cancerous cells (Morimoto et al. 2008). An interaction between CD155 on the cancerous cells and DNAM-1 on platelets results in the arrest of the cancerous cells in pulmonary vessels and subsequent entry into tissue (Morimoto et al. 2008). Depletion of platelets reduced the rate of metastasis into the lungs.

CD155 also interacts with CD96 (Fuchs et al. 2004). CD96 was first identified as a T cell activation antigen and originally called Tactile (T cell activation, increased late expression) (Wang et al. 1992). It is an Immunoglobulin superfamily member with homology to both CD155 and DNAM1 (Shibuya et al. 1996; Wang et al. 1992). CD96 is expressed on T cells and NK cells and binds CD155, but not nectin-2. Ligation of CD96 with CD155 enhances NK cell-mediated cytotoxicity. However, CD96 does not directly enhance killing, rather it increase the stability of the cell-cell contact (Fuchs et al. 2004). The increased stability of the cell-cell interaction allows for more efficient killing. Little is known about the intracellular signalling induced by ligation of CD96. The cytoplasmic tail contains a putative immune receptor tyrosine-based inhibitor receptor (ITIM), however, ligation of CD96 enhances rather then inhibits NK cell cytotoxicity (Fuchs et al. 2004).

## 1.7 AIMS

Interest in UL141 has focused on its role in suppressing cell surface expression of the powerful NK cell activating ligand CD155. However, CD155 has important roles in regulating cell motility, growth and in intercellular signalling. The downregulation of CD155 by UL141 has the potential to impact significantly on the biology of the host cell. This study sought to gain a greater appreciation of the role played by UL141 during productive HCMV infection. To this end I had the following aims:

1) To characterise the effects of gpUL141 expression on cell adhesion and motility.
2) To investigate the physical relationship between CD155 and gpUL141
3) To determine whether gpUL141 is a component of the HCMV virion

# 2 MATERIALS AND METHODS

## 2.1 SOLUTIONS

Ampicillin stock

Ampicillin (Sigma-Aldrich, Poole, UK) was dissolved in water at 50mg/ml and stored at -20°C.

Chloramphenicol stock

Chloramphenicol (Sigma-Aldrich) was dissolved in ethanol at 12.5mg/ml and stored at -20°C.

0.1% Crystal violet solution

0.1% (w/v) Crystal violet (BDH ltd. Poole, UK) was dissolved in phosphate buffered solution (PBS) and filtered through a 0.2μm filter.

DABCO

2% (w/v) 1,4-Diazabicyclo[2,2,2]octane (DABCO) (Sigma-Aldrich) and 10% PBS in glycerol (Fisher Scientific, Loughborough, UK)

DNA loading buffer

30% glycerol in de-ionised water with 0.25% (w/v) bromophenol blue (Sigma-Aldrich) in 0.25% (w/v) xylene cyanol FF (Sigma-Aldrich).

Freezing mixture

90% foetal calf serum (FCS) and 10% (v/v) dimethyl sulphoxide (DMSO) (Sigma-Aldrich)

IPTG Stock

23.8mg Isopropyl β-D-1-thiogalactopyranoside (IPTG) (Melford, Ipswich) dissolved in 1ml water to generate a 100mM stock solution.

Kanamycin stock

Kanamycin (Roche, Mannheim, Germany) was dissolved in water at 50mg/ml and stored at -20°C.

Luria Bertani (LB) agar

As for LB broth but with 1.5% (w/v) agar (Fisher Scientific) added before autoclaving. Antibiotics were added before setting in plates.

LB broth

1% (w/v) tryptone, 1% (w/v) sodium chloride (Sigma-Aldrich) 0.5% yeast extract (Sigma-Aldrich) dissolved in water then autoclaved.

LB sucrose selection plates

1% (w/v) tryptone, 0.5% (w/v) yeast extract (Sigma-Aldrich), 5% (w/v) sucrose 1.5% (w/v) agar (Sigma-Aldrich) dissolved in water then autoclaved. 1:1000 chloramphenicol stock, 1:500 X-gal stock and 1:500 IPTG stock were added before setting in plates.

20% NP40 5% deoxycolate stock

20% (v/v) NP-40 alternative (Calbiochem, California, USA) and 5% (w/v) sodium deoxycholate (Sigma-Aldrich) dissolved in sodium phosphate buffer.

PBS

One PBS tablet (Oxoid, Hampshire, UK) was dissolved per 100ml water to generate buffer containing 8% (w/v) sodium chloride, 0.2% (w/v) potassium chloride, 1.15% (w/v) disodium hydrogen phosphate and 0.2% (w/v) potassium dihydrogen phosphate at pH7.3.

PBST

PBS with 0.1% Tween-20 (Fisher Scientific)

10% SDS stock

10% (w/v) sodium dodecyl sulphate (SDS) (Fisher Scientific) dissolved in sodium phosphate buffer

SDSPAGE sample buffer

0.225M tris(hydroxymethyl)aminomethan (Tris)-Cl, pH6.8, 50% (v/v) glycerol, 5% (w/v) SDS, 0.05% (w/v) bromophenol blue, 50mM dithiothreitol (Sigma-Aldrich) and 1% (v/v) 2-mercaptoethanol (Sigma-Aldrich) were made to 10ml with water.

Semi-dry transfer buffer

48mM Tris, 39mM glycine (Sigma-Aldrich), 1.3mM SDS and 200ml methanol made up to 1l with water.

35% Sodium-tartrate buffer

35% (w/v) sodium tartrate (Sigma-Aldrich) dissolved in sodium phosphate buffer.

15% Sodium-tartrate/ 30% glycerol buffer

15% (w/v) sodium tartrate dissolved in 30% (v/v) glycerol and sodium phosphate buffer.

Sodium phosphate buffer

4.8g sodium dihydrogen phosphate (BDH Ltd, Poole, UK) was dissolved in 1l water to generate a 0.04M solution. 5.7g disodium hydrogen phosphate (Sigma-Aldrich) was dissolved in 1l water to produce a 0.04M solution. The solutions were mixed to produce a buffer with final concentrations of 7.6mM sodium dihydrogen phosphate and 0.032M disodium hydrogen phosphate.

TAE (50x)

242g Tris base, 57.1ml glacial acetic acid (Fisher scientific) and 100ml 0.5M ethylenediaminetetraacetic acid (EDTA), pH8.0 were mixed with water in a final volume of 1l.

0.7% TAE agarose gel

0.7g agarose (Invitrogen) dissolved in 100ml TAE buffer by heating, then poured into a mould and left to set at room temperature.

Tris Buffer

10ml of 1M Tris-Cl pH7.4 was mixed with 2ml 0.5M EDTA, pH8.0 with water added to a final volume of 1l.

1M Tris-Cl

121.1g Tris base was dissolved in 1l water and adjusted to desired pH with hydrogen chloride.

0.5% Triton X-100

0.5% (v/v) Triton X-100 (Sigma-Aldrich) was dissolved in water.

X-gal stock

5-bromo-4-chloro-3-indoyl-β-D-galactopyranoside (X-gal) (Melford, Ipswich) was dissolved in N,N-dimethyl formamide (DMF) (Sigma-Aldrich) to generate a 40mg/ml stock solution. Aliquots were stored at -20°C.

## 2.2 CELL CULTURE

### 2.2.1 Cells

Human foreskin foetal fibroblasts (HFFF) (kindly supplied by Dr G. Farrar, Porton Down) were immortalised with human telomerase reverse transcriptase by S Llewellyn-Lacey as described in McSharry *et al* (2001). HFFF were maintained in 175cm$^2$ tissue culture flasks in DMEM-10. 293 cells (kindly provided by F Graham, McMaster University), 293 cells stably expressing gpUL141GFP and GFP (293-UL141GFP and 293-GFP, kindly provided by Dr P Tomasec (Tomasec et al. 2005), 293-TREx cells (Invitrogen), human Caucasian glioblastoma-astrocytoma U373 (kindly provided by Dr M. Wills, Cambridge University), and U373 cell lines stably expressing CD155YFP (kindly provided by Prof. G Wilkinson) were maintained in 175cm$^2$ tissue culture flasks. All cell lines were grown in incubators at 37°C in 5% $CO_2$.

### 2.2.2 Passage Of Cell Lines

Confluent monolayers of adherent cells were passaged by removing medium, washing with PBS then incubating the monolayer with an appropriate volume of trypsin/EDTA (Invitrogen) until the cells detached. An equal volume of fresh DMEM-10 was then added to inhibit the trypsin and the cells were split between 1:2 and 1:5 with fresh DMEM-10 and added to a 175cm$^2$ tissue culture flask.

### 2.2.3 Transfection Of DNA

#### 2.2.3.1 Transfection With Effectene

Cells were transfected with Effectene transfection reagent (Qiagen, Sussex, UK) according to the manufacturer's protocols. This technique gave high transfection efficiency for 293 and U373 cells (greater than 80% efficiency) but was less efficient transfecting fibroblasts (less than 10% efficiency). Plasmids used for transfections are described in table 2.1. Cells seeded at 40 to 80% confluency in 6 well tissue culture plates were used for transfection. 0.4μg of DNA was diluted in EC buffer to a total volume of 100μl then 3.2μl of enhancer was added. Following brief mixing and incubation at room temperature for 5 minutes, 10μl of Effectene transfection reagent was added. The DNA-Effectene reagent mixture was incubated for a further 5 minutes then mixed with fresh DMEM-10 and added to the cells. The cells were then incubated for three days at 37°C for three days then used in the appropriate assay.

**Table 2.1. Transfection vectors**

| Name | Background | Generated by | Official Designation |
|---|---|---|---|
| pEYFP-N1 | n/a | Clontech (California, USA) | pAL 839 |
| pECFP-N1 | n/a | Clontech (California, USA) | pAL 295 |
| pCD155YFP | pAL 839 | D. Cochrane | pAL 880 |
| pCD155CFP | pAL 295 | D. Cochrane | pAL 881 |
| pUL141YFP | pAL 839 | D. Cochrane | pAL 882 |
| pUL141CFP | pAL 295 | D. Cochrane | pAL 883 |

### 2.2.3.2 Transfection With Nucleofector

For higher efficiency of fibroblast transfection Amaxa basic Nucleofector kit for primary mammalian fibroblasts (Lonza, Cologne, Germany) was used according to the manufacturer's protocol. Recently passaged fibroblasts at approximately 80-90% confluency were detached from the growth substrate with trypsin and resuspended in fresh DMEM-10. $1x10^6$ cells per transfection were then centrifuged at 90g for 10 minutes at room temperature then resuspended in 100µl per transfection of Nucleofector solution. 100µl of the cell suspension was mixed with 2µg of DNA and added to a Nucleofector cuvette. The cuvette was then place in a Nucleofector II device and electroporated on program T016. Following electroporation the cuvette was removed from the device and free pre-warmed media was added to the cell suspension then transferred to a six well tissue culture plate. The cells were then incubated for three days at 37°C for three days then used in the appropriate assay.

### 2.2.4 Lentivirus Vector Delivery To Human Fibroblasts

Confluent fibroblasts in 12 well tissue culture plates were infected with one of five lentiviral vectors expressing CD155 specific shRNAs (Sigma) or with a lentiviral vector expressing scramble RNA (Sigma) for 20 hours in a minimal volume of DMEM-10 with 8µg hexadimethrine bromide at MOIs of 1, 5 and 10. The virus was then removed from the cells and fresh media was added. After incubation for 3 days the media was replaced with fresh DMEM-10 containing 2.5mg/ml puromycin (Sigma-Aldrich). The lentivirus-

infected fibroblasts were monitored daily with fresh DMEM-10 puromycin added every three days. During recovery the cell lines were expanded from one well of a 12 well tissue culture plate to a 25cm$^2$ tissue culture flask. They were then assayed for CD155 expression by FACS then cryopreserved.

### 2.2.5 Cryopreservation Of Cell Lines

Adherent cells in log phase growth were treated with a minimal volume to cover the monolayer, e.g 1ml for a 25cm$^2$ flask of trypsin/EDTA for 5 minutes at room temperature until the cells detached from the tissue culture flask. The cell were recovered by centrifugation at 400g for 5 minutes then resuspended in freezing mixture (90%FCS 10%DMSO). 1ml aliquots were transferred to cryovials and placed in a Nalgene 5100 cryo 1°C freezing container (Merck, West Drayton, UK) containing isopropanol at room temperature. The freezing container was stored at -70°C overnight then the cryovials were transferred to liquid nitrogen for storage.

To resurrect cells from liquid nitrogen storage, they were rapidly thawed, resuspended in DMEM containing 50% (v/v) FCS the centrifuged at 400g for 5 minutes. The cells were resuspended in DMEM-10 then centrifuged at 400g for 5 minutes. The cells were then resuspended in DMEM-10 and transferred to a 25cm$^2$ tissue culture flask and incubated at 37°C.

### 2.2.6 Cell Counting

A 10µl aliquot of cells was diluted 1:1 with Trypan blue (Sigma-Aldrich) and counted on a glass haemocytometer (Sigma-Aldrich) under white light. Viable cells were identified by the exclusion of Trypan blue. Cells were counted in the four outer grid regions of the haemocytometer and the number of cells per ml was determined using the following equation:

Number of cells/ml = [(Total number of cells counted) x $10^4$ x 2] / 4

## 2.3 VIRUSES

### 2.3.1 Propagation Of HCMV

HCMV strain Merlin, strain AD169, HCMVUL32GFP and HCMVΔUL141 were all grown in fibroblasts. HFFFs were cultured in 175cm$^2$ tissue culture flasks until they reached 70% confluence. They were then infected with virus at a MOI of 0.1 in 5ml of DMEM and rocked for 4 hours at 37°C. After the incubation the media was replaced with 25ml of fresh 10% FCS DMEM and incubated at 37°C. The cells were monitored for cytopathic effects (cpe) daily and the media was renewed weekly. When extensive cpe was apparent through the monolayer, media was removed to storage at -70°C and fresh media was added to the cells. During the following days, the growth media continued to be replaced and stored every two days until the infected cells disintegrate.

To prepare HCMV virions the aliquots of supernatant were defrosted and cell debris was removed by centrifugation at 600g for 10 minutes. The supernatant was pooled and then spun at 23000g for 2 hours to pellet the virus. Following centrifugation the supernatant was discarded and the pellet was resuspended in DMEM. To reduce aggregation of the viral particles the resuspended pellet was aspirated repeatedly through a 21G needle. The resuspended virus pellet was then frozen at -70°C in 100μl aliquots.

### 2.3.2 Propagation Of Recombinant Adenovirus (Rad) Stocks

RAd stocks were propagated in 293 cells. RAd viruses used are shown in table 2.2 along with their formal designations in the laboratory. 293 cells were grown to 70% confluency in a 175cm$^2$ tissue culture flask, infected with virus at a moi of 0.1 in a minimal volume of media then incubated overnight in a rocking incubator at 37°C. The following day the virus was removed and replaced with fresh DMEM-10. Cells were monitored for cpe and the media was replaced as needed. When 100% of cells exhibited cpe, they were detached from the flask by gentle tapping and resuspended in DMEM. Infected cells were recovered by centrifugation at 900g for 5 minutes and the cell pellet resuspended in PBS. Arklone P was then added to the cells at a 1:1 ratio and mixed vigorously before centrifugation at 900g for 5 minutes. The aqueous phase containing the virus was removed, aliquoted and stored at -70°C.

**Table 2.2. Recombinant Viruses**

| Name | Background | Generated by | Official Designation |
|---|---|---|---|
| **RAd** | | | |
| RAd control | AdEasy | P. Tomasec | RAd 592 |
| RAdGFP | AdEasy | P. Tomasec | RAd 502 |
| RAdUL141 | AdEasy | P. Tomasec | RAd 587 |
| RAdUL141GFP | AdEasy | P. Tomasec | RAd 522 |
| RAdCD155mCh | AdZ | B. McSharry | RAd 1225 |
| RAdUL141CFP | AdZ | D. Cochrane | RAd 1281 |
| | | | |
| **HCMV** | | | |
| HCMVUL32GFP | Merlin | R. Stanton | RCMV 1172 |
| HCMVΔUL141 | Merlin | V. Prod'Homme | RCMV 1149 |

### 2.3.3 Titration Of Virus Stocks

HCMV and RAd virus stocks were titrated using a limited dilution assay. Confluent HFFFs (for HCMV titration) or 293 cells (for RAd titration) were trypsinised and added to 24 well tissue culture plates (HCMV) or 96 well plate (RAd) and allowed to adhere overnight. Cells were plated to 80% confluency. Serial dilutions between $10^{-2}$ and $10^{-10}$ of the virus stocks were made in DMEM-10 and 1ml (HCMV) or 100µl (RAd) of each dilution was added to 10 wells. Following incubation for 24 hours, all media was replaced. The cells were monitored for cpe and the media was replaced as necessary. After 4 weeks for HCMV, or 10 days for RAd, cpe was marked in each well. The virus titre was calculated as tissue culture infectious dose ($TCID_{50}$) using the Reed-Muench formula:

$$TCID_{50} = log_{10}\text{dilution} \left( \frac{\%\text{ infection at next dilution above 50\% - 50}}{(\%\text{ infection dilution above 50\% - \% infection dilution below 50\%})} \right)$$

$TCID_{50}$ units were converted into pfu/ml for convenience using the accepted conversion factor of 1 $TCID_{50}$ = 0.7 infectious units (Davis 1990).

### 2.3.4 HCMV purification

HCMV virus particle were purified by ultracentrifugation over a continuous sodium tartrate gradient. HCMV was grown as described in section 2.3.1 and the clarified supernatant was recovered by centrifugation for 2 hours at 4°C then the pellet was

resuspended in sodium phosphate buffer. The gradients were made in ultra clear ultracentrifuge tubes (Beckman Coulter, California, USA) by combining 4ml 35% sodium-tartrate and 5ml 15% sodium tartrate/30% glycerol in a gradient mixer. The resuspended pellet was then layered over the gradients and balanced to 100mg. The gradients were then centrifuged for 45 minutes at 4°C. Following centrifugation the virus particle band was removed from the gradient with a 20G needle, washed in sodium phosphate buffer at for 1 hour at 4°C then resuspended in 100µl sodium phosphate buffer and stored at -80°C. For flow cytometry experiments the virus was first inactivated by irradiated with a 22 TBq caesium-137 source for 24 hours.

### 2.3.5 Fractionation of HCMV

Purified HCMV particles were separated into detergent soluble and insoluble fractions using a procedure adapted from (Adair et al. 2002). Purified virions were incubated at 4°C with 1% Triton X-100 for 30 minutes. The insoluble component was recovered by centrifugation at 18000g for 30 minutes, then resuspended in sodium phosphate buffer. Both fractions were stored at -70°C before use in western blotting.

An alternative detergent extraction buffer (Wang et al. 2004c) was also used to fractionate the virions. Purified virions were incubated with 1% NP-40 and 0.5% deoxycholate for 30 minutes at room temperature. At 5 minute intervals the sample was vigorously mixed to ensure separation of the viral envelope. After the incubation the insoluble fraction was recovered by centrifugation at 18000g for 30 minutes before being

resuspended in sodium phosphate buffer. Both fractions were stored at -70°C before use in western blotting.

### 2.3.6 Infection Of Cells For Assays

RAd were routinely delivered to HFFF, U373 cells and 293 cells, while HCMV infections were done in HFFF cells. Table 2.2 lists the viruses used as well as their official laboratory designations. Confluent 175cm$^2$ tissue culture flasks of the appropriate cell line were trypsinised, resuspended in DMEM-10, seeded into 25cm$^2$ tissue culture flasks or 6 well tissue culture plates then incubated overnight at 37°C.

When the cells had reach 70-80% confluency the media was removed and an appropriate volume of virus was added in a minimal volume. The cells were then incubated for 2-4 hours in a rocking incubator at 37°C. The inoculum was then removed and replaced with fresh pre-warmed DMEM-10 then incubated for three days at 37°C before use in the relevant experiment.

Multiplicity of infection for RAd infections were 50, 100 and 150 pfu/cell and for HCMV was 5 and 10 pfu/cell. RAds were titred on permissive 293 cells, which express high level of the Coxsackie adenovirus receptor (CAR). HFFFs express extremely low levels of CAR and are ~10 fold less susceptible to RAd infection. In order to provide for efficient virus delivery, it is necessary to use 10 fold more virus. All virus infections

included an independent negative control; RAd control for RAd infections and mock infection (media only) control for HCMV infections.

## 2.4 MOLECULAR BIOLOGY

### 2.4.1 PCR

PCR reactions were carried out using Expand high fidelity PCR system (Roche) with 1µl of the manufacturers supplied buffer, 0.5µl dNTP (10mM) and 0.5µl of each primer (100pmol/ml) (made to order from Invitrogen). The following thermocycling reaction was used:

95°C for 2 minutes

95°C for 30 seconds

58°C for 30 seconds 35 cycles

72°C for 90 seconds

### 2.4.2 Agarose Gel Electrophoresis

Separation of DNA fragments by size was performed by electrophoresis in 0.7% w/v agarose TAE gel. DNA samples were mixed with DNA loading buffer then transferred into wells. The gel was then run at 75V for approximately 1 hour, depending on resolution required. The gel was then stained with ethidium bromide buffer for ten minutes, washed with water then visualised under UV light in an Autochemi system (UVP Bioimaging systems, Cambridge, UK).

### 2.4.3 Isolation Of DNA From Agarose Gel

DNA was isolated from agarose gels using a GFX PCR DNA and Gel Band Purification Kit (GE healthcare, Buckinghamshire, UK) following the manufacturers protocol. The kit works on the principle that DNA will bind to a glass fibre matrix in high salt concentration while protein and salt contaminants do not. The DNA is eluted from the glass fibre matrix column by washing with a low salt concentration buffer.

### 2.4.4 Plasmid DNA Minipreps

Small scale plasmid preparations were performed using a QIAprep Spin Miniprep Kit (Qiagen). The kit is based on alkaline lysis of bacterial cells followed by the binding of DNA onto a silica column in the presence of high salt concentration. Bacteria containing the plasmid of interest were cultured in 5ml of LB overnight then recovered by centrifugation at 10000g for 5 minutes. The bacteria were resuspended in 250µl of manufacturer's P1 buffer then of then lysed in buffer P2 (250µl). After 5 minutes the neutralisation buffer N3 (350µl) was added to allow denatured DNA to reanneal; bacterial cell debris and precipitated chromosomal DNA was then cleared by centrifugation at 18000g for 10 minutes. The supernatant was then decanted into a silica column, which was then centrifuged at 18000g for 60 seconds. The column was washed with the manufacturers' buffer PB then the DNA was eluted from the column in 50µl Tris buffer. DNA was stored at -20°C until required.

### 2.4.5 Plasmid Purification By Maxiprep

Large scale plasmid purification was performed using QIAfilter Plasmid Maxi Kit (Qiagen). The principles of the kit are similar to those of the miniprep kit described above. The protocol is based on the alkaline lysis of bacteria cells followed by the binding of plasmid DNA to an anion exchange resin under low salt conditions. RNA and protein contaminants are washed from the resin under medium salt concentration while the plasmid DNA is eluted with high salt buffer. The DNA is then desalted by isopropanol precipitation.

A starter culture of 5ml of LB medium was inoculated with the bacteria containing the plasmid of interest. After 8 hours of incubation at 37°C with vigorous shaking, 25ml of LB medium was inoculated with 25µl of the starter culture. This main culture was then incubated overnight at 37°C with vigorous shaking. The bacteria cells were then harvested by centrifugation at 6000g for 15 minutes at 4°C then resuspended in 4ml of the manufacturers P1 buffer. The cells were then lysed by the addition of an equal volume of the manufacturer's P2 buffer then incubated at room temperature for 5 minutes. The lysate was then neutralised by the addition of P3 buffer (4ml), and cleared by passing through a filter cartridge into the resin column. Once the lysate has entered the resin by gravity flow it was washed twice with 10ml of the manufacturers QC buffer under gravity flow. The DNA is then eluted from the resin with 5ml of the manufacturer's QF buffer and then precipitated by mixing with 3.5ml isopropanol and

centrifuging at 15000rpm for 30 min at 4°C. The precipitated DNA was then washed twice with 70% ethanol, allowed to air dry then redissolved in Tris buffer. To determine the yield of the maxiprep purification the DNA concentration was determined by UV spectrophotometry at 260nm and by analysis on an agarose gel.

### 2.4.6 Restriction Enzyme Digestion

Restriction enzymes used in this study were *Bam*HI (Promega, Wisconsin, USA), *Age*I, (NEB, Massachusetts, USA) and *Hin*dIII (NEB, Massachusetts, USA). All digestions were carried out according to the manufacturers' instructions. Reactions consisted of DNA template, 5µl 10x reaction buffer (NEB) and de-ionised water to a total volume of 50µl. Restriction enzyme digests were incubated for 2-16 hours at 37°C. Following digestion, DNA fragments were separated by agarose gel electrophoresis (section 2.4.2) and purified by GFX PCR DNA and Gel Band Purification Kit (GE lifesciences) (section 2.4.3).

### 2.4.7 DNA Ligation

To clone DNA sequences, linearised vector and insert were mixed with 1µl T4 DNA ligase enzyme and 1µl 10 x ligase buffer (NEB) in a total volume of 10µl. The reaction was incubated for 1 hour at 16°C. After the incubation, the DNA was purified by GFX

PCR DNA and Gel Band Purification Kit or ethanol/sodium acetate precipitation then used to transform bacteria.

### 2.4.8 Ethanol/Sodium Acetate Precipitation Of DNA

Ligation reactions and restriction nuclease digestion products were purified by ethanol/sodium acetate precipitation. 10% (v/v) sodium acetate (Invitrogen) was added to the sample in a total volume of 10µl. 250µl of ethanol was added and the sample was centrifuged at 18000g for 30 minutes. The supernatant was removed and the pellet washed twice in 70% (v/v) ethanol. The purified DNA was then resuspended in an appropriate volume of Tris buffer or water.

### 2.4.9 Transformation of *E.coli*

Plasmids were transformed into the electrocompetent *E.coli* TOP10 (Invitrogen) by electroporation. Briefly, 1µl DNA was mixed with an aliquot of *E.coli* TOP10 and incubated at 4°C for 15 minutes then transferred to a 0.2cm electroporation cuvette. The bacteria were then electroporated at 2.5kV using an electroporator (BioRad Gene Pulser). The bacteria we then allowed to recover in LB for 2 hour at 37°C. After recovery, the bacteria were plated on selective LB agar plates and incubated overnight at 37°C.

### 2.4.10 Glycerol Stock

*E. coli* containing plasmids of interest were stored as glycerol stocks. 500µl of an overnight bacteria culture was mixed with 500µl of 80% (v/v) glycerol in a cryovial and stored at -70°C.

### 2.4.11 DNA Sequencing

Inserts were sequenced using BigDye 3.1 terminator cycle sequencing kit (PerkinElmer, Boston, USA) and dideoxy terminator cycle sequencing. The reaction mixture consisted of DNA sample, 4µl reaction mix, 1µl sequencing primer (see table 2.3 for primer sequences) in a total volume of 10µl. The following thermal cycling conditions were used:

95°C for 30 seconds

50°C for 15 seconds 25 cycles

60°C for 4 minutes

Following the thermocycling reaction, the products were precipitated by sodium acetate/ethanol precipitation and the sequencing products separated on an ABI model 377 sequencer (Applied Biosystems, Foster City, USA) by a dedicated technician at Central Biotechnology Services (Cardiff University)

**Table 2.3. PCR primer sequences**

| Name | Sequence | Notes | Produced by |
|---|---|---|---|
| CD155 5prime | CATGAAGCTTAGCTGCT CGGAGCAACTGGCAT | *HindIII* site added | Invitrogen (Paisley, UK) |
| CD155 3prime | GATCACCGGTGCCCTTG TGCCCTCTGTCTGTGGA | *AgeI* site added | Invitrogen (Paisley, UK) |
| CD155 seq1 | TTCGGGTTGCGCGTAGA GGA | CD155 sequencing primer | Invitrogen (Paisley, UK) |
| CD155 seq2 | ATTGGAGCACGACCAT GG | CD155 sequencing primer | Invitrogen (Paisley, UK) |
| CD155 seq3 | CAGAAGGTCCAGCTCA CTGG | CD155 sequencing primer | Invitrogen (Paisley, UK) |
| UL141 5prime | CATGAAGCTTAGATCAT GTGCCGCCGGGAGTCG | *HindIII* site added | Invitrogen (Paisley, UK) |
| UL141 3prime | GATGGATCCAGCCTCTT CATCTTTCTAACACC | *BamHI* site added | Invitrogen (Paisley, UK) |

### 2.4.12 Cloning Using The AdZ Vector.

The Ad recombinant RAdUL141CFP was produced in a novel vector system that exploits DNA recombineering technology (Stanton et al. 2008). The AdZ vector consists of the entire genome of a replication-deficient Ad5 vector inserted into a single copy prokaryotic BAC (bacterial artificial chromosome) plasmid (fig 2.1). Dual selectable markers (ampicillin resistance and sucrose sensitivity) within an HCMV major IE promoter expression cassette are present in the E1 locus. The AdZ vector is maintained in *E. coli* SW102, which carries an integrated copy of the lambda red genes. The red genes promote DNA recombination between short arms of homology, and their expression can be transiently induced by heat-shock. The transgene, generated with short arms of homology (usually by PCR) overlapping the HCMV IE promoter expression cassette, is transformed directly into *E. coli* SW102 as linear DNA. Expression of the red genes is induced; enabling the transgene to be inserted under the control of the IE promoter by homologous recombination (recombineering). Recombinants are selected by loss of the dual selectable markers, and the resultant BAC transfected into 293 cells to produce the recombinant virus.

### 2.4.13 PCR

The UL141CFP ORF was amplified from pUL141CFP using primers with 80 nucleotide 5` homology to the AdZ vector. The reaction was performed using Expand Hi-Fi

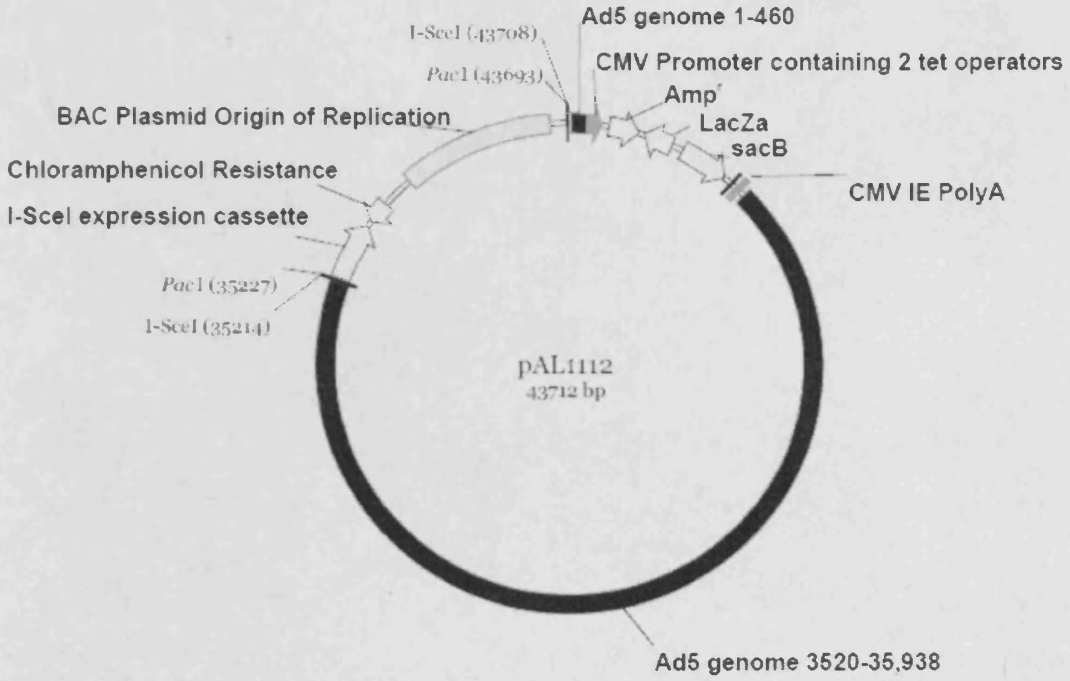


**Figure 2.1. AdZ vector map.**
The AdZ vector contains the Ad5 vector deleted for E1 and E3 regions in a single copy vector. It contains a selection cassette encoding ampicillin resistance, *lacZα* and *sacB* (sucrose sensitivity) between the CMV promoter and the CMV IE PolyA. Inserts are generated with arms of homology to the promoter and PolyA replacing the selection cassette. Adapted from (Stanton et al. 2008).

polymerase (Roche) in the manufactures buffer (containing Mg), 50 pmol primer and nucleotides. The reaction conditions were as described in section 2.4.1.

The sequences of the primers used were (arms of homology in normal text, UL141 specific sequence in bold):

5` UL141 primer

5`AACCGTCAGATCGCCTGGAGACGCCATCCACGCTGTTTTGACCTCCATAGA

AGACACCGGGACCGATCCAGCCTGGATCC**ATGTGCCGCCGGGAGTCG-3'**

3` UL141 Primer

GGCGTGACACGTTTATTGAGTAGGATTACAGAGTATAACATAGAGTATAATA

TAGAGTATACAATAGTGACGTGGGATCC**TTACTTGTACAGCTCGTCCA**

Following the reaction the product was gel purified using GFX PCR DNA and Gel Band Purification Kit (GE lifesciences) as described in section 2.4.3.

### 2.4.14 Transformation of Bacteria

An overnight starter culture of SW102 bacteria containing the AdZ vector was grown in 5ml of LB containing ampicillin and chlorampenicol at 32°C. 0.5ml of the starter culture was then inoculated into 25ml LB containing ampicillin then incubated at 32°C in a shacking incubator. The absorbance at 600nm was monitored until it reached a value of 0.6. At this point the culture was transferred to a water bath and incubated at 42°C for 15

minutes to induce the lambda red genes. The culture was then transferred to ice and cooled for 15 minutes then centrifuged for 5 minutes at 0°C. The bacteria cells were resuspended in ice-cold water and centrifuged again. Following the final centrifugation the pellet was resuspended in a minimal volume of water and transferred to Eppendorf tubes in 25µl aliquots. 3µl of the purified PCR product was added then the bacteria and PCR product transferred to a pre-chilled 0.2cm cuvette and electroporated at 2.5kV. The electroporated bacteria were transferred into 5ml LB, incubated for 4 hours to allow for recovery. A 50µl aliquot was plated on L-agar sucrose containing sucrose and X-gal, and incubated for 48 hours at 32°C. Following incubation, white colonies that grew in the presence of sucrose were selected for screening.

### 2.4.15 Preparation of BAC DNA

The standard miniprep protocol (described in section 2.4.4) does not produce sufficient AdZ DNA; this is because the vector is based on a single copy BAC vector. To maximise DNA yields, a modified miniprep spin (Qiagen) protocol was used. A white colony from the sucrose selection plate was selected and grown overnight in 5ml chloramphenicol LB at 32°C in a shacking incubator. The bacteria cells were recoverred by centrifugation at 18000g for 5 minutes then resuspended in 250µl buffer P1. 250µl buffer P2 was then added to lyse the cells. After 5 minutes, 250µl buffer N3 was added to neutralise the lysis reaction. This solution was centrifuged at 18000g for 10 minutes, the supernatant transferred to a fresh Eppendorf tube and DNA precipitated by the addition of 750µl 70% isopropanol. Following centrifugation at 18000g for 10 minutes

the DNA was washed with 70% (v/v) ethanol, air dried and finally resuspended in 30µl of buffer EB.

To test whether the desired recombination event had occurred, the vector DNA was digested with *Bam*HI (Promega). 8µl of miniprep purified plasmid DNA was incubated at 37°C for one hour with 1µl of the recommended buffer and 1µl *Bam*HI (NEB). The entire reaction was then separated on an agarose gel as described in section 2.4.2. The AdZ vector produces seven bands when digested with *Bam*HI, however two are from in the selection cassette. If these bands, 2.5kbp and 1.7kbp, are not present then recombination has occurred.

### 2.4.16 Sequencing

The sequencing reaction consists of 5µl DNA, 1µl primer (3.2pmol/µl) and 4µl BigDye 3.1 (Perkin-Elmer). The sequence of the primers used were; 5'-AATGTCGTAACAACTCCG-3' and 5'-ACCTGATGGTGATAAGAAG-3'. The reaction conditions were as follows:

95°C for 5minutes
95°C for 30 seconds
55°C for 10 seconds 100 cycles
60°C for 4 minutes

The reaction products were cleaned using Performa DTR columns (EdgeBio, Maryland, USA) according to manufacturer's instructions. Briefly, the product is added to the column and centrifuged. The gel filtration matrix removes dye terminators and salts purifying the PCR products. The products were then sequenced as described in section 2.4.11.

### 2.4.17 Maxiprep

NucleoBond BacMAX 100 kit (Clontech) was used for large scale purification of AdZ vector DNA. This kit is based on a modified alkaline/SDS lysis procedure followed by potassium acetate precipitation of chromosomal DNA. Plasmid is first bound to an anion exchange resin, which is then washed then the plasmid DNA is eluted. A single bacterial colony was inoculated into a 5ml starter culture and incubated for 6 hours at 32°C in a shaking incubator. The starter culture was then diluted into 250ml LB and incubated overnight at 32°C. The bacteria were harvested by centrifugation at 5000g for 15 minutes at 4°C then resuspended in 24ml of buffer S1(Clontech). 24ml of the manufacturers buffer S2 is then added to lyse the cells. After three minutes, pre-cooled buffer S3 is added to the cells to neutralise the reaction. The bacteria suspension was then clarified by centrifugation at 12000g for 15 minutes at 4°C then by filtration. The cleared lysate was then loaded onto an equilibrated NucleoBond column containing the anion exchange resin. The column was then washed twice with 18ml of the manufacturer's buffer N3 then the DNA was eluted by the addition of 15ml buffer N5 pre-heated to 50°C to the column. The plasmid DNA was then precipitated with

isopropanol washed with 70% (v/v) ethanol then resuspended in 100µl 10mM Tris pH8.5. DNA concentration was measure by absorbance at 260nm.

### 2.4.18 Generation of RAd Virus

RAd were generated by transfecting the AdZ vector into 293TREx cells using Polyfect (Qiagen). 293TREx cells were seeded in a 25cm$^2$ tissue culture flask and incubated overnight at 37°C. 4µg of the AdZ BAC DNA was diluted to 100µl with DMEM, then 40µl of Polyfect reagent added and the sample incubated 10 minutes. The volume was made up to 1ml with DMEM-10 before the transfection mix was added directly to 293TREx cells. After 24 hours at 37°C, the media was removed, discarded and replenished with fresh DMEM-10. Cells were monitored for cpe, and stocks made from resulting virus 2.3.2 and 2.3.3.

## 2.5 WESTERN BLOTTING

Proteins separated by SDSPAGE were detected by western blotting. Pre-set 10% Nupage Novex acrylamide gels were used in conjunction with the Nupage electrophoresis equipment (Invitrogen). MOPS or MES buffer was used for electrophoresis, depending on the required resolution. To prepare cell extracts, monolayers were washed once with PBS, removed from the tissue culture flask by mechanical scraping and resuspended in 10 ml PBS. Cells were centrifuged at 400g for 5 minutes, washed again in 10 ml fresh PBS Before being resuspended in 100µl SDSPAGE sample buffer. To prepare virus samples, irradiated purified HCMV virions (described in section 2.3.4) or detergent treated virion fractions (described in section 2.3.5) were diluted 1:4 in 4xSDSPAGE sample buffer.

Samples were then denatured at 99°C for 10 minutes before loading 7-10µl of the samples into the wells of the acrylamide gel, alongside a 5µl sample of Novex sharp standard pre-stained markers (Invitrogen). Proteins were separated by SDSPAGE at 150V for 1-2 hours, depending on the resolution required and running buffer used. Proteins were transferred to nitrocellulose membrane (GE Biosciences, UK) by semi-dry transfer. Blotting paper and nitrocellulose membrane were pre-soaked in transfer buffer then layered onto the transfer apparatus (TransferBlot SD, BioRad, Heucules, California, USA) with a sheet of blotting paper on the negative electrode, then the nitrocellulose on top. The gel was then removed from the electrophoresis equipment and layered over the nitrocellulose membrane. A final sheet of blotting paper was layered on top of the gel.

After ensuring that all air bubbles were removed the transfer apparatus was assembled and the proteins were transferred by semi-dry transfer for 1 hour at 10V.

Following the transfer the nitrocellulose membrane was removed from the transfer apparatus. The position of the pre-stained markers were marked on the membrane using an Antigen-Antibody (mouse) Pen (Alpha Diagnostics, USA) before the membrane was blocked with 5% (w/v) milk powder/PBST for 1 hour at room temperature or overnight at 4°C. After the incubation the blot was washed for 30 minutes with an appropriate volume of PBST, the PBST being replaced three times then an appropriate dilution of primary antibody in 5% (w/v) milk powder/PBST was added to the membrane for 1 hour at room temperature or overnight at 4°C. Table 2.4 shows the primary antibodies and the dilutions used. The blot was then washed with PBST as above, then goat anti-mouse horse-radish peroxidase conjugated monoclonal antibody (BioRad) diluted 1:1000 in 5% (w/v) milk powder/PBST added to the blot and incubated for 1 hour at room temperature. Blots were washed a final time in PBST before incubation with the horse-radish peroxidase chemiluminescent substrate (Thermo Scientific, Waltham, Massachusetts, USA) for 5 minutes. The blots were analysed with Chemidoc chemilumenescence imaging system (UVP, Cambridge).

To re-probe a blot they were washed three times in PBST then incubated with ReStore (Pierce, Rockford, USA) for 2 hours before being washed a further three times in PBST. The stripped blots were re-blocked with in 5% (w/v) milk powder/PBST for 1 hour at room temperature or overnight at 4°C then the staining was carried out as described above.

**Table 2.4. Primary antibodies used for western blots**

| Antibody | Dilution | Isotype | Company |
|---|---|---|---|
| α-CD155 | 1:5000 | Mouse IgG1 | Abcam (Cambridge, UK) |
| α-gB | 1:5000 | Mouse IgG1 | Abcam (Cambridge, UK) |
| α-IE-1 | 1:6000 | Mouse IgG2a | Chemicon (Massachusetts, USA) |
| α-pp65 | 1:6000 | Mouse IgG1 | Abcam (Cambridge, UK) |
| α-UL14 | 1:2000 | Mouse IgG1 | In house |
| α-UL141 | 1:10000 | Mouse IgG1 | Tomasec *et al* (2005) |
| α-UL99 | 1:5000 | Mouse IgG2a | Abcam (Cambridge, UK) |

### 2.5.1 Deglycosidase Treatment

To deglycosylate proteins, samples were digested with either endoglycosidase H (Endo H) or peptide N-glycosidase F (PNGase) (NEB). Cells or purified virions were resuspended in denaturing buffer (NEB) to a total volume of 90µl and incubated at 99°C for 10 minutes. The sample was then split into three aliquots for Endo H digestion, PNGase digestion and a control aliquot processed without enzyme. For Endo H, 1µl (500 Units) enzyme and 5µl buffer G5 (NEB) were added to a total volume of 50µl. For PNGase. 1µl (500 Units) PNGase enzyme, 5µl of the supplied NP40 solution and 5µl of the buffer G7 was added to a total volume of 50µl. For the control aliquot, 5µl of buffer G5 was added the PBS added to a total volume of 50µl. All samples were then incubated overnight at 37°C. After the incubation the samples were mixed with SDSPAGE sample buffer and blotted as described above.

## 2.6 MICROSCOPY

### 2.6.1 Preparation Of Cells

For microscopy experiments, cells were grown on sterilised coverslips placed in 6 well tissue culture plates, either transfected (as described in section 2.2.2) or infected with RAds or HCMV (as described in section 2.3.6) and incubated for three days at 37°C. The coverslips were removed from the tissue culture dish, washed with PBS and where appropriate immunofluorescence performed (Section 2.6.2) then mounted on microscope slides with DABCO to preserve fluorescence signal. The slides were then imaged directly under phase and fluorescent light using a Leica DM IRBE (Leica). For live cell imaging, cells were cultured directly on microscope slides (Nunc Flask on Slide) then imaged directly.

For confocal microscopy the slides were fixed by immersion in a 1:1 mixture of acetone and methanol for 30 seconds then mounted onto microscope slides. The slides were imaged on a Leica SP5 confocal microscope (Leica) with the following settings. Stimulation with argon laser. CFP emission 465-505 nm, YFP emission 525-600 nm. AF 549 emission 605-700 nm. Microscope images were obtained using OpenLab (Improvision, Coventry, UK) or Leica LAS AF software (Leica) then analysed with Adobe Photoshop CS2 (Adobe, California, USA).

### 2.6.2 Immunofluorescence

Cells, washed in PBS, were fixed on coverslips with 4% paraformaldehyde in PBS for 20 minutes at room temperature. Paraformaldehyde was removed by washing the coverslips three times with PBS, then incubated with 1:200 dilution of mouse anti-calnexin monoclonal antibody (Chemicon, Massachusetts, USA) for 1 hour at 37°C in a humidified chamber. The coverslips were then washed three times in PBS then incubated with a 1:500 dilution of AF549-conjugated goat anti-mouse IgG monoclonal antibody (Invitrogen) for 1 hour at 37°C in a humidified chamber. Following a final round of washes the coverslips were mounted onto microscope slides and imaged by confocal microscopy.

## 2.7 FACS

### 2.7.1 Cell Staining Protocol

Primary and secondary antibodies used in FACS analysis are detailed in table 2.5. Between $5x10^5$ and $1x10^6$ cells were added per FACS tubes and washed in 3ml of 0.2%BSA-PBS at 400g for 5 minutes. Cells were then incubated with the primary antibody in 150µl 0.2%BSA-PBS for 30 minutes at 4°C in the dark, washed in

**Table 2.5. Antibodies used for FACS experiments**

| Antibody | Dilution | Isotype | Company |
|---|---|---|---|
| Primary Antibodies | | | |
| α-CD155 | 1:500 | Mouse IgG1 | Abcam (Cambridge, UK) |
| α-gB | 1:50 | Mouse IgG1 | Abcam (Cambridge, UK) |
| α-pp65 | 1:50 | Mouse IgG1 | Abcam (Cambridge, UK) |
| α-UL141 | 1:50 | Mouse IgG1 | Tomasec *et al* (2005) |
| α-UL99 | 1:50 | Mouse IgG2a | Abcam (Cambridge, UK) |
| Mouse IgG1 | | Mouse IgG1 | Sigma-Aldrich (Missouri, USA) |
| Mouse IgG2a | | Mouse IgG2a | Sigma-Aldrich (Missouri, USA) |
| | | | |
| Secondary Antibodies | | | |
| Alexa Fluor 647 F(ab')2 fragment of goat anti-mouse IgG ( H +L) | 1:400 | Goat IgG | Invitrogen (Paisley, UK) |
| Alexa Fluor 488 F(ab')2 fragment of goat anti-mouse IgG ( H +L) | 1:400 | Goat IgG | Invitrogen (Paisley, UK) |
| Alexa Fluor 594 F(ab')2 fragment of goat anti-mouse IgG ( H +L) | 1:400 | Goat IgG | Invitrogen (Paisley, UK) |

0.2%BSA-PBS and incubated with an isotype specific fluorochrome conjugated secondary antibody at an appropriate dilution in 150µl 0.2%BSA-PBS for 30 minutes at 4°C in the dark. Cells were washed in 0.2%BSA-PBS then resuspended in 300µl 0.2%BSA-PBS before analysing by flow cytometry. FACS analysis was performed using a FACSCalibur (BD, New Jersey, USA) and CellQuest Pro software (BD).

### 2.7.2 Virus Staining Protocol

See table 2.5 for antibodies and dilutions used. Irradiated purified HCMV virions were washed in 200µl 0.2%BSA-PBS and centrifuged at 18000g for 20 minutes. Virions were resuspended in 10µl 0.2%BSA-PBS containing the primary unconjugated antibody for 30 minutes at 4°C in the dark, washed with 3ml 0.2%BSA-PBS and resuspended with an isotype-specific, fluorochrome-conjugated secondary antibody (in 10µl 0.2%BSA-PBS) for 30 minutes at 4°C in the dark. Cells were washed in 0.2%BSA-PBS then resuspended in 300µl 0.2%BSA-PBS before analysing by flow cytometry. FACS analysis was performed using a FACSCalibur and CellQuest Pro software.

For experiments using purified virions and fibroblasts the following procedure was followed. Fibroblasts were infected with RAdCD155mCh or the same vector lacking an insert (RAd-control). After three days the media was removed and the cells were washed in PBS. HCMVUL32GFP was added to the cells at a moi of 10 and incubated at 4°C on a rocking platform for 4 hours. After the incubation, the inoculate was removed, the cells were washed with PBS then incubated with 4% paraformaldehyde. The cells were then

incubated with trypsin/EDTA (Invitrogen) until the cells detached. The cells were resuspended in 0.2% (w/v)BSA-PBS, centrifuged at 400g for 5 minutes at 4°C then resuspended in 400µl 0.2% (w/v)BSA-PBS. FACS analysis was performed using a FACSCalibur and CellQuest Pro software.

## 2.8 ADHESION ASSAY

Cells were seeded in a 96 well tissue culture dish ($2x10^5$ cells/well) then incubated at 37°C. At various times after addition of cells (time-points defined in figure legends) triplicate wells were washed gently with PBS, fixed with methanol then washed again with PBS. At the end of the time course all PBS was removed and the fixed cells were stained with 0.1% crystal violet for 30 min, washed three times in water then dissolved with 0.5% Triton x-100 overnight. Absorbance at 550nm was used as a measurement of the number of adherent cells, and analysed using Graphpad Prism.

A modified protocol was also used. The adhesion assay was performed as described above, except the stained cells were dissolved in 33% acetic acid for 30 min. The acetic acid dissolved the staining quicker, reducing the possibility of evaporation or incomplete dissolving. Absorbance at 550nm was measured and analysed using Graphpad Prism (Graphpad, California, USA).

## 2.9 *IN VITRO* SCRATCH ASSAY

Cells were seeded in a 60mm tissue culture dish then incubated overnight. The following day an area of the tissue culture dish was denuded by scoring a plastic tip across the surface creating an approximately 1mm wound in the confluent monolayer. The lid was replaced and sealed with Parafilm.

Time-lapse microscopy was performed with a Leica DM IRBE inverted microscope (Leica) in an incubator set to 37°C. Images were taken every 5 minutes for 16 hours using Improvision OpenLab 3 (Improvision) then converted into movies using Apple QuickTime (Apple, California, USA).

To quantify the assay images taken each hour were analysed by three different techniques: manual measurement of area, manual measurement of distance and automatic measurement of area.

1) Manual measurement of area

The leading edges of the monolayer were defined manually and the area of the wound was calculated using Improvision OpenLab 3 software giving a measurement of area in pixels. This value was then converted to percentage of initial wound area for comparison.

2) Manual measurement of distance

Using Improvision OpenLab 3 software the distance between the leading edges were measured at three separate points per frame. The average distance was calculated for each frame then converted to a percentage of the initial wound size.

3) Automatic measurement of area

Individual images were imported into Adobe Photoshop CS2 (Adobe). The area of the wound was calculated using the colour selection tool to automatically select the wound. This technique gave a value in pixels for each frame; these values were converted into percentage of initial area for comparison with the other techniques.

## 2.10 NEUTRALISATION ASSAY

Fibroblasts from a confluent 175cm$^2$ tissue culture flask were detached with trypsin, seeded in a 96 well tissue culture plate and incubated overnight to attach. Doubling dilutions of antibodies and positive and negative human sera from 1:40 to 1:2560 were made in DMEM and mixed with 100 pfu of HCMVUL32GFP. After 30 minutes incubation, the serial dilutions plus virus were added to the HFFF in the 96 well plate. The cells were incubated for 4 hours in a rocking incubator then the media was replaced with fresh DMEM-10. After three days the cells were imaged with an inverted fluorescent microscope for GFP fluorescence caused by infection with HCMVUL32GFP. GFP positive cells were counted for each well and analysed with Graphpad Prism software (Graphpad).

# 3 THE EFFECT OF UL141 ON CELL ADHESION AND MIGRATION

UL141 was initially defined to be an NK evasion function through its capacity to downregulate cell surface expression of CD155, thus sequestering the ligand for DNAM-1 and CD96. However, CD155 also participates in intercellular connections through binding to nectin-3 (Sato et al. 2004) and adhesion to the extracellular matrix via its capacity to bind vitronectin (Lange et al. 2001). CD155 locates both to focal complexes and the leading edge of migrating fibroblasts where ligand stimulation promotes intracellular signalling to stimulate movement (Oda et al. 2004). CD155 upregulation is an important step in the metastasis of certain cancers, including gliomas (Sloan et al. 2005) and sarcomas (Sloan et al. 2004), due to the reduced adherence and promotion of motility.

I was therefore interested in determining whether HCMV UL141-mediated downregulation of CD155 would impact on normal cell process involved in intercellular communication, adhesion and motility. Cell adhesion can be readily measured *in vitro* simply by measure the time taken for cells to settle and attach to surface of tissue culture dishes. To provide further insight into the possible consequence of UL141 expression on cell motility, an *in vitro* wound healing assay was performed. The assay involves artificially introducing a gap in a cell monolayer and tracking the capacity of cells to repair this 'wound'. The assay thus measures the capacity of cells to respond to their environment, then migrate or proliferate to repair the damage. In these studies, UL141

was analysed by expression in continuous 293 cells lines, and following transient expression when delivered by using an Ad vector. A HCMV UL141 deletion mutant became available in the later stages of the study, and was then included in experiments.

## 3.1 EFFECT OF UL141 EXPRESSION ON THE ADHERENT PROPERTIES OF 293 CELLS

A 293 continuous cell line expressing a UL141GFP fusion protein was instrumental in identifying the mechanism by which UL141 modulated NK cell function (Tomasec et al. 2005). By fluorescence microscopy, expression of the UL141GFP fusion protein was readily detected, although expression levels varied between cells. UL141GFP exhibited a restricted intracytoplasmic distribution that in cells expressing particularly high levels looked like inclusion bodies (fig 3.1A). In contrast GFP expressed alone has a more generalised distribution, not trafficking to a specific organelle (fig 3.1B). Endogenous CD155 expression could readily be detected on the surface of 293-GFP control cells by flow cytometry, and was efficiently downregulated in cells expressing UL141GFP (fig 3.1C). This study reproduces and supports the findings of Tomasec et al (2005). It was apparent, however, that the 293 UL141GFP cell line proved relatively difficult to culture relative to 293-GFP cells, taking much longer to reach confluency.

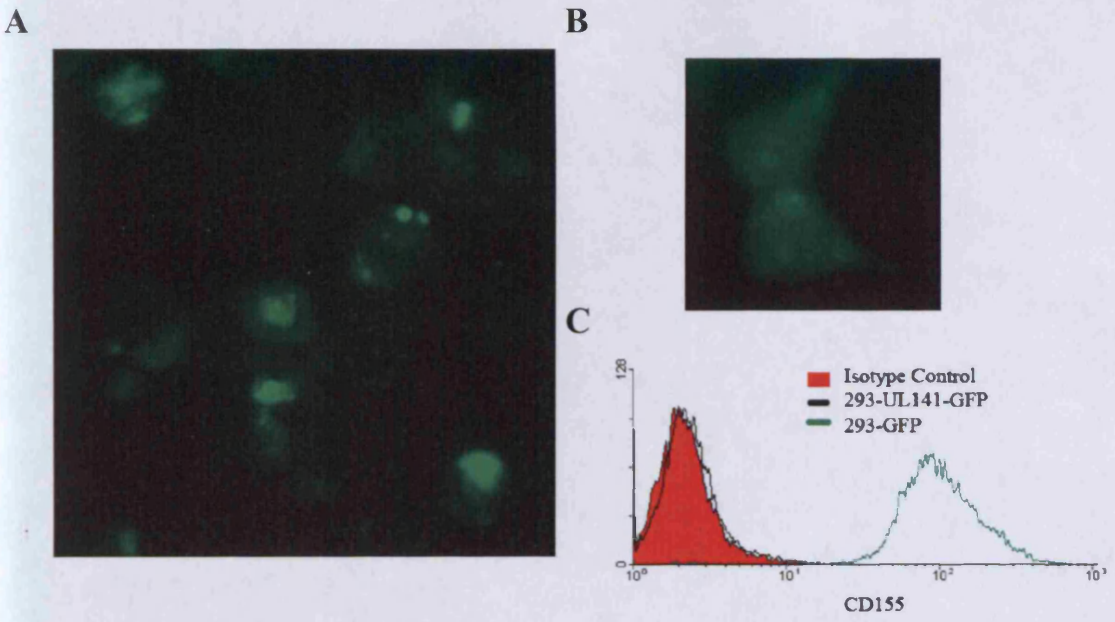


**Figure 3.1. Downregulation of cell surface CD155 in 293 Cells.**
Continuous 293 cell-line expressing UL141GFP or GFP and grown under selection with Geneticin. (A) Fluorescent image of 293-UL141GFP cells. (B) Fluorescent image of 293-GFP cells. (C) Comparison of CD155 cell surface expression on 293-UL141GFP and 293-GFP cells. Cells were stained with anti-CD155 monoclonal antibody then AF594 – tagged secondary goat anti-mouse antibody. Solid red is isotype control, black line is 293-UL141GFP and green is 293-GFP.

I was interested in the poor growth properties of this cell line. The effect of UL141GFP expression on the capacity of cells to adhere to the substrate was therefore studied using a crystal violet adherence assay. Cells removed from monolayers, by minimal treatment with trypsin, were allowed to adhere to the surface of 96 well plates. At various timepoints non-adherent cells were washed off and the adherent cells were fixed with methanol. At the end of the timecourse all wells were stained with crystal violet then lysed in a solution containing Triton X-100 (materials and methods section 2.8). Absorbance of the Triton x-100-crystal violet solution at 570nm was interpreted to be a quantitative measurement of the number of adherent cells. To measure total cell numbers in each experiment, wells were included where the non-adherent cells are not washed off. Comparison of the absorbance of these wells demonstrated that similar numbers of cells were added initially.

Either 293-GFP cells or 293-UL141GFP cells ($2x10^5$ per well) were plated in triplicate, non adherent cells were washed off and adherent cells were fixed at the time indicated in fig 3.2. Cell adhesion increased over time for both lines, yet 293-GFP cells clearly attached more efficiently than 293-UL141GFP cells (fig 3.2A). While the difference varied over time at all time points, 293-GFP cells exhibited more efficient adhesion (up to 3 fold at 2h). 293 UL141GFP cells adhered to the growth substrate at a slower rate than 293-GFP cells.

A

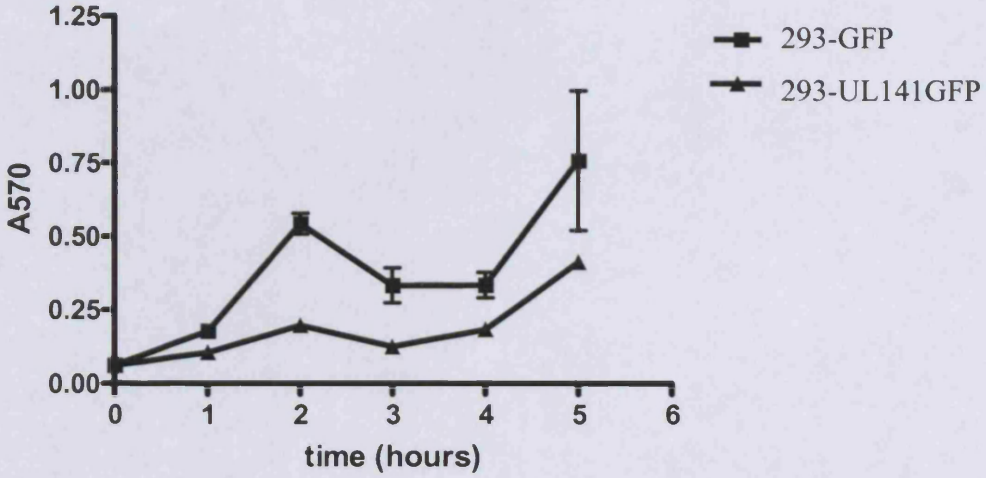


B

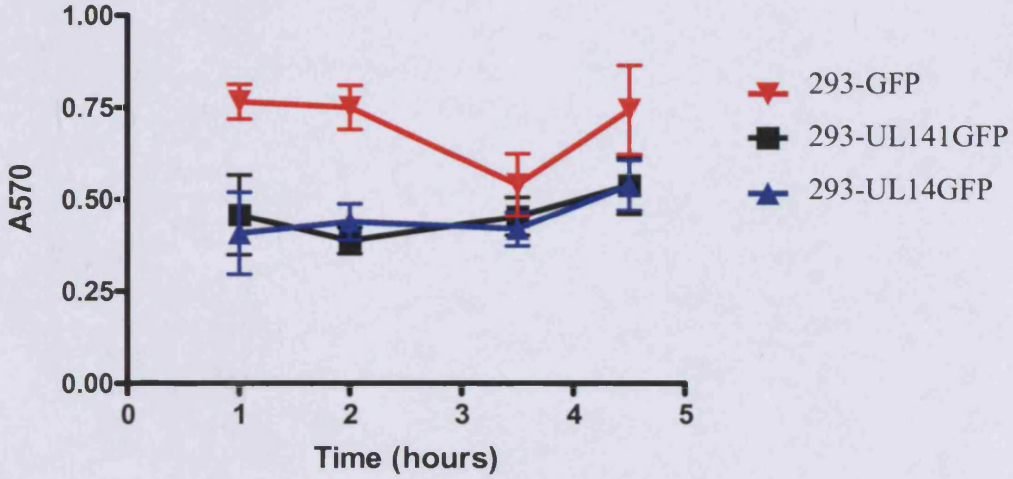


**Figure 3.2. UL141 expression reduces 293 cell adhesion.**
(A) Assay measuring 293-UL141GFP or 293-GFP cell adherence to plastic substrate over time. Absorbance at 570nm was measured. Data shown is the average of three replicates with error bars representing standard deviation and representative of three independent experiments. (B) Assay measuring 293-GFP, 293-UL141GFP or 293-UL14GFP cell adherence to plastic substrate over time. Data shown is the average of three replicates with error bars representing standard deviation and representative of three independent experiments.

There are only two members of the HCMV UL14 gene family: UL14 and UL141 (Davison et al. 2003; Dolan et al. 2004). Although the function of UL14 has yet to be determined, like UL141, it encodes an Endo H-sensitive glycoprotein that traffics to the ER but it is known not to downregulate CD155 (Tomasec et al. 2005, M. Armstrong, PhD thesis). When repeating this assay, a 293 cell line stably expressing a UL14GFP fusion protein was included to compare the relative effect of the UL14-family members on cell adhesion (fig 3.2B). UL14GFP expression also reduces 293 cell adherences when compared to control 293-GFP cells. UL14GFP reduces cell adhesion to a similar extent to UL141GFP without downregulating cell surface CD155.

## 3.2 EFFECT OF UL141 EXPRESSION ON THE ADHESIVE PROPERTIES OF U373 CELLS

U373 cells are a human glioblastoma line semi-permissive for HCMV, which were observed to express CD155 on the cell surface (fig 3.3A). Ad vectors provide for efficient transient expression of transgenes; an Ad vector encoding UL141 (RAdUL141) was available to this study (Tomasec, 2005). Upon expression of UL141 cell surface CD155 is downregulated (fig 3.3A) compared to the CD155 expression levels observed in RAd control infected U373 cells. A biphasic response was observed, indicative of two populations of cells. One population in which there is efficient suppression of CD155, and a second with partial downregulation.

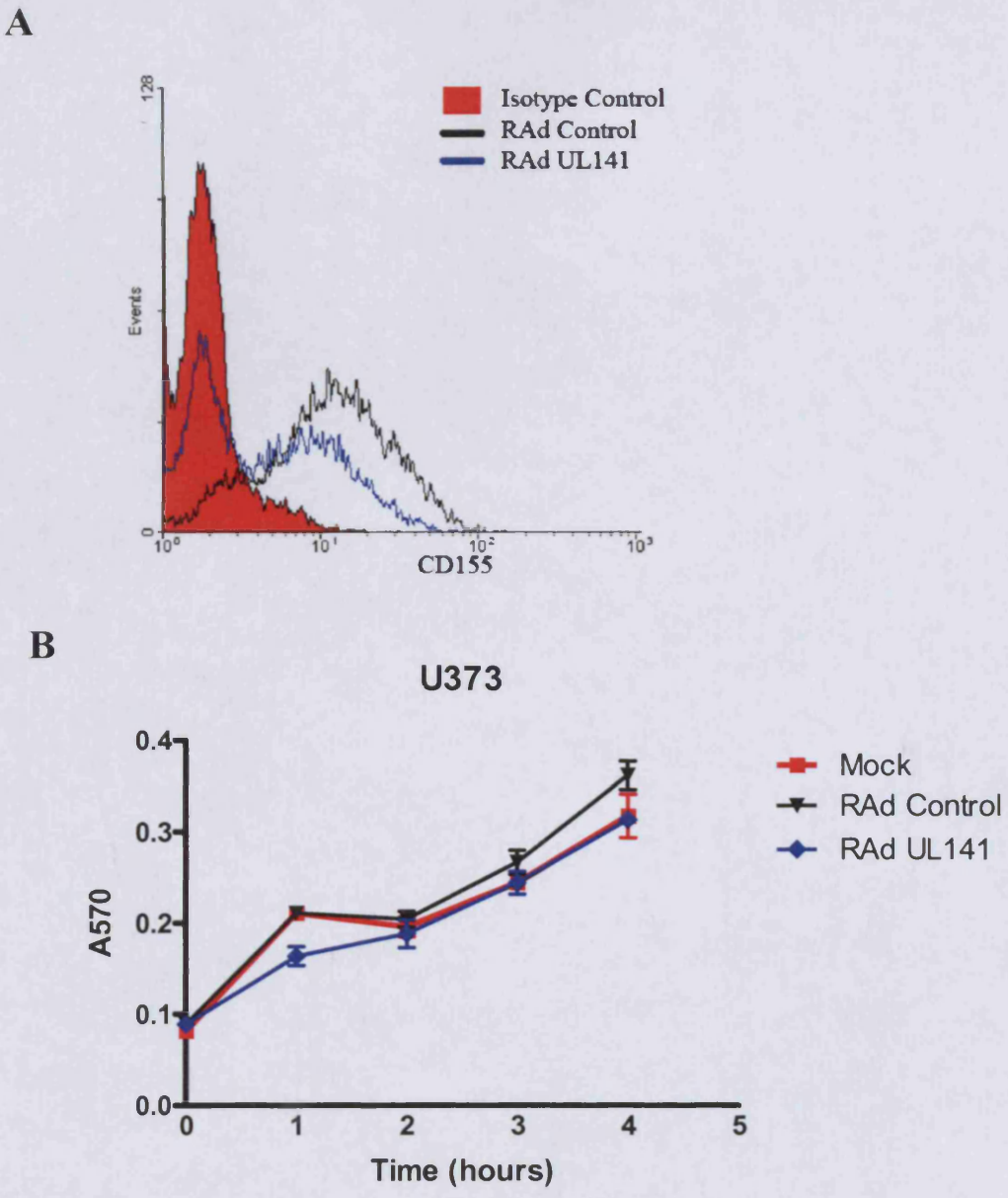


**Figure 3.3. The effect of UL141 on U373 cell adhesion.**
(A) Cell surface expression of CD155 on U373 cells infected with RAdUL141 (black line) or a control vector (RAd Control, blue line). Cells stained with mouse anti-CD155 monoclonal or isotype control (red) then stained with goat anti-mouse AF594 were analysed by flow cytometry. (B) U373 cells infected with RAd Control (▼), RAdUL141 (♦) or mock infected (▼) were used in a crystal violet adhesion assay. Error bars are the standard deviation between three replicates.

U373 cells were infected with RAd UL141, RAd control and mock infected. The control Ad vector was based in the same vector background (AdEASY-1), contained the HCMV major IE promoter and SV40 polyadenylation sequence, but lacked a transgene insert. Throughout this study, the control Ad vector used will be of equivalent construction to the adenovirus recombinant under test. Three days post infection the adherence of the cells on cell culture plastic was studied (fig 3.3C). Mock infected U373 cells and cells infected with an empty vector both adhere to the plastic growth substrate at the same rate. There is a slight deficit in adhesion in cells infected with RAd-UL141 at one hour; however, this difference does not persist during the rest of the experiment. When expressed in the context of an Ad vector, UL141 did not substantially alter the capacity of U373 cells to adhere to the susbstrate.

### 3.2.1 Effect of Overexpression of CD155 on the Adhesive Properties of U373 Cells

To determine the role of CD155 in the initiation of adhesion of U373 cells, U373 cell-lines stably expressing a CD155CFP fusion protein were created. U373 cells were transfected with the plasmid pAL881, then plated 24 hours late on 100mm diameter tissue culture dishes at a range of low cell densities, by sequential 10 ten-fold dilutions. Geneticin-resistant cell colonies were selected, a panel of 10 expanded. Two clones, U373-A6 and U373-A3, expressed higher levels of cell-surface CD155 than the parental cells when measured by flow cytometry (fig 3.4A). These cell-lines were used in an adhesion assay to see if increased expression of CD155 could affect U373 cells adhesion.

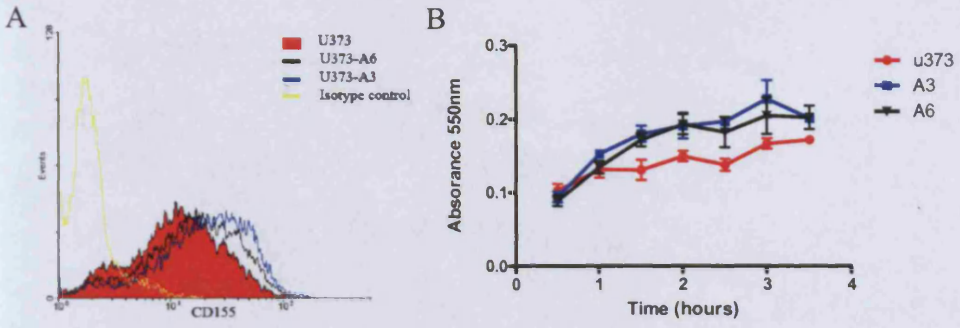


**Figure 3.4. Ectopic expression of CD155 increases adhesion of U373 cells.** Continuous U373 cell lines expressing CD155CFP were analysed in an adhesion assay. (A) Cell surface expression of CD155 on the parental U373 cells (solid red) and two transfected cell lines U373-A6 (Black line) and U373-A3 (blue line). Cells stained with an anti-CD155 mAb or an isotype control were analysed by flow cytometry. (B) The three cell lines were used in an adhesion assay as described previously. Cells were washed and fixed at thirty minute intervals. Data shown is the mean of three replicates with the error bars showing the standard deviation.

During the first hour no difference was apparent, but as the time course proceeded, the two CD155CFP cell lines consistently exhibited greater adherence (fig 3.4B). U373 cells express a relatively low amount of CD155 as measured by FACS.

UL141 downregulation of cell-surface endogenous CD155 did not score in the adhesion assay (fig 3.3), yet it is clear that CD155 can influence U373 cells adhesion. It is possible that UL141 was not expressed efficiently enough in U373 cells to significantly impair adhesion, or that the endogenous CD155 levels did not reach a threshold level of expression to be a rate-limiting factor. The over-expressing cell lines potentially could be used to aid functional studies.

## 3.3 EFFECT OF UL141 EXPRESSION ON THE ADHERENT PROPERTIES OF HUMAN FIBROBLASTS

Human fibroblasts support a fully productive infection with both low and high passage HCMV strains, and exhibit strong adherence to plastic growth substrate. In contrast, 293 cells adhere weakly to the plastic and fail to support productive HCMV infection. Whilst I wished to study the effect of UL141 influence on fibroblasts adhesion, continuous cell lines cannot readily be established in this cell type. An Ad vector was therefore used to deliver and express UL141 in HFFFs. The capacity of the recombinant RAd-UL141 to downregulate cell surface expression of CD155 in this experimental system was established in a FACS experiment. HFFF cells were infected for three days prior with RAd-UL141, RAd-control or mock infected. While RAd-UL141 efficiently

downregulated CD155 relative to mock-infected and cells infected with the control vector (fig 3.5A).

The cells were then trypsanised and used in a crystal violet adherence assay as described. The cell number control wells had equal absorbencies (data not shown). There was no consistent difference in adherence between mock-infected cells and RAd-control infected fibroblasts across the time course (fig 3.5B) showing that infection with the vector did not substantially alter the adherence of the cells. RAd-UL141 cells followed the same dynamics as the control cells but with much lower adherence. At all time points RAd-UL141 had approximately half the absorbance of either the mock-infected cells or the RAd-control infected cells. This data shows that UL141 expression alter the rate of adherence of HFFF cells

## 3.4 EFFECT OF UL141 EXPRESSION ON ADHERENCE DURING HCMV INFECTION

Expression of UL141 alters the ability of HFFFs to adhere to the growth substrate. A recombinant HCMV virus with a deletion in UL141 (HCMVΔUL141) was used to study whether the UL141-dependant reduction of adherence occurs during HCMV infection. HCMVΔUL141 has lost the capacity to downregulate CD155 and nectin 2, plus infected cells are more vulnerable to NK cell attack than those infected with the parental virus

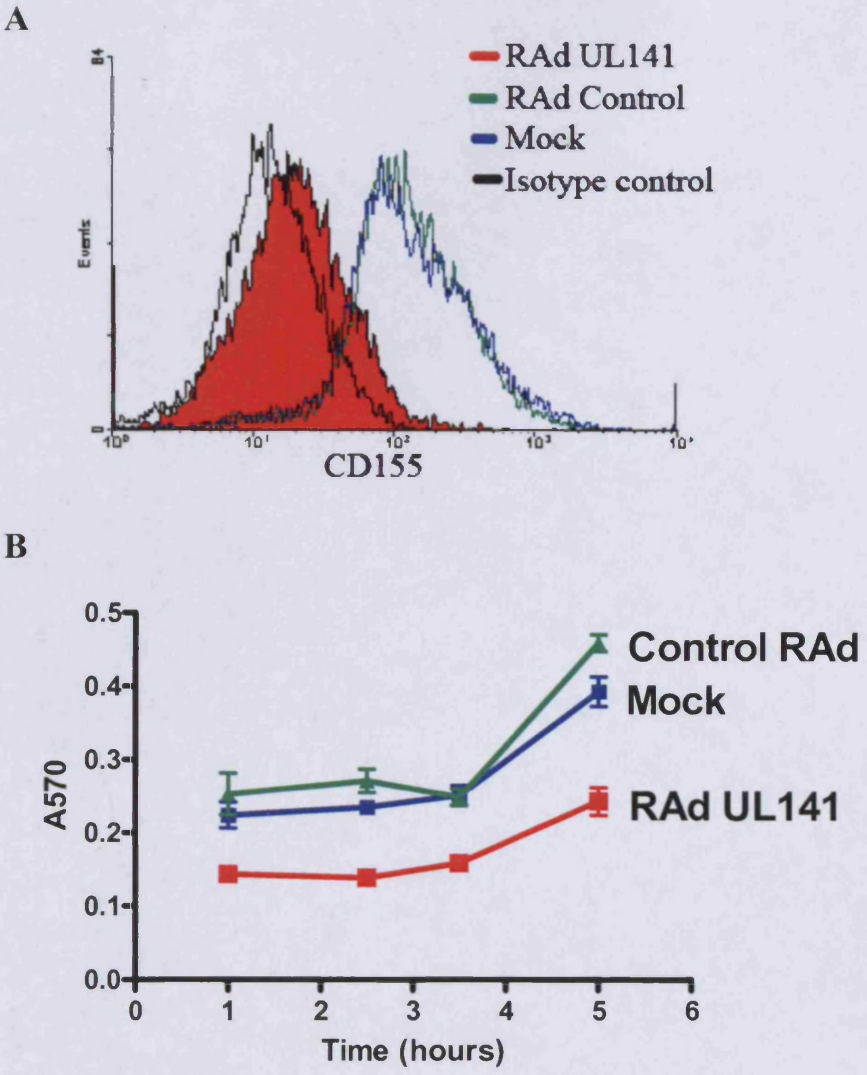


**Figure 3.5. Expression of UL141 reduces adhesion of human fibroblasts**
HFFF were mock infected or infected with RAdUL141 or RAd control. (A) Three days p.i. cells stained with anti-CD155 mAb or isotype control were analysed by flow cytometry. (B) Assay measuring cell adherence to plastic substrate over time. Data shown is the mean of three independent replicates with error bars showing standard deviation.

(Prod'homme, personal communication). HFFFs were infected with the parental HCMV strain Merlin, HCMVΔUL141 virus or mock infected for three days then used in an adhesion assay using a slightly modified technique (described in section 2.8.1).

Infection with either strain Merlin or the ΔUL141 virus resulted in greatly reduced adherence of cells compared to the mock-infected controls (fig 3.6). The adherence of HCMVΔUL141 infected fibroblasts was comparable to that of strain Merlin-infected cells at all time points. HCMV infection alters many aspects of cell binding including the destruction of focal adhesions (Stanton et al. 2007) and the downregulation of integrins (Warren et al. 1994c), the effect of UL141 on cell adhesion was not detectable against a background of other major changes to adhesion molecules in infected cells.

## 3.5 ESTABLISHMENT OF AN *IN VITRO* WOUND HEALING ASSAY

To investigate the effect of UL141 expression on cell migration an *in vitro* wound healing assay was performed. A linear gap is first introduced into a confluent monolayer using a plastic tip; the cells are then imaged in real time to track the repair of the wound. This assay provides a measure of the rate cell migration to repair the lesion in the monolayer.

To ensure an accurate and objective assessment of scratch closure three measurement techniques were used to compare the same images following the migration of a 293-UL141 cell monolayer: distance measurement, manual area measurement and automatic area measurement (fig 3.7). For the first technique, the distance between the two leading

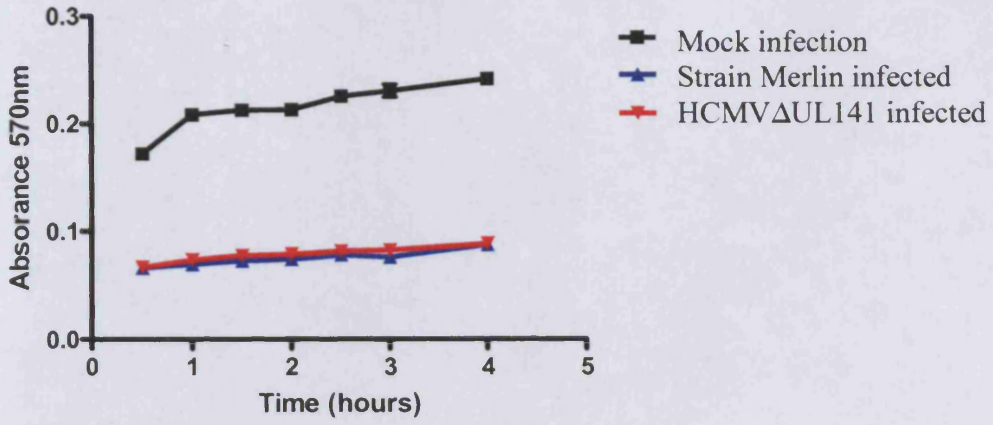


**Figure 3.6. Effect of UL141 expression on cell adhesion during HCMV infection**
Human fibroblasts were infected with Merlin strain HCMV, HCMVΔUL141or mock infected. Data shown is the mean of three independent replicates with error bars showing standard deviation.

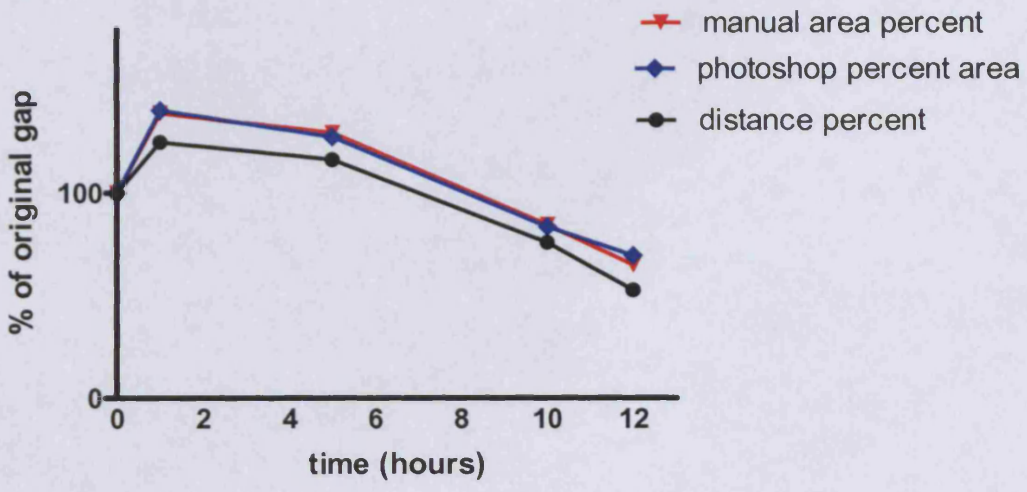


**Figure 3.7. Comparison of techniques for measurement of scratch assay wound size.** A monolayer of 293-UL141GFP cells was wounded with a plastic tip then incubated for 12 hours at 37°C. Images were taken at 0,1,5,10 and 12 hours post wounding. The size of the void in the monolayer was measured either by (▼) measurement of the distance between leading edges, (♦) automatic calculation of area by Adobe Photoshop or by (●)manual area calculation. All values are expressed as percentage of initial wound size to standardise values.

edges was measured at each time point. For manual area measurement the perimeter of the wound was defined manually on screen for each frame then the area was calculated using Improvision OpenLab software. Automatic area measurement used Adobe Photoshop CS2 software to calculate the area of the wound. After conversion to percentage measurements, the initial scratch being set at 100%, the three techniques produced comparable results. The area measurements varied by less than one percent at one hour post wounding and by five percent at 12 hours post wounding, whilst the distance measurement gave consistently lower values at each timepoint studied. At one hour post wounding distance measurement was lower than automatic area measurement by 10% and at 12 hours post wounding the difference was 25%. The variation in the distance measurement technique is because the leading edges do not move uniformly with parts of the leading edges moving faster than other. Area measurement was therefore considered a more accurate assay. For all further wound assays Photoshop software was used to quantify scratch assays as it is straightforward and potentially less subjective.

### 3.5.1 Effect Of UL141 On 293 Cell Migration In An *in vitro* Wound Healing Assay

To determine the effect if UL141 expression altered cell migration 293 cells expressing UL141GFP or GFP (fig 3.8A) were used in the *in vitro* wound assay. A small area of a confluent monolayer was denuded with a plastic tip and was incubated at 37°C for 16 hours. Images were acquired every five minutes, with a subset selected at hourly intervals analysis quantitatively using Adobe Photoshop. The 293-GFP monolayer closed at a relatively consistent rate, averaging 3.1% / hour over the course of the

experiment (fig 3.8A and B and video 3.1). At 14 hours post wounding the two leading edges have began to make contact and only small voids in the monolayer remain.

293-UL141GFP cells exhibited reproducible differences to the control cells (fig 3.8A). Within minutes of wounding, the area of the wound increased, peaking at 1 h post wounding with an increase of up to 30% of the initial size. Directly following wounding the edges of the monolayer detach from the substrate (video 3.2) and over the course of an hour either reattaches to the substrate or settled on top of the monolayer.

The expanded wound size remained stable for 4 hours then a phase of rapid closure followed. From 4 to 14 hours post wounding the rate of closure was 9% per hour, three times greater than closure in the control cells. The leading edges of 293-UL141GFP begin to meet at 14 hours post wounding. The total time to wound resolution for both cell lines is similar; however, the dynamics of closure are markedly different.

Although the assay was set up to investigate cell migration, no clear UL141GFP-mediated effect on motility could be deduced from this assay. UL141GFP appeared to act to reduce cell:substrate adhesion, and as a consequence the monolayer adjacent to the lesion detached. Unexpectedly, a more rapid peak rate of gap closure was observed with the 293-UL141GFP cells. However, these cells were able to recruit displaced cells to the gap. Cell surface CD155 expression helped to protect the cell monolayer from damage, but did not accelerate repair.

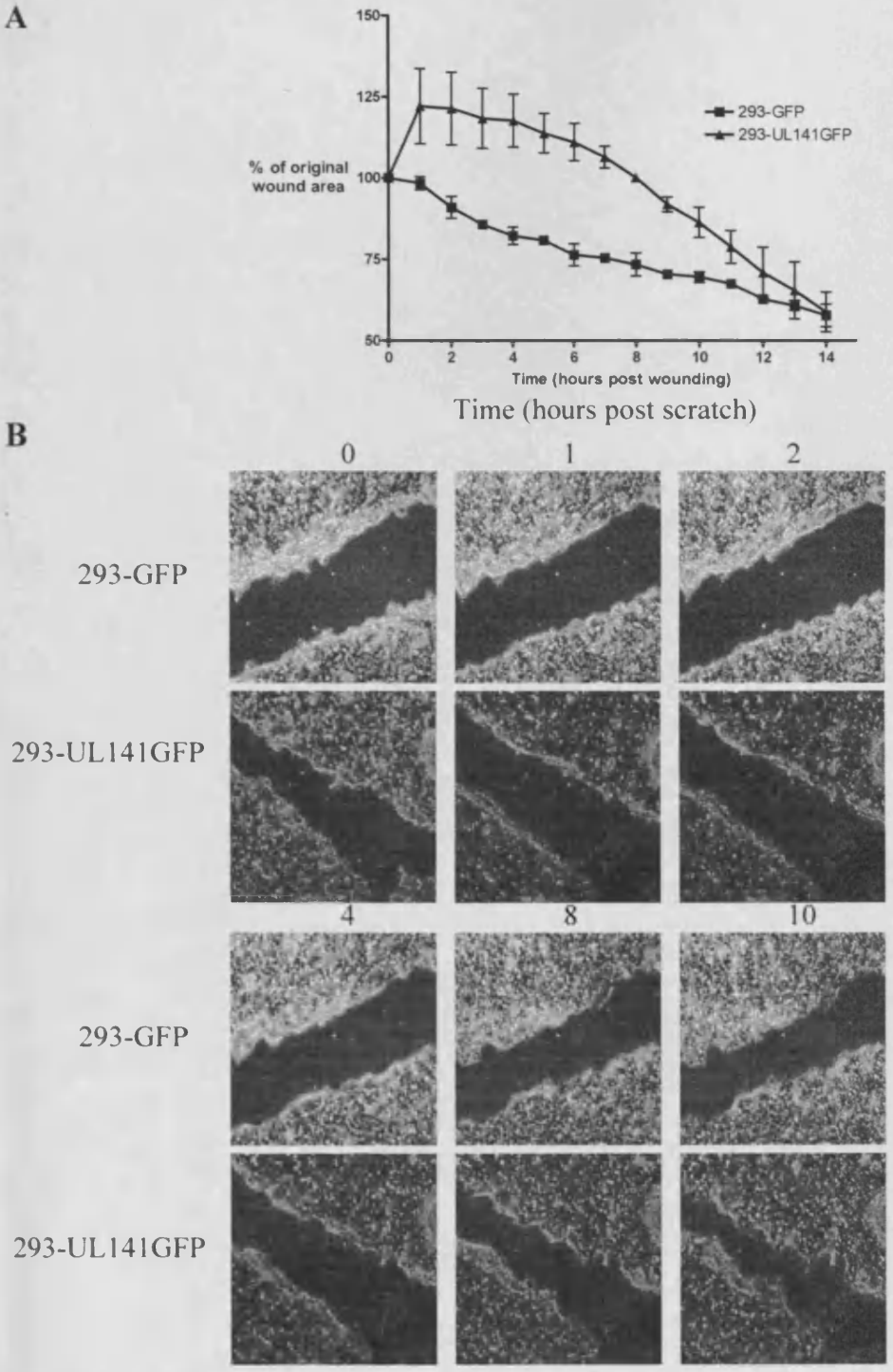


**Figure 3.8. Effect of UL141 on 293 cell migration in an *in vitro* wound healing assay.** 293-GFP or 293-UL141GFP cells were used in an *in vitro* wound healing assay (A) Images at hourly intervals were analysed using Adobe Photoshop. Results are expressed as percentage of initial wound area Data shown is the average of three independent experiments, error bars are standard deviation. (B) Images from an individual experiment. Images are representative of three independent experiments.

## 3.6 SUMMARY

The study consolidated previous findings from this laboratory, UL141 downregulated cell surface CD155 expression in transfected 293 cells, and in both U373 and human fibroblasts when expressed by using an Ad vector. CD155, like the other members of the nectins and nectin-like family of proteins, has important adhesion properties. It was postulated by Tomasec et al (2005) that UL141 suppression of CD155 could have implications for HCMV-infected cells distinct from NK cell evasion. This study provides the first demonstration that UL141 can also affect the adhesive properties of cells. UL141 mediated downregulation of cell surface CD155 in 293 cells and fibroblasts, but nor U373 cells, was observed to reduces cell:substrate adhesion. Productive HCMV infection was demonstrated to have a major suppressive effect on cell substrate adhesion. However, experiments with a HCMV deletion mutant showed this to be a redundant function, the contribution made by UL141 could not detected in the context of lytic infection. In this context, it is demonstrated that UL14 when expressed in isolation also inhibited cell:substrate adhesion.

# 4 CHARACTERISATION OF THE INTERACTION BETWEEN gpUL141 AND CD155

The proposed model for UL141-mediated evasion of NK recognition involves gpUL141 forming a stable complex with de novo synthesised CD155 and this complex being retained in the ER. Direct imaging of this complex by immunofluorescence has proved problematical. The only mAb available for CD155 compatible with immunohistochemistry was only capable of detecting the fully mature glycosylated form of the protein; CD155 remains in an immature (Endo H-sensitive) form in the presence of gpUL141. Whilst gpUL141 was readily detected, it was associated with inclusion bodies that co-localised with ER markers. Only the surface of these inclusion bodies could be stained, it was not clear if this was because gpUL141 was only on the surface or because the antibody could not penetrate into the inclusion. To enable to direct visualisation of CD155 and UL141, they were expressed with C-terminal fluorescent tags; variously yellow fluorescent protein (YFP), cyan fluorescent protein (CFP) and mCherry (mCh). This procedure allowed co-expression of the two proteins to be followed simultaneously without using antibodies and live cell imaging to be performed.

## 4.1 GENERATION OF CD155 AND gpUL141 FUSION CONSTRUCTS.

The cDNA of UL141 was amplified by PCR, digested with restriction endonuclease and ligated into the plasmids pECFP-N1 and pEYFP-N1. Insertion of the appropriate size into

the vector was established first by restriction nuclease digestion (fig 4.1A) then by DNA sequencing. Figure 4.2 shows plasmid map of pUL141YFP and pUL141CFP.

Occasionally, fluorescent tags are cleaved from fusion proteins by cellular proteases, leaving GFP expressed in isolation. It is therefore prudent to check the expressed fusion protein is of the appropriate molecular weight. Cell extracts were prepared from HFFFs transfected with pUL141CFP or pUL141YFP, and infected with strain Merlin infected (positive control) were used in a western blot (fig 4.1B). Cyan fluorescent protein and yellow fluorescent protein both have a molecular weight of 27kDa; therefore the predicated weight of both the gpUL141CFP and gpUL141YFP fusion proteins is 61kDa. On the western blot both proteins migrated to 60 kDa, very close to the predicted size.

Similarly, CD155 sequence was also amplified and inserted into the same plasmids to generate pCD155CFP or pCD155YFP (fig 4.2). Correct insertion was verified by restriction digestion (fig 4.1C) and sequencing. To ensure that these fusion proteins expressed CD155 HFFF cells transfected with pCD155YFP were analysed by flow cytometry (fig 4.1D). Transfection was measured by the presence of YFP fluorescence and cell surface CD155 expression was measured by staining with anti-CD155. 7% of the fibroblasts had been transfected successfully, of these half had greater CD155 levels than the untransfected cells showing that pCD155YFP is causing an increase in CD155 expression.

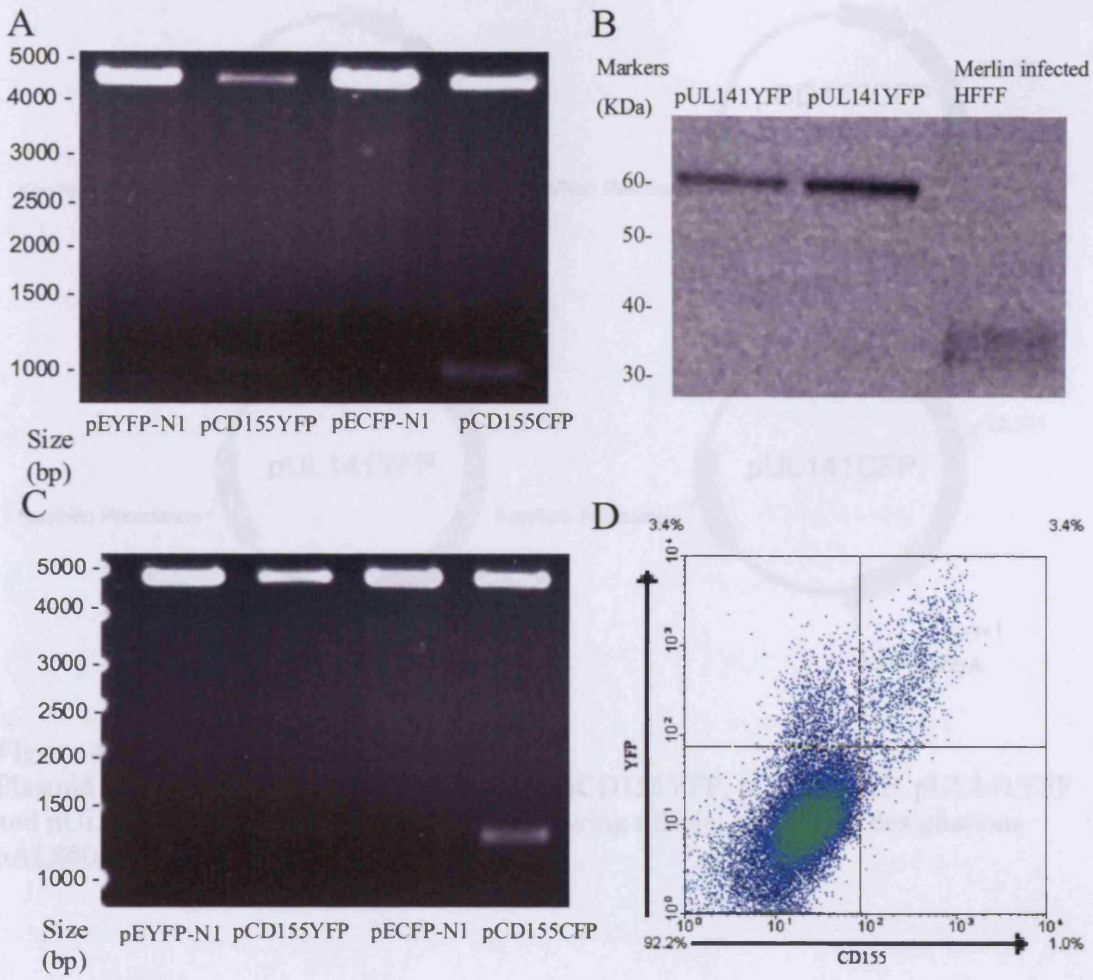


**Figure 4.1. Construction of CD155 and UL141 fluorescent fusion proteins**
(A) The Merlin HCMV UL141 sequence was cloned into pEYFP-1 and pECFP-1 to create the constructs pUL141YFP and pUL141CFP. The plasmids were digested with *HindIII* and *BamHI* to confirm insertion. (B) gpUL141 expression in HFFF transfected with pUL141CFP or pUL141YFP. gpUL141 expression was detected with the M550 series of mAbs. (C) The CD155 sequence was cloned into pEYFP-1 and pECFP-1 to create the constructs pCD155YFP and pCD155CFP. The plasmids were digested with *HindIII* and *AgeI* to confirm insertion. pCD155YFP and pCD155CFP were then transfected into HFFF cells to confirm CD155 expression by flow cytometry. (D) pCD155YFP transfected HFFFs stained with anti-CD155 and goat anti-mouse AF647 fluorescent-conjugated secondary

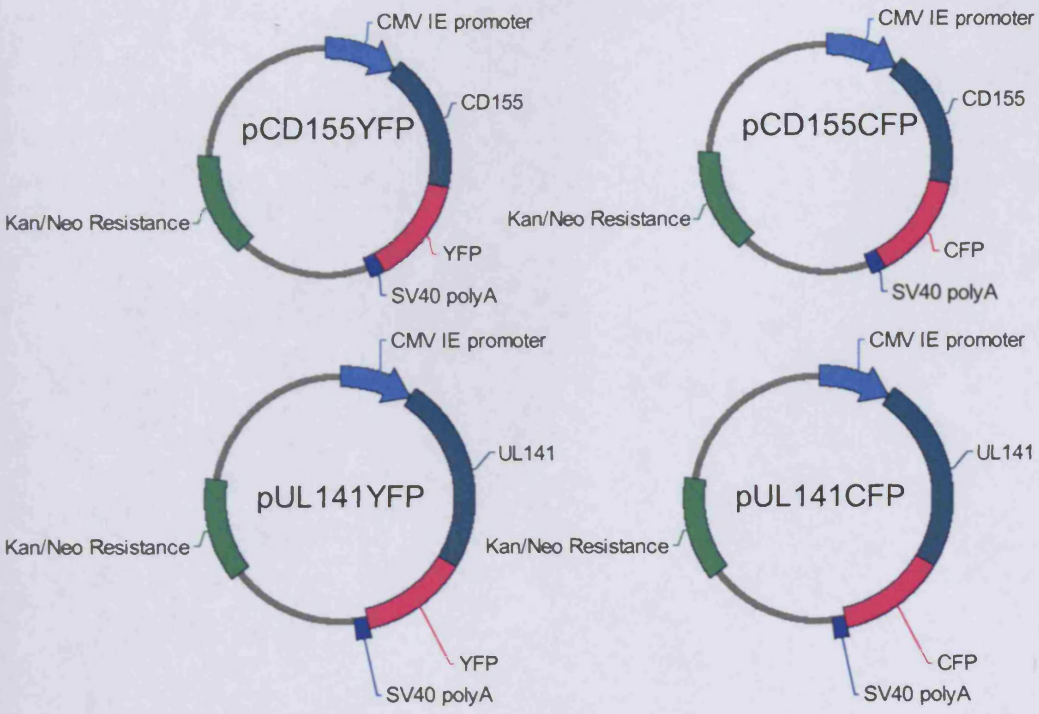


**Figure 4.2. Expression plasmid maps**
Plasmid maps of the four expression vectors; pCD155YFP, pCD155CFP, pUL141YFP and pUL141CFP. The plasmids have the following official laboratory designations pAL880, pAL881, pAL882 and pAL883.

## 4.2 UL141 AND CD155 TRANSFECTION OF 293 CELLS

The plasmid constructs were tested first in 293 cells because these cells can be readily transfected at high efficiency. 293 cells were transfected singly with pUL141CFP (fig 4.3A), pUL141YFP (fig 4.3B), pCD155CFP (fig 4.3C) or pCD155YFP (fig 4.3D), and co-transfected with pCD155CFP and pUL141YFP (fig 4.4A) or with pCD155YFP and pUL141CFP (fig 4.4B). Three days post transfection the cells were fixed and imaged directly. CD155 appeared to be expressed on the cell surface (fig 4.3), although intracellular accumulations were also observed. In 293 cells surface expression of CD155 appeared to localise strongly to regions of cell-cell contact. In contrast, gpUL141 was exclusively intracellular with a structured perinuclear distribution consistent with it trafficking to the ER (fig 4.3A and B; Tomasec et al 2005). This is consistent with the 293 UL141GFP cells in chapter 3.

When CD155 and gpUL141 are co-expressed in 293 cells gpUL141 retains the perinuclear staining observed in the single transfections (fig 4.4). Utilising the CD155 fusion protein it is possible to directly visualise the immature CD155 form retained within the cell. CD155 is downregulated from the cell surface and is now predominantly intracellular. Intracellular CD155 co-localises closely with gpUL141. The co-localisation is mainly concentrated in the inclusion bodies with a diffuse area of staining surrounding the structures. CD155 and gpUL141 are both present throughout the inclusion bodies. The dimensions and quantity of these structures are not constant and vary between cells. The close co-localisation throughout the cell suggests that gpUL141 is directly interacting CD155 within the cell.

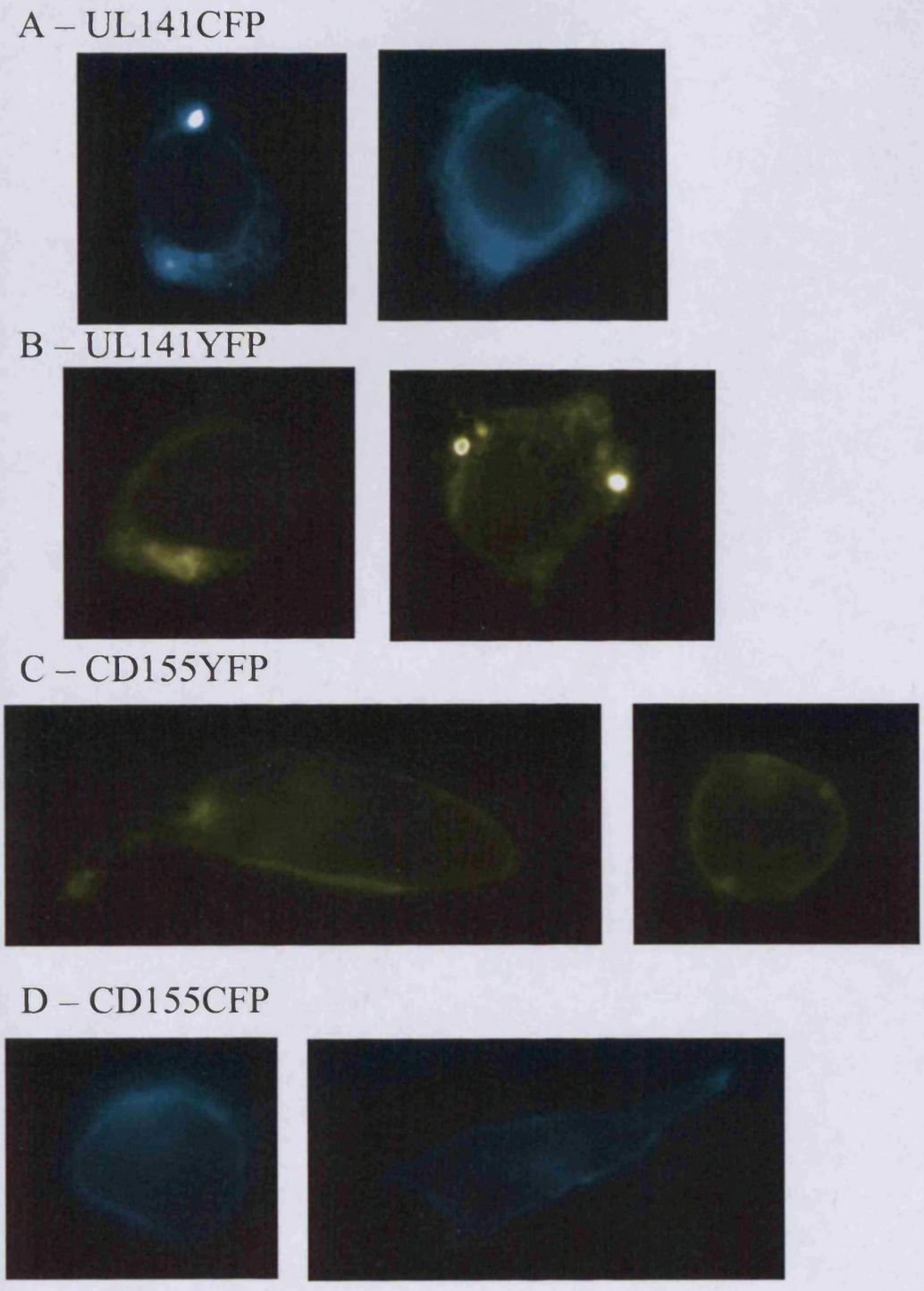


**Figure 4.3. Distribution of gpUL141 and CD155 in 293 cells.**
293 cells were transiently transfected with expression plasmids expressing (A) gpUL141-CFP fusion protein (pUL141CFP), (B) gpUL141-YFP fusion protein (pUL141YFP), (C) CD155-YFP (pCD155YFP) or (D) CD155-CFP fusion protein (pCD155CFP) using Effectene. Three days following transfection, cells were fixed and imaged directly at 100x magnification under oil immersion. Fluorescence was detected and analyzed with a Leica DMIRBE microscope with Improvision Openlab software.

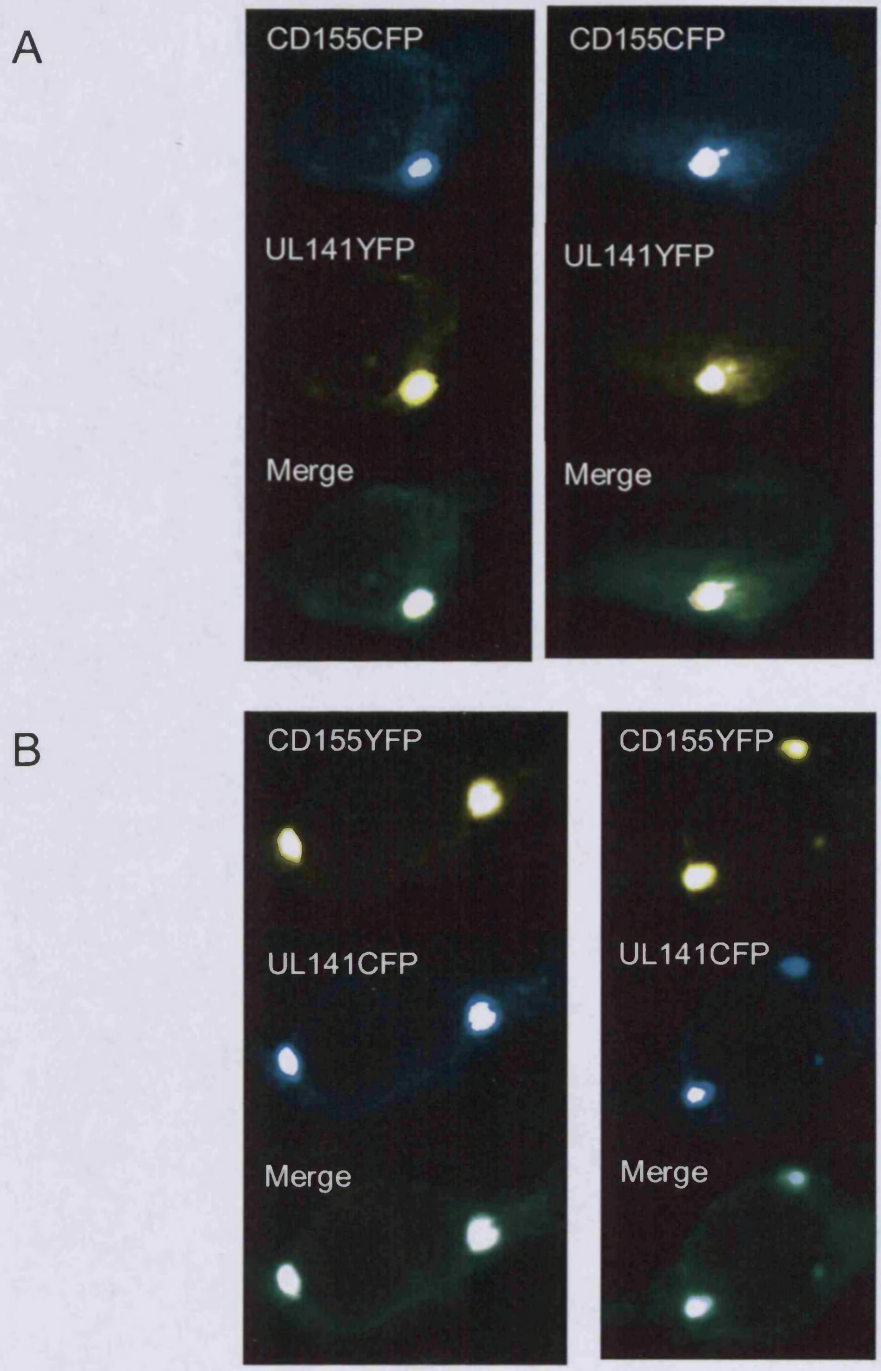


**Figure 4.4. Co-localisation of gpUL141 and CD155 in 293 cells.**
293 cells were transiently transfected with expression plasmids expressing (A) CD155-CFP fusion protein (pCD155CFP) and gpUL141-YFP fusion protein (pUL141YFP) or (B) CD155-YFP (pCD155YFP) and gpUL141-CFP fusion protein (pUL141CFP), using Effectene. Three days following transfection, cells were fixed and imaged directly. Fluorescence was detected and analyzed with a Leica DMIRBE microscope with Improvision Openlab software.

## 4.3 gpUL141 AND CD155 TRANSFECTION OF HUMAN FIBROBLASTS

Following the imaging in 293 cells, the experiment was repeated in human primary fibroblasts (HFFF cells). Although fibroblasts exhibited a much lower levels of transfection by standard techniques, they are a more valid target cell to study as they can support full productive HCMV infection. Initial experiments used transfectene while latter experiments were performed using nucleofection as it gave a higher rate of transfection. Use of transfectene resulted in 4% of fibroblasts transfected while nucleofection resulted in greater than 60% efficiency.

Reassuringly, transfection with pCD155YFP (fig 4.5A) or pCD155CFP (fig 4.5B) resulted in identical expression profiles: localising predominantly at the cell membrane, with small intracellular concentrations. Most noticeably, CD155 was associated with 'nanotubule'-like extrusions that are visible extending from cells. Although in 293 cells CD155 was clearly concentrated to cell-cell contacts, in HFFFs CD155 this phenomenon was much less pronounced (fig 4.5A).

HFFFs transfected with either pUL141YFP or pUL141CFP were directly imaged. Both constructs produce proteins with the same distribution (fig 4.6). gpUL141 expressed in HFFFs exhibit an intracellular perinuclear distribution. The inclusion bodies observed in 293 cells are not present in transfected HFFFs. Endogenous CD155 present in the transfected fibroblasts will complex with the UL141 fusion protein.

A – CD155YCP

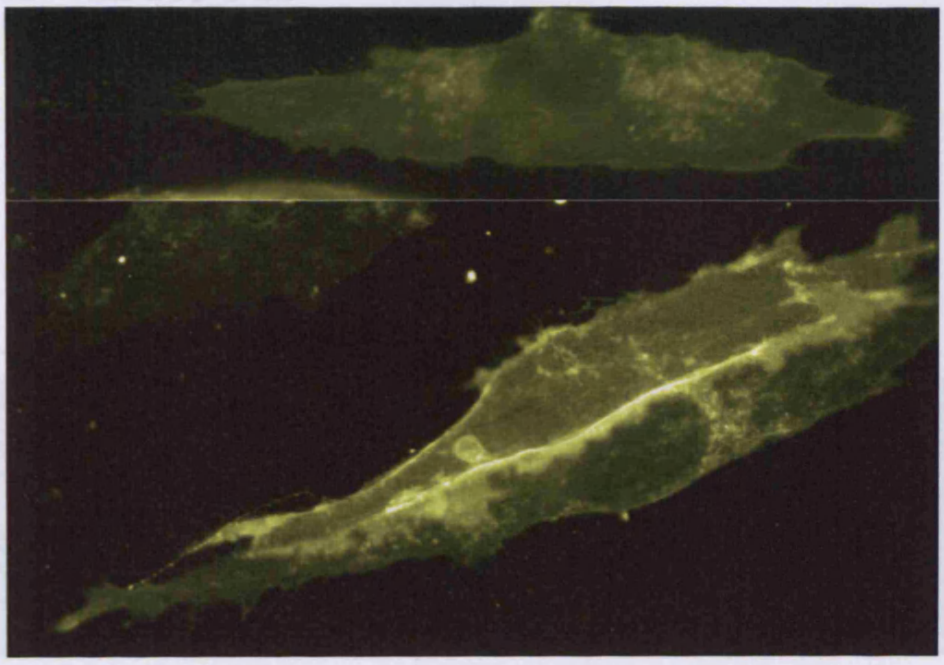

B – CD155CFP

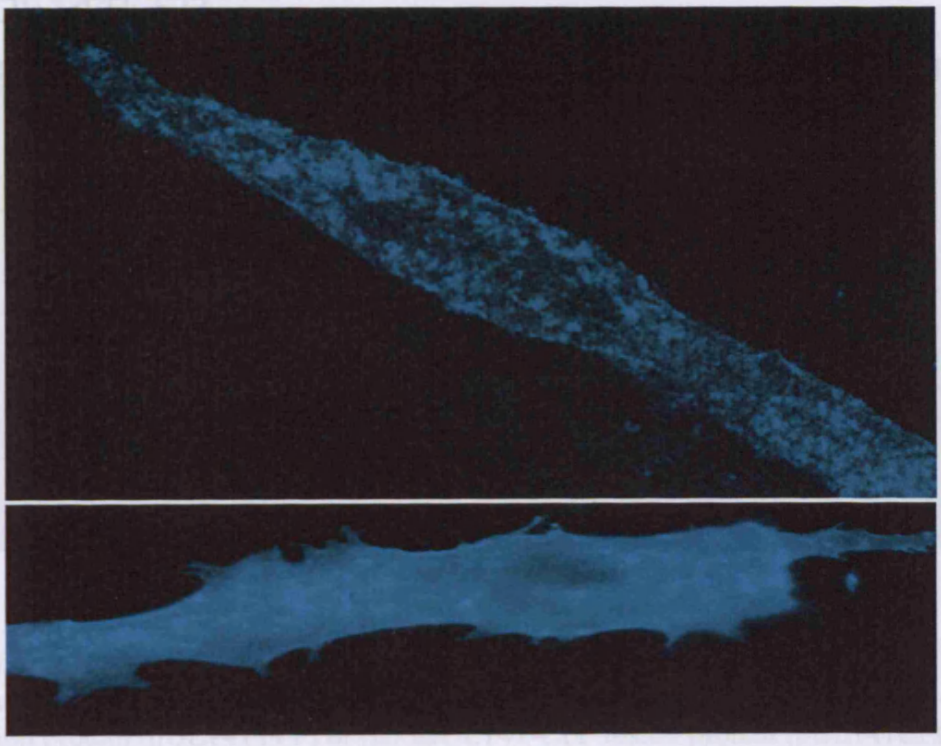

**Figure 4.5. Distribution of CD155 in transfected fibroblasts**
HFFFs were transiently transfected with expression plasmids expressing (A) CD155-YFP (pCD155YFP) or (B) CD155-CFP fusion protein (pCD155CFP) using Effectene. Three days following transfection, cells were fixed and imaged directly at 100x magnification under oil immersion. Fluorescence was detected and analyzed with a Leica DMIRBE microscope with Improvision Openlab software.

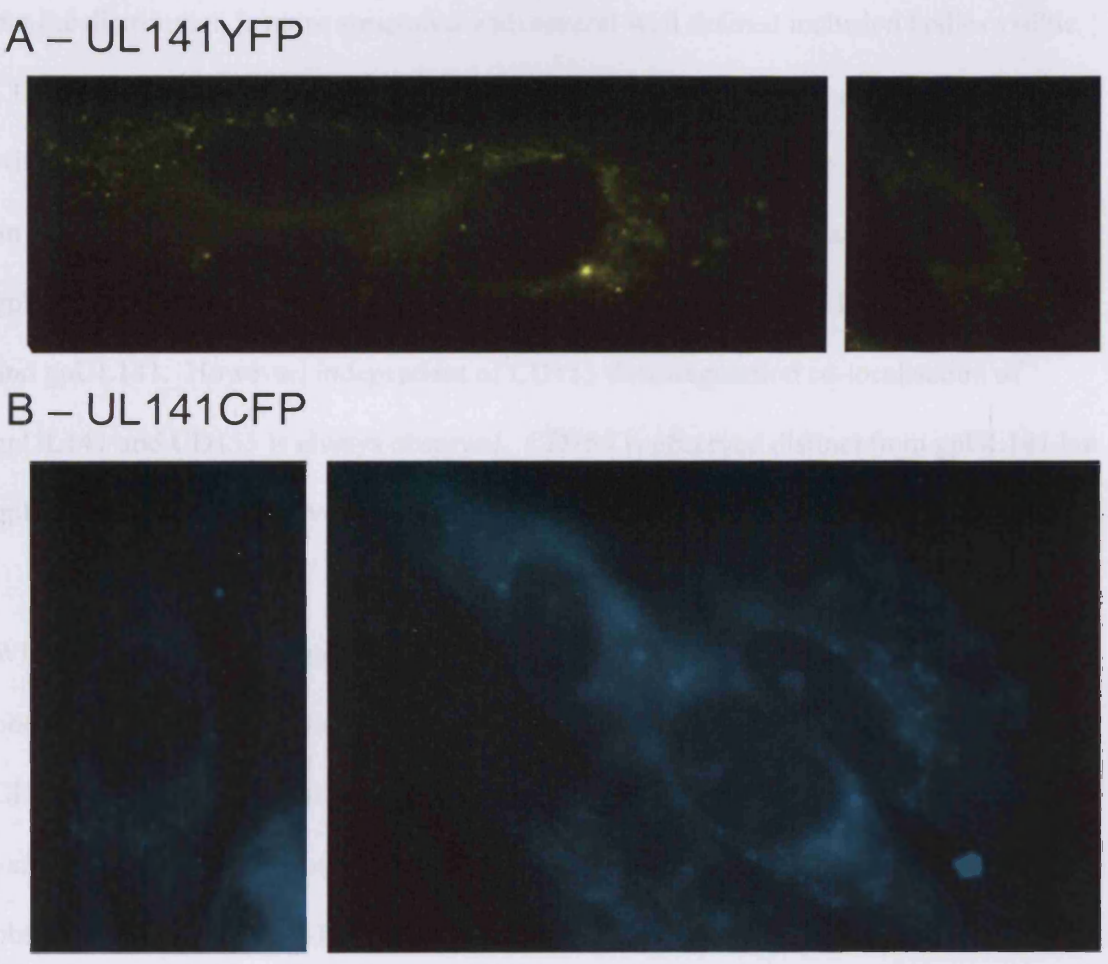


**Figure 4.6. Distribution of UL141 in transfected fibroblasts**
HFFFs were transiently transfected with expression plasmids expressing (A) gpUL141-YFP fusion protein (pUL141YFP) or (B) gpUL141-CFP fusion protein (pUL141CFP) using Nucleofector. Three days following transfection, cells were fixed and imaged directly at 100x magnification under oil immersion. Fluorescence was detected and analyzed with a Leica DMIRBE microscope with Improvision Openlab software.

Next, HFFF were co-transfected with the CD155 and gpUL141 fusion proteins to visualise the interaction. pUL141CFP and pCD155YFP (fig 4.7A) or pUL141YFP and pCD155CFP (fig 4.7B) were co-transfected into HFFF cells. The distribution of the UL141 fusion protein is altered in HFFFs overexpressing CD155; it is still intracellular but the distribution is more structured with several well defined inclusion bodies visible. CD155 is now retained within the cell and closely co-localises with gpUL141 including within the inclusion bodies. As observed in the 293 cells above, the inclusion bodies are an amalgam of gpUL141 and CD155. The downregulation of cell surface CD155 by gpUL141 is not absolute. It is dependant on the relative expression levels of both CD155 and gpUL141. However, independent of CD155 downregulation co-localisation of gpUL141 and CD155 is always observed. CD155 is observed distinct from gpUL141 but gpUL141 is always observed co-localised with CD155.

When CD155 is incompletely retained (fig 4.7) CD155 displays an intermediate phenotype where it is partially cell surface and partially intracellular. All intracellular CD155 invariably co-localises with gpUL141, while cell surface CD155 does not. The variable downregulation of cell surface CD155 is in agreement with previous observations that gpUL141 downregulates cell surface CD155 but does not completely eradicate surface expression (chapter 3).

Figure 4.7

A – CD155YFP and UL141CFP

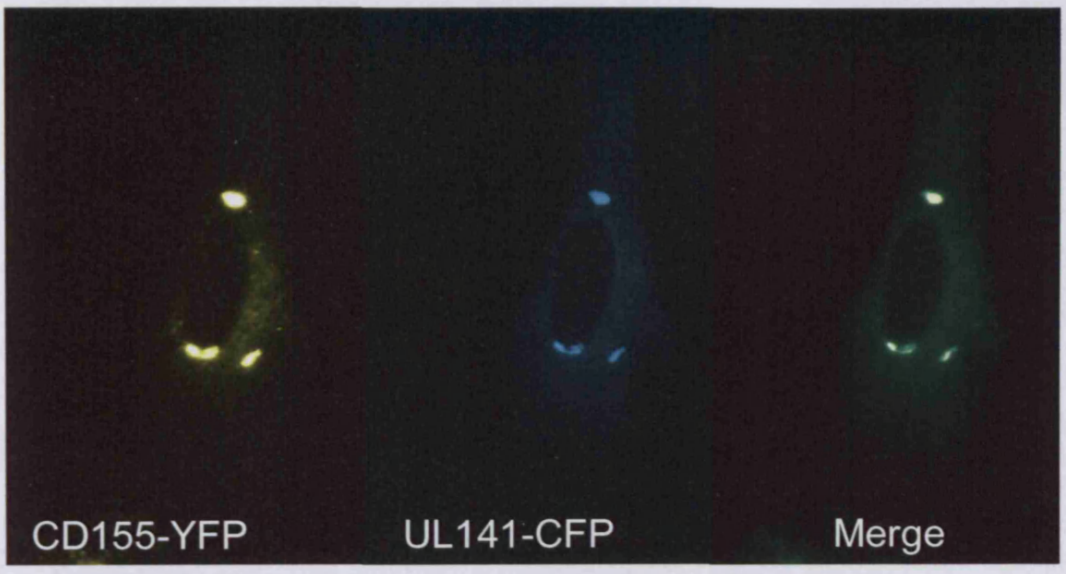


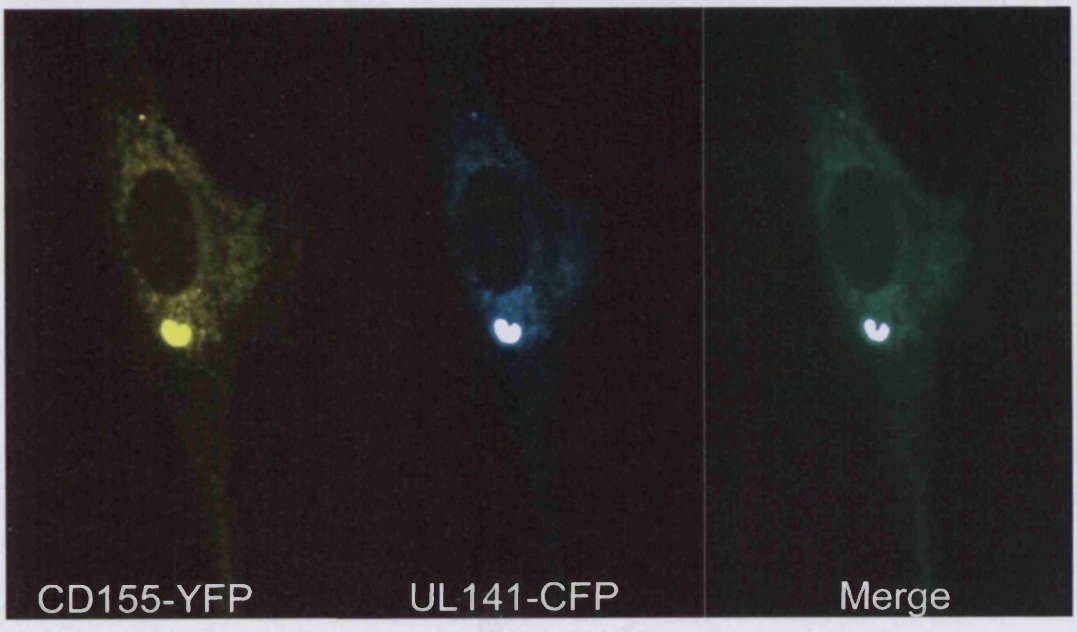

B – CD155CFP and UL141YFP

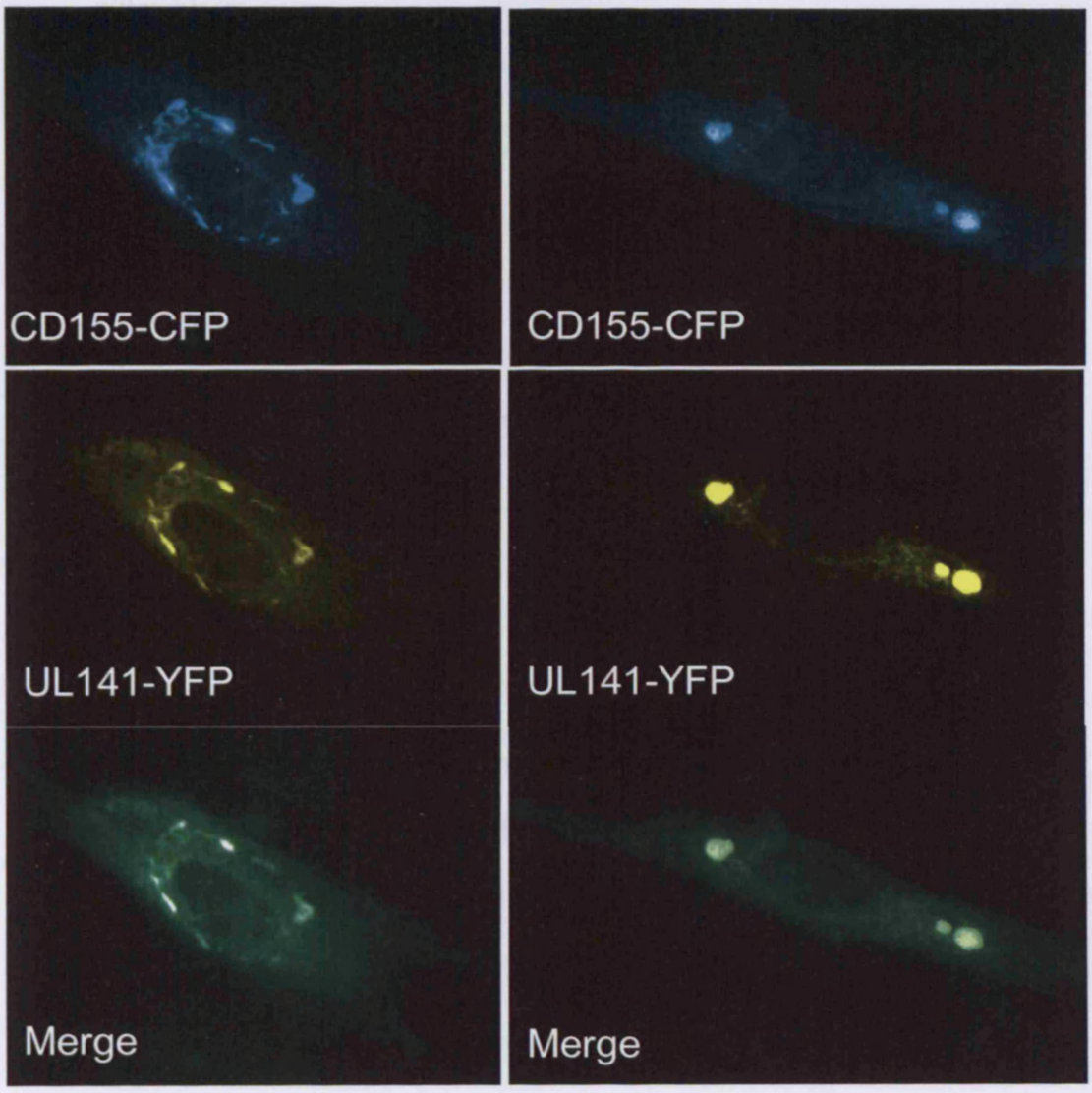


**Figure 4.7. Co-localisation of gpUL141 and CD155 in HFFF.**
HFFFs were transiently transfected with expression plasmids expressing (A) CD155-YFP (pCD155YFP) and gpUL141-CFP fusion protein (pUL141CFP) or (B) CD155-CFP fusion protein (pCD155CFP) and gpUL141-YFP fusion protein (pUL141YFP) using Nucleofector. Three days following transfection, cells were fixed and imaged directly. Fluorescence was detected and analyzed with a Leica DMIRBE microscope with Improvision Openlab software.

### 4.3.1 Confocal Imaging of gpUL141 and CD155 Transfection of Human Fibroblasts

To image the interaction between UL141 and CD155 in greater resolution confocal microscopy was used. In transfected HFFFs UL141CFP exhibited the same diffuse perinuclear distribution, but was observed to be granular with many foci of intense fluorescence (fig 4.8A). Inclusion bodies were well-defined and varied in both size and shape. Intracellular CD155YFP also exhibited a more granular appearance within cell, and finely labelled the outline of the cell membrane with the protein being more concentrated in some regions (fig 4.8B).

In co-transfection experiments, UL141CFP and CD155YFP co-localised within cells (fig 4.8B). The two proteins exhibited a granular distribution with many bodies of high fluorescence. The inclusion bodies, both large and small, consist of co-localised gpUL141 and CD155. While not all CD155 is intracellular, cell surface CD155 is not associated with gpUL141. This is likely to be breakthrough expression where CD155 is able to reach the cell surface without being retained by gpUL141.

To resolve the three-dimension structure of the gpUL141-CD155 inclusion bodies in HFFFs a series of images were taken along the z-axis at 1μm intervals (fig 4.9). CD155 and gpUL141 co-localise throughout the inclusion body. The inclusion bodies occur within the cell not at the cell surface and consist of a homogeneous mixture of

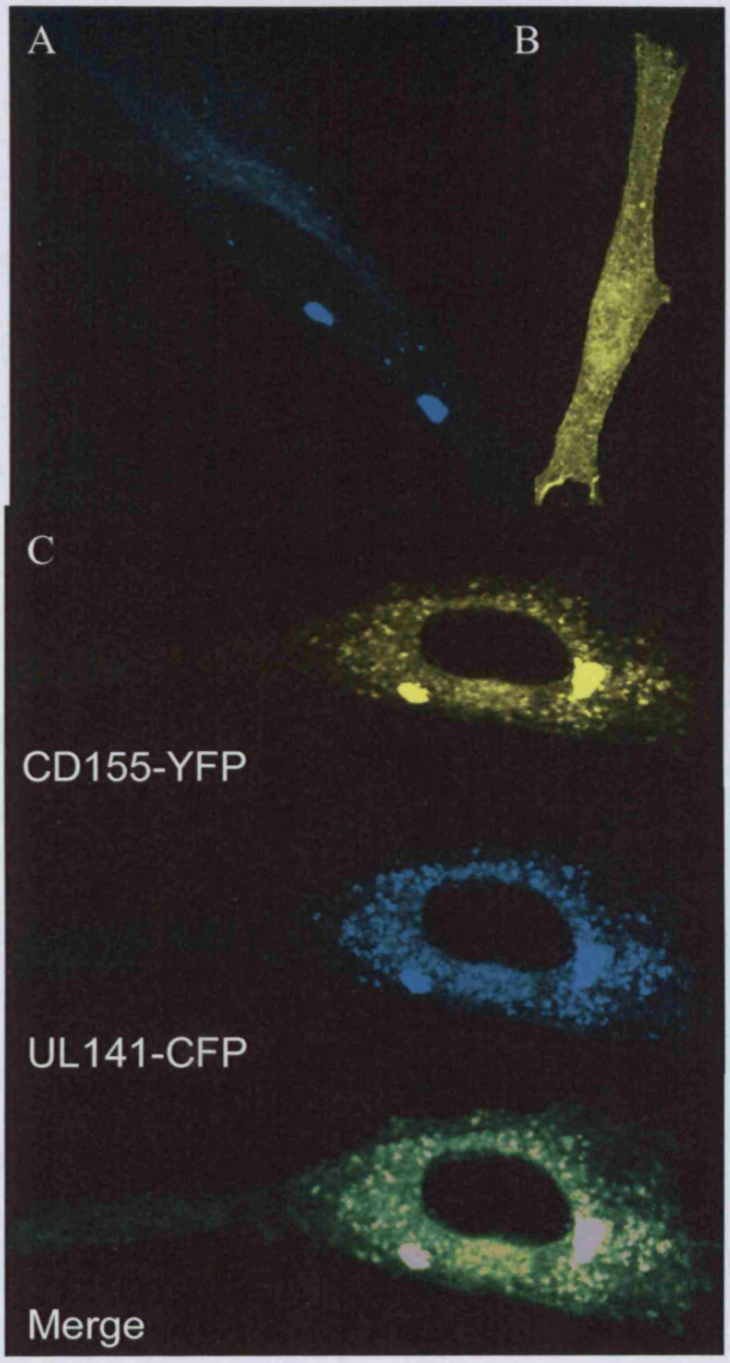


**Figure 4.8. Confocal microscopy of CD155YFP and UL141CFP**
HFFFs were transiently transfected with expression plasmids expressing (A) gpUL141-CFP fusion protein (pUL141CFP), (B) CD155-YFP fusion protein (pCD155YFP) or (C) CD155-YFP (pCD155YFP) and gpUL141-CFP fusion protein (pUL141CFP) using Nucleofector. Three days following transfection, cells were fixed and imaged directly. Fluorescence was detected and analyzed with a Leica SP5 resonant scanning confocal microscope. Cyan Channel – UL141-CFP, Yellow channel – CD155-YFP.

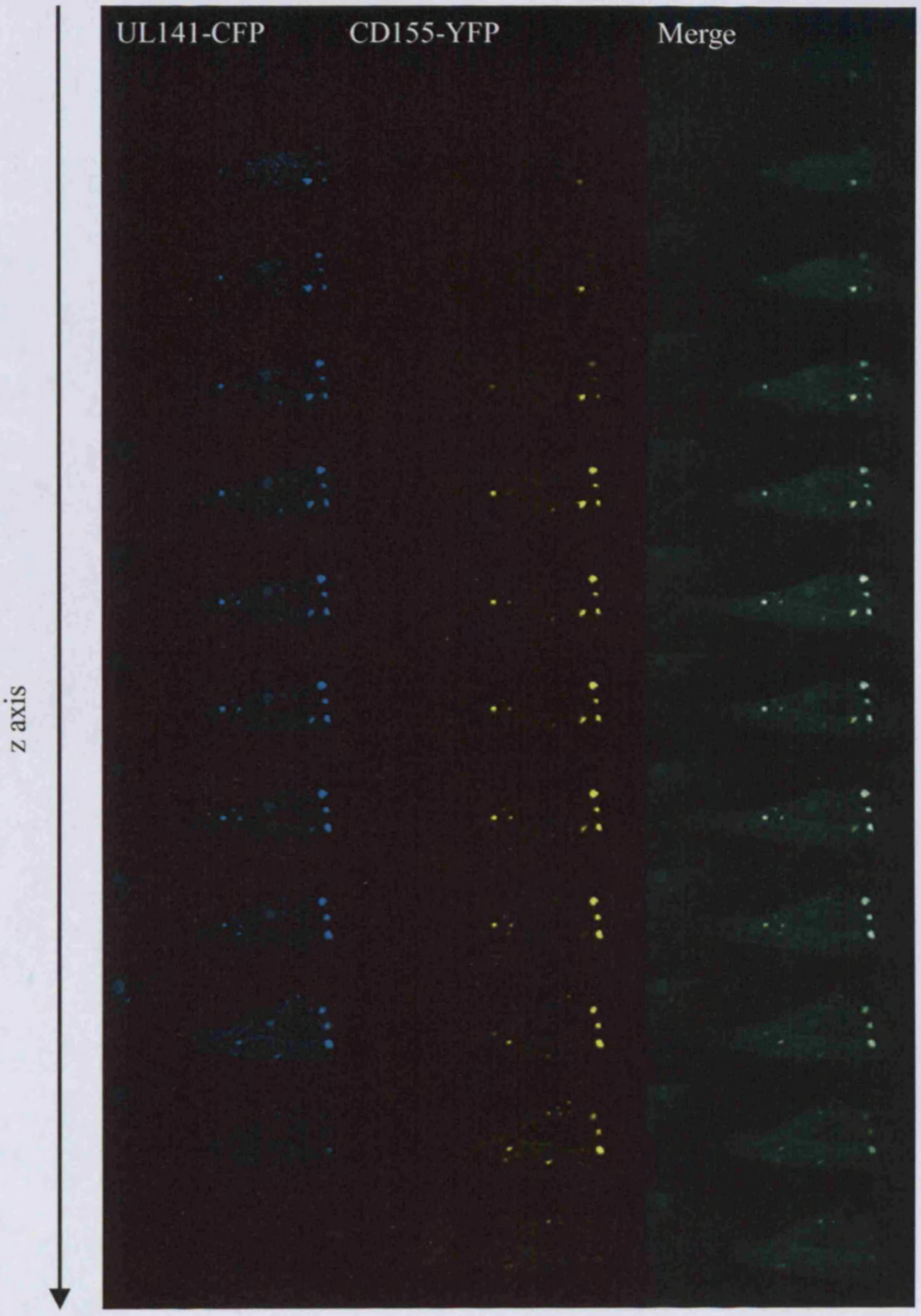


**Figure 4.9. Three dimensional co-localisation of CD155 and UL141.**
HFFFs were transiently transfected with expression plasmids expressing CD155-YFP (pCD155YFP) and gpUL141-CFP fusion proteins (pUL141CFP) using Nucleofector. Three days following transfection, cells were fixed and imaged directly. Fluorescence was detected and analyzed with a Leica SP5 resonant scanning confocal microscope. Serial images along the z-axis were taken at 1μm intervals. Yellow channel is CD155YFP, cyan channel is UL141CFP and the double overlay is shown.

gpUL141CFP and CD155YFP. In contrast to the immunofluorescence staining, where gpUL141 was only detected on the outer surface of inclusion bodies, UL141CFP and CD155YFP were present throughout the inclusion.

### 4.3.2 Intracellular localisation of CD155 and gpUL141

While gpUL141 was shown previously (by immunofluorescence) to be expressed in the ER (Tomasec et al. 2005), it was not possible at that time to image the retained intracellular form of CD155 with antibodies. HFFFs transfected with pCD155YFP and pUL141CFP were therefore stained for the ER marker calnexin. Calnexin associated closely with CD155 and gpUL141 (fig 4.10); indeed it was detected both in inclusion bodies and granular particles. There are occasional points of calnexin staining which do not correspond to CD155 or gpUL141 but the majority does co-localise. The distribution of calnexin show that the interaction between CD155 and gpUL141 occurs in the endoplasmic reticulum. The presence of large areas of calnexin staining corresponding with inclusion bodies suggest that the endoplasmic reticulum has been distended by the complex formation. The high level of calnexin co-localisation with the CD155-gpUL141 complex indicates that calnexin is also involved in the complex. Calnexin is a chaperon protein that binds N-linked glycoprotein in the endoplasmic reticulum. Both gpUL141 and the immature ER-resident form of CD155 have N-linked oligosaccharides so an interaction with calnexin is to be expected.

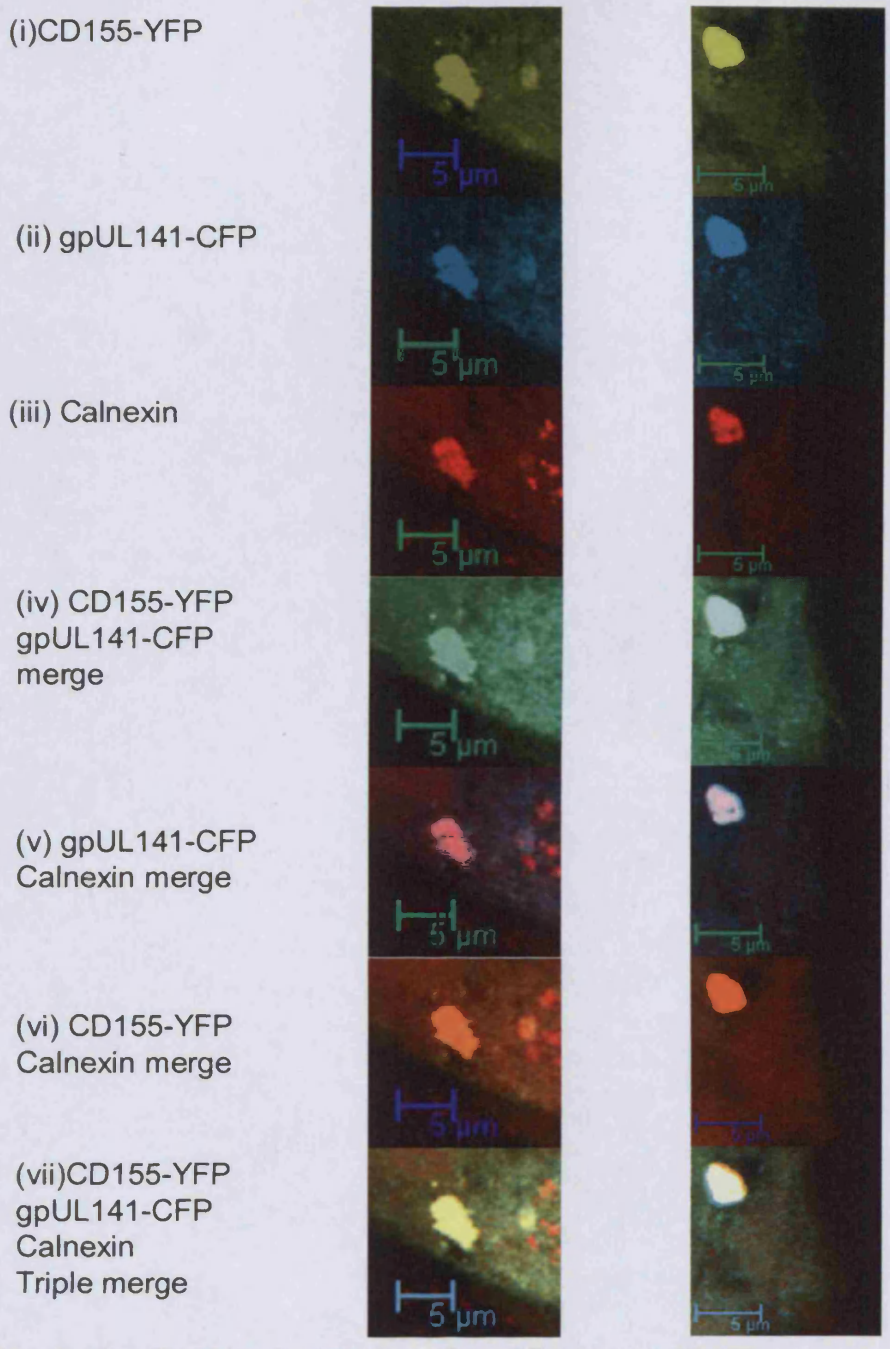


**Figure 4.10. Co-localisation of calnexin with gpUL141 and CD155.**
HFFFs were transiently transfected with expression plasmids expressing (A) gpUL141-CFP fusion protein (pUL141CFP), (B) CD155-YFP fusion protein (pCD155YFP) or (C) CD155-YFP (pCD155YFP) and gpUL141-CFP fusion protein (pUL141CFP) using Nucleofector. Three days following transfection, cells were fixed, stained with the anti-calnexin monoclonal C8.B6 (Chemicon) with goat anti-mouse AF647 as the secondary monoclonal then imaged directly. Fluorescence was detected and analyzed with a Leica SP5 resonant scanning confocal microscope. Images shown are of two separate cells, scale bar is 5µm. (A) CD155YFP is shown in yellow, (B) gpUL141CFP is shown in cyan, (C) Calnexin staining is shown in red (D) overlay of yellow and cyan channels, (E) overlay of cyan and red channels (F) overlay of yellow and red channels (G) overlay of all three channels.

## 4.4 Ad RECOMBINANTS ENCODING UL141 AND CD155 IN LIVE HUMAN FIBROBLASTS

RAd expressing UL141 and CD155 were created to overcome the limitations of transfection. Fibroblasts transfect at low efficiency, even the higher efficiency Nucleofection technique does not transfect all cells. Additionally, Nucleofection requires the cells to be in suspension during electroporation which is inappropriate for the study of UL141. UL141 expression reduces the ability of HFFF to adhere (chapter 3), this system may be selecting against high expression of UL141. RAd vectors overcome these limitations. RAd infections are much more controllable and reproducible, which means that 100% of cells can easily be infected. Additionally, RAd infections are performed on pre-adhered cells which is ideal for the study of adhesion-modifying factors. A RAd expressing UL141CFP (RAdUL141CFP) was generated by recombineering as described in materials and methods and used in concert with a RAd expressing CD155mCherry (RAdCD155mCh) that had already been generated in the laboratory.

Initially, cells were infected individually with RAdCD155mCh or with RAdUL141CFP. Reassuringly, both viruses produced distributions in agreement with the transfection studies. RAdUL141CFP infection produced fluorescence with intracellular distribution (fig 4.11A). However, the distribution is much more diffuse and without the inclusion bodies observed previously in the transfection images. CD155 had a cell surface distribution (fig 4.11B). The fluorescence is less even than when CD155 is expressed following transfection. There are intracellular

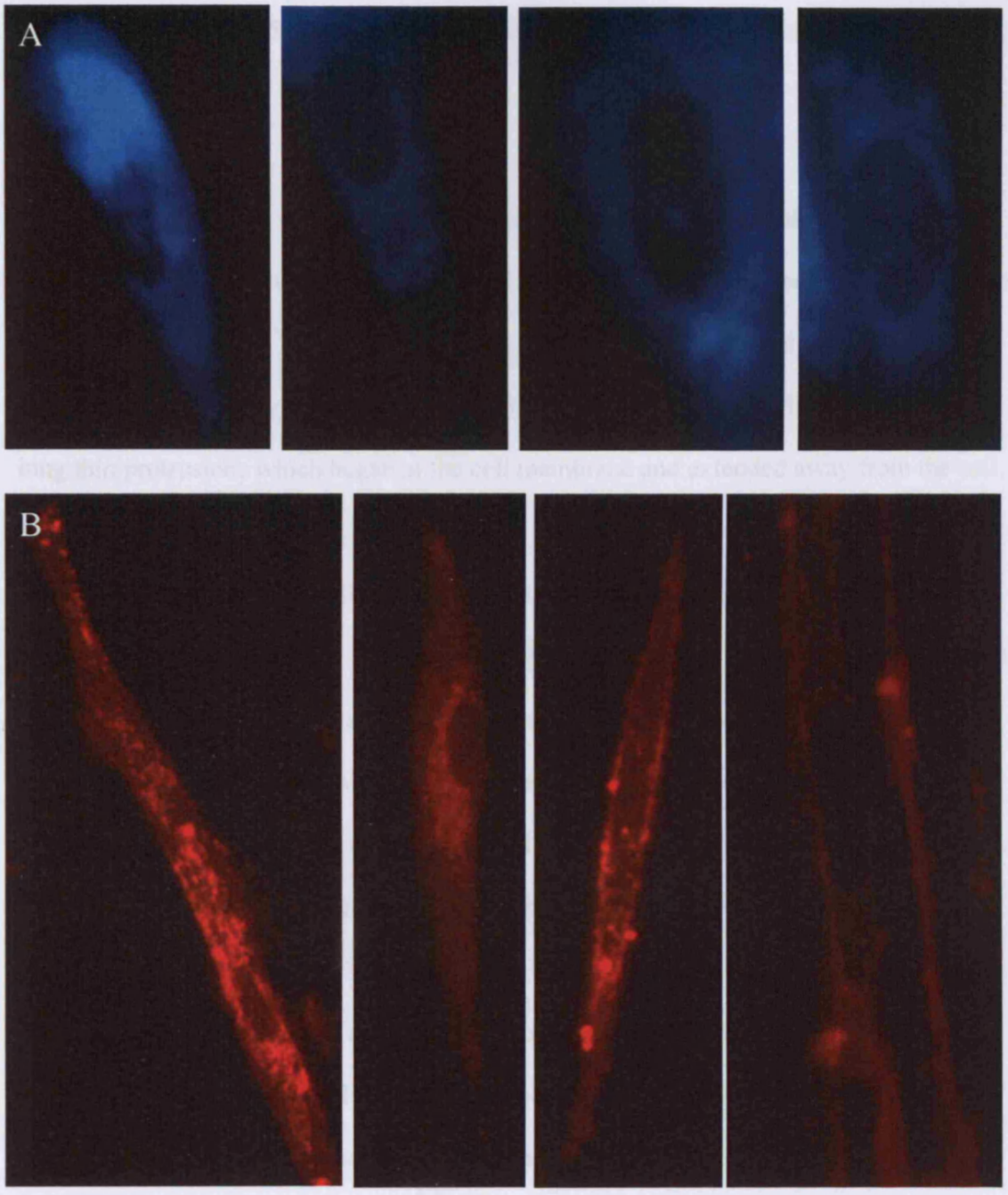


**Figure 4.11. Recombinant adenoviral vectors encoding CD155 and UL141.** HFFFs were infected with (A) RAdUL141CFP or (B) RAdCD155mCh incubated for three days then imaged directly.

concentrations of CD155 visible which are likely CD155 expressing intracellular vesicles.

Interestingly, infection with RAdCD155mCh had a marked effect on the morphology of the fibroblasts. Cells overexpressing CD155 appeared thinner and elongated compared to uninfected fibroblasts. This change in morphology is probably caused by an increase in cell adhesion caused by the overexpression of CD155. Also, these cells frequently had long thin protrusions which began at the cell membrane and extended away from the cell.

In co-infection experiments CD155 is retained within the cell and co-localises with gpUL141 (fig 4.12). As with the transfection system, inclusion bodies, consisting of both UL141CFP and CD155mCh, are observed. However, the inclusion bodies are generally larger and less well defined than those observed previously. The suppression of CD155 from the cell surface was less efficient in RAd infected cells compared to transfected cells. CD155, without gpUL141, was visible on the surface of RAd infected cells.

When UL141 is expressed in the presence of only endogenous CD155 there was few to no inclusion bodies present. However when both UL141 and CD155 are massively overexpressed by RAd infection, the inclusion bodies were frequently observed and were generally larger. The variation in size is likely because of the variable expression levels of both proteins. This suggests that the inclusion bodies form by CD155 complexing with gpUL141 and not by gpUL141 alone. Previously, gpUL141 had been shown to form large multimeric complexes with itself (Mel Armstrong, PhD thesis) which had

been hypothesised to be responsible for creating the bodies of high gpUL141 concentration.

## 4.5 IMAGING CD155YFP IN HUMAN FIBROBLASTS DURING HCMV INFECTION

Having established that gpUL141 and CD155 co-localise when both proteins are expressed via transfection or RAd infection, it was then important to study the distribution of CD155 during HCMV infection. All studies described so far have excluded all other HCMV proteins to image the interaction between CD155 and gpUL141. However the situation is more complex during HCMV infection. Recently, it has been identified that gpUL141 functions in concert with another, yet unidentified, HCMV protein to suppress the cell surface expression of nectin-2 (Tomasec, personal communication).

Previous attempts to visualise CD155 during HCMV infection used immunofluoresence (Tomasec et al. 2005). As stated above, the immature intracellular form of CD155 is not recognised by available antibodies. However, the CD155 fluorescent fusion protein enables the direct visualisation of intracellular CD155, so it is ideal for visualising CD155 during HCMV infection. Fibroblasts were transfected with pCD155YFP, allowed to adhere that infected with HCMVΔUL141 or the parental Merlin strain HCMV. After three days the cells were imaged directly.

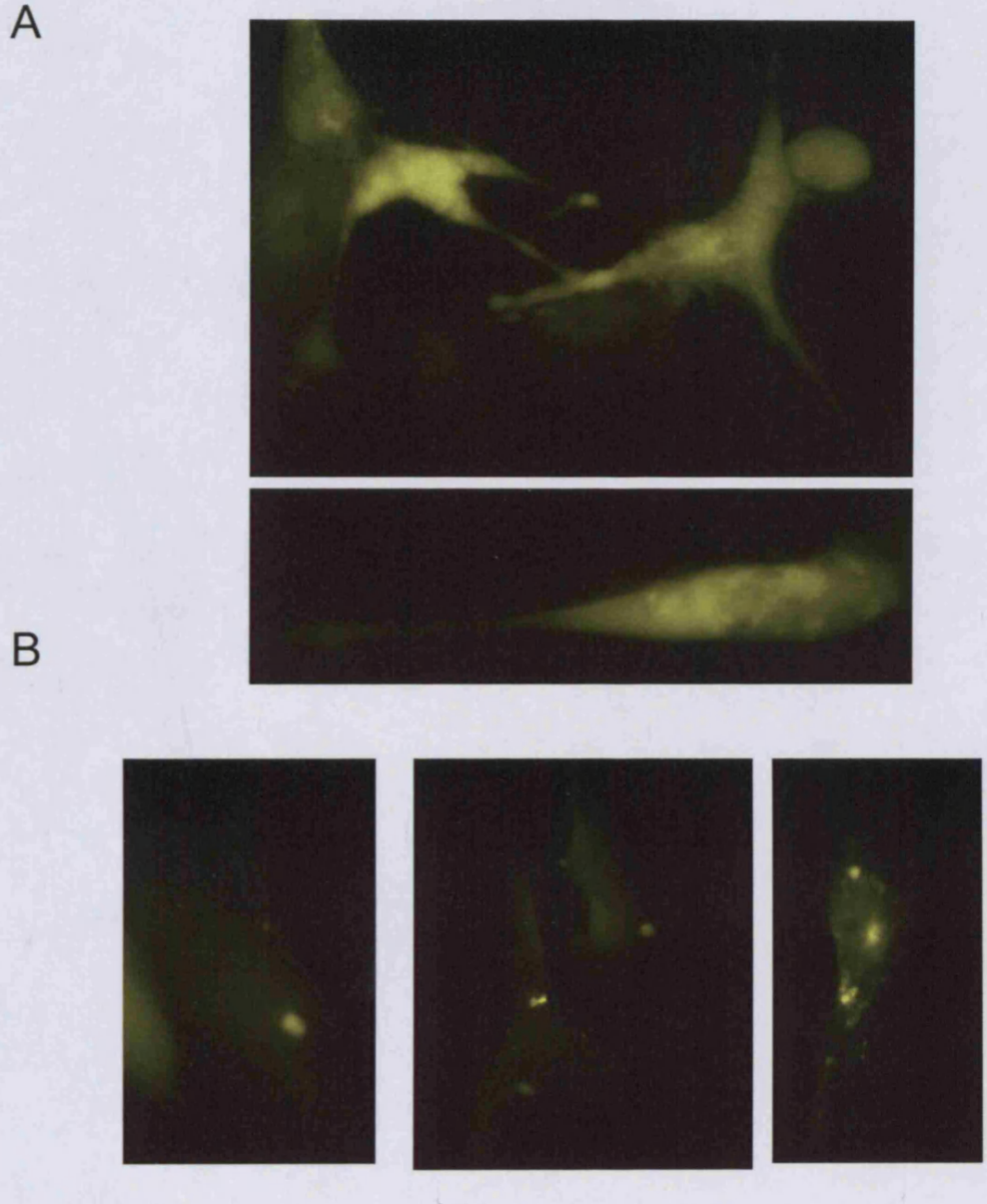


**Figure 4.13. CD155 distribution in HCMV-infected fibroblasts**
HFFF were transfected with pCD155YFP then infected with either (A) ΔUL141HCMV or (B) Merlin HCMV ΔUL141 HCMV then imaged after three days

The HCMVΔUL141 had been described as losing the ability to suppress cell surface expression of CD155 (Prod'homme, personal communication) and this was confirmed by the images (fig 4.13A). In CD155YFP-expressing fibroblasts infected with HCMVΔUL141, CD155 displayed the standard cell surface fluorescence with no intracellular fluorescence. Indeed, as previously described for laboratory strain which lack UL141 (Tomasec et al. 2005), cells appeared to have upregulated cell surface expression of CD155.

CD155YFP-expressing fibroblasts infected with Merlin strain HCMV displayed downregulation of cell surface CD155 with the characteristic inclusion bodies present (fig 4.13B). The inclusion bodies observed were generally smaller than those observed previously. The downregulation of CD155 was not as efficient as observed in both the transfection and RAd infection experiments. Extensive cell surface CD155 fluorescence is observed in addition to the intracellular fluorescence. This is to be expected as CD155 is hugely overexpressed compared to normal cellular levels.

This shows direct visual evidence that CD155 is downregulated from the cell surface and retained within the cell during HCMV infection. Despite any other interactions involving gpUL141 that occur during HCMV infection, the interaction with CD155 and formation of inclusion bodies originally observed in the transfection system are preserved during HCMV infection.

## 4.6 SUMMARY

When CD155 is expressed in the presence of UL141 it is retained within the cell as in an immature form. This immature form is not recognised by anti-CD155 mAbs, which, therefore, prevents the visualisation of the interaction between CD155 and gpUL141. Fluorescent fusion proteins of both CD155 and UL141 were generated to enable the direct visualisation and characterisation of the interaction between CD155 and gpUL141. Initially, this was important to confirm the findings of Tomasec and colleagues (2005), then used to further our understanding of the interaction. The fusion proteins had distributions consistent with previously published observations when expressed individually. When co-expressed, either by transfection or RAd infection, CD155 was downregulated from the cell surface and retained within the cell in agreement with Tomasec (2005). However, because of the fluorescent moiety fused to CD155 it was possible to directly image the immature intracellular form (see table 4.1 for summary of fluorescence results). When co-expressed with UL141, CD155 was intracellular and co-localised closely with gpUL141 in the ER. Large bodies of high fluorescence were often observed. These inclusion bodies were comprised evenly of both gpUL141 and CD155.

Additionally, I show that the ER chaperone, calnexin, closely co-localises with CD155 and gpUL141 and is included in the inclusion bodies. As both CD155 and gpUL141 are glycoproteins it is likely that calnexin interacts with both proteins.

The size and frequency of the inclusion bodies vary considerably. It appears that size and prevalence of these bodies depend on the relative expression levels of both proteins;

when UL141 is expressed only in the presence of endogenous CD155 (high gpUL141, low CD155) there were very few inclusion bodies present, while when both proteins are expressed by RAd infection (high gpUL141, high CD155) the inclusion bodies are large and plentiful.

Finally, the distribution of CD155 during HCMV infection was studied. Fibroblasts infected with HCMVΔUL141 did not downregulate cell surface CD155, while infection with the parental strain Merlin HCMV did result in the downregulation of CD155. As with the transfection and RAd infection experiments, intracellular CD155 accumulated in inclusion bodies. This shows that despite the function of gpUL141 being more complex during HCMV infection the interaction with CD155 is maintained.

**Table 4.1. Summary of Fluorescent imaging results**

| Cell Type | Expression Method | Expression construct/virus | Expression | Distribution |
|---|---|---|---|---|
| 293 Cells | Effectene transfection | pCD155CFP | CD155CFP | Cell Surface |
| | | pCD155YFP | CD155YFP | Cell Surface |
| | | pUL141CFP | UL141CFP | Intracellular |
| | | pUL141YFP | UL141YFP | Intracellular |
| | | pCD155CFP, pUL141YFP | CD155CFP, UL141YFP | Intracellular, CD155 and UL141 co-localise |
| | | pCD155YFP, pUL141CFP | CD155YFP, UL141CFP | Intracellular, CD155 and UL141 co-localise |
| HFFF | Nucleofector Transfection | pCD155CFP | CD155CFP | Cell Surface |
| | | pCD155YFP | CD155YFP | Cell Surface |
| | | pUL141CFP | UL141CFP | Intracellular |
| | | pUL141YFP | UL141YFP | Intracellular |
| | | pCD155CFP, pUL141YFP | CD155CFP, UL141YFP | Intracellular, CD155 and UL141 co-localise |
| | | pCD155YFP, pUL141CFP | CD155YFP, UL141CFP | Intracellular, CD155 and UL141 co-localise |
| | Nucleofector transfection with anti-Calnexin immunofluorescence | pCD155YFP, pUL141CFP | CD155YFP, UL141CFP | Intracellular, CD155, UL141 and calnexin co-localise |
| | RAd Infection | RAdUL141CFP | UL141CFP | Intracellular |
| | | RAdCD155mCh | CD155mCh | Cell Surface |
| | | RAdUL141CFP, RAdCD155mCh | UL141CFP, CD155mCh | Intracellular, CD155 and UL141 co-localise |
| | Nucleofector transfection with HCMV infection | pCD155YFP, strain Merlin HCMV | CD155YFP | Intracellular CD155 |
| | | pCD155YFP, ΔUL141 HCMV | CD155YFP | Cell Surface CD155 |

# 5 CHARACTERISATION OF gpUL141 IN HCMV VIRUS PARTICLES

HCMV disease can be associated with the infection of an extremely wide range of cell types *in vivo*, however in vitro efficient virus production is best achieved in primary human fibroblasts. Recent studies have revealed that to adapt to growth in fibroblasts HCMV clinical isolates reproducibly develop mutations in the UL128-131A locus (Dolan et al. 2004; Sinzger et al. 2000) and UL135 (Stanton et al, manuscript in preparation). Mutation in UL128-131A is associated with loss of endothelial and myeloid cell tropism (section 1.2.4). Interesting, UL141 is also often deleted from the genome of HCMV clinical isolates, although the selective pressure is clearly much less than for UL135 and UL128-131A (Davison, personal communication).

Although gpUL141 is a HCMV-encoded transmembrane glycoprotein, it was not initially considered to be a strong candidate to be a virion protein. The protein was shown to be retained in the ER, which is not the site for virion production. Additionally, UL141 has a recognised function in suppressing NK cell recognition during productive infection. However, CD155 is a recognised receptor for poliovirus and a range of herpesviruses (section 1.6.3). If gpUL141 were to be in the virion, it is possible that the interaction between gpUL141 and CD155 could potentially be involved during virus entry. Most studies of HCMV virion glycoproteins have been performed using the laboratory strain AD169 and Towne, which are both deleted in UL141. I therefore set out to determine whether gpUL141 was a component of virions.

## 5.1 gpUL141 IS A COMPONENT OF MERLIN HCMV VIRUS PARTICLES

To study the composition of HCMV virions, it is necessary first to purify them free from the cellular debris. Strains Merlin and AD169 strain were cultured in HFFF cells, then purified by ultracentrifugation over a continuous glycerol-sodium tartrate gradient. Following centrifugation three bands are visible; NIEPs at the top, mature virus particles in the middle and dense bodies at the bottom. The mature virus particle band was removed from the gradients with a large gauge needle then washed and resuspended in sodium phosphate buffer. The presence of virus particles was tested by blotting for the HCMV envelope glycoprotein gB. Occasionally virion envelopes can be lost through osmotic shock, thus gB was indicative that the virions were intact. To control for cellular protein contamination the samples were probed for the major immediate-early protein IE1p72, which is known not incorporated into virions. Strain Merlin-infected HFFF extract, purified strain Merlin virions and purified strain AD169 virions were all positive for gB (fig 5.1A), with a 55 kDa band visible in all three lanes. The mAb used for detection of gB recognises only the cleaved 55kDa transmembrane component but not the extracellular component or uncleaved precursor. The detection of the 72 kDa IE1 protein was in strain Merlin-infected cell extracts, but in neither of the two purified virion preparations (fig 5.1B), was evidence that the purified virus preparation are not contaminated with extraneous protein from infected cells.

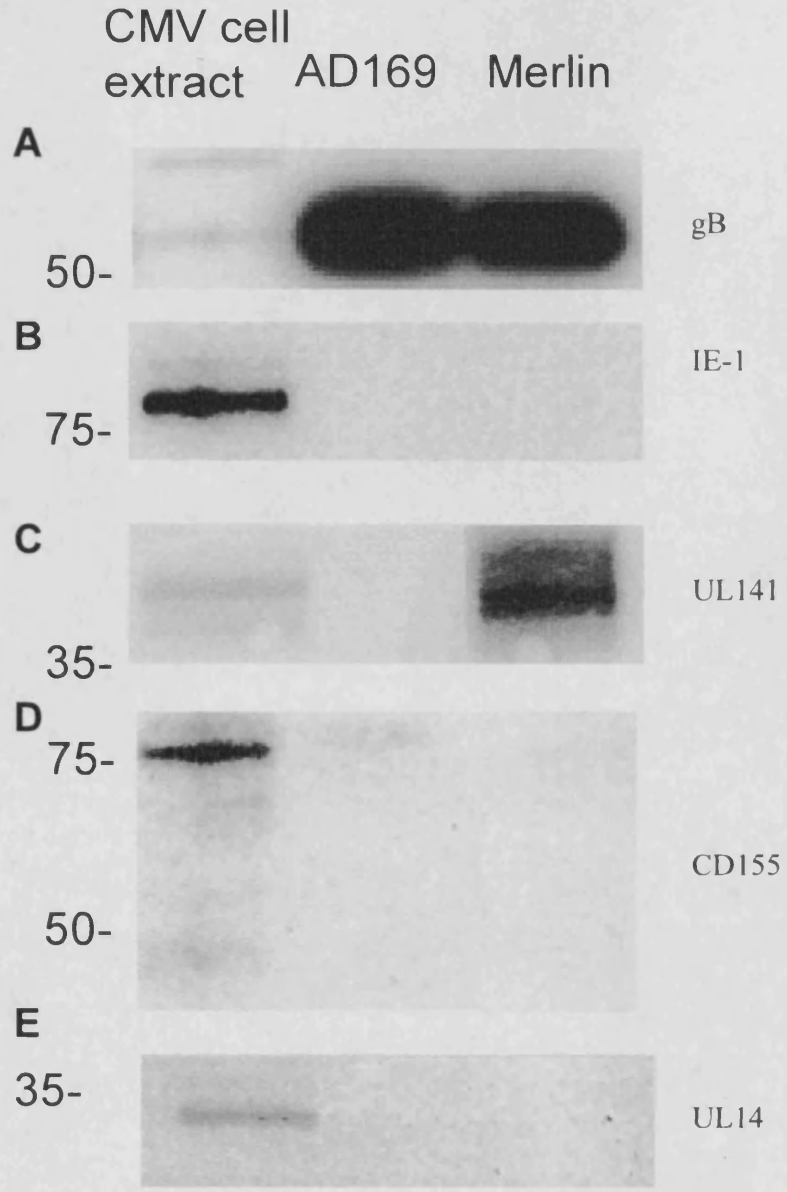


**Figure 5.1. gpUL141 but not gpUL14 or CD155 is a component of the Merlin HCMV virus particle.**
Strain AD169 HCMV and strain Merlin HCMV were purified by ultracentrifugation in a glycerol-tartrate gradient. Purified virus particles and the cell extract of HCMV infected HFFF were blotted with the (A) 2F12 mAb specific for the envelope glycoprotein gB, (B) 8b1.2 mAb to the immediate-early protein IE-1, (C) the gpUL141-specific M550 mAbs, (D) 5D1 mAb to CD155 and (E) mAbUL14 specific for gpUL14. Left margin, molecular sizes (in kDa).

Having established that the purified viruses were free of cellular contamination, they were then blotted for gpUL141 (fig 5.1C). Strain Merlin-infected cell extract was positive for gpUL141 with a double band visible at 37 and 40 kDa. UL141 is encoded by UL/*b*' sequence that is missing from all passaged strains of HCMV, strain AD169 virions were therefore included as a negative control for non-specific antibody binding. Purified strain AD169 virions were negative for staining with the gpUL141 mAb.

Purified strain Merlin virions were positive for gpUL141 staining. gpUL141 stained as a doublet approximately the same size as the gpUL141 staining in Merlin strain HCMV-infected cell extract. Additionally, there is a selective concentration of gpUL141 in the virion, as was observed also for gB. The gpUL141 staining of the purified strain Merlin virion is not because of contamination with cellular proteins as the strain Merlin virions stain negative for the intracellular localised immediate early protein IE1p72. Therefore, gpUL141 is a component of the strain Merlin HCMV virion.

gpUL141 and CD155 co-localise within infected cells when co-expressed, indicative of the proteins being in a complex (Chapter 4). To determine if CD155 is also incorporated into the virus the purified virus was blotted for CD155 (Fig 5.1D). When blotted for CD155, strain Merlin-infected HFFF displays bands at 75 and 50 kDa. However, both Merlin and AD169 purified virus particles are negative for CD155.

Although gpUL141 and CD155 co-associate in fibroblasts, only gpUL141 was incorporated into the virion. The selective incorporation of gpUL141 was consistent with it being an active process rather than non-specific incorporation of infected cell

glycoproteins. Cellular proteins can detected in purified virions, and it may be possible that more sensitive assays could detect the presence of low amounts of CD155 in the virion. However, there is no concentration of CD155 as there is for gpUL141 and gB. Therefore, CD155 is not intentionally incorporated into the virion. The result also implies that since gpUL141 in virions may yet have the capacity to bind CD155 during the infection process.

gpUL14 is the only known homologue to gpUL141. There are functional similarities between the two proteins; when expressed from an Ad vector gpUL14 can suppress NK cell function (Wilkinson, personal communication), and gpUL14 also reduces cell adhesion to the same extent as gpUL141 (Chapter 3.2). Because of the structural and functional similarities, the purified virus particles were then blotted for gpUL14. Strain Merlin-infected cell extract produced a band at 30 kDa, while both strains Merlin and AD169 purified virions were negative. Both strains of HCMV used encode UL14, express gpUL14 during productive infection but neither incorporates gpUL14 into their virions. This is further evidence that the incorporation of gpUL141 into the virion was selective.

## 5.2 LOCATION OF gpUL141 IN THE VIRION

HCMV virus particles consist of three parts: capsid, tegument and envelope (fig 1.3). Glycoproteins involved in virus attachment and entry are invariably associated with the

envelope. If gpUL141 is in the envelope, it may be on the outside surface of the virion and in a topologically appropriate location to be involved in virion attachment and entry

Purified strain Merlin virus particles were dissolved in Triton X-100 for one hour at 4°C. The precipitate was centrifuged and the soluble fraction was extracted. Following the re-suspension of the insoluble precipitate the two fractions, plus whole purified Merlin virions were examined on Western blots using mAbs to the tegument protein pp65, the envelope glycoprotein gB and gpUL141 (fig 5.2A). pp65 was only present in the insoluble fraction, consistent with the tegument protein remaining attached to capsids during the extraction process. gB was present in both the soluble fraction and the insoluble fraction, indicating that the virion envelope has not been completely dissolved. Parts of the envelope may remain attached to the tegument following detergent treatment (Farrar and Oram 1984). If the envelope was completely dissolved gB would be only present in the soluble fraction. gpUL141 follows the same pattern as gB; gpUL141 is present in both the insoluble and soluble fractions. As the soluble fraction was free from tegument and capsid, this implied that gpUL141 was present in the envelope of the virion. However, because of the incomplete separation of the envelope from the tegument and capsid it was not possible to rule that gpUL141 was present only in the

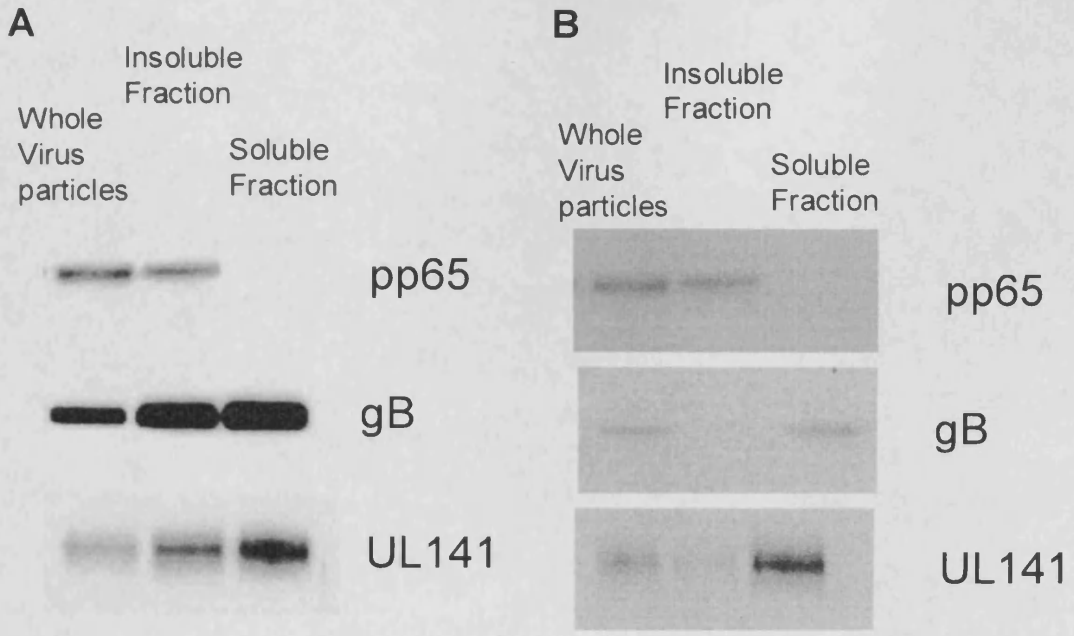


**Figure 5.2. Detergent fractionation of the Merlin virion.**
Purified strain Merlin virus particles were dissolved in either Triton x-100 (A) or 1% NP-40 and 0.5% deoxycholoate (B). The insoluble portion was spun down and the soluble portion was removed. The pelleted insoluble portion of the virus particles was resuspended. Purified Merlin virus and both the insoluble fraction and the soluble fraction were blotted for pp65, gB and UL141.

envelope. Triton X-100 has reduced effectiveness at low temperatures, which may prevent complete separation of the envelope (Roberts 2008).

The previous method used Triton X-100, a non-ionic detergent. Non-ionic detergents are typically milder and less likely to denature proteins than ionic detergents. To enhance the separation of the membrane, a mixture of non-ionic and ionic detergents were used. Purified Merlin virus particles were dissolved in NP40, a non-ionic detergent, and sodium deoxycholate, an ionic detergent, for one hour at room temperature (Wang et al. 2004c). The soluble fraction was removed and the insoluble precipitate was redissolved in sodium phosphate buffer. Both fractions plus whole virus particles were blotted for pp65, gB and gpUL141 (fig 5.2B). pp65 is present only in the whole virus particles and in the insoluble fraction (fig 5.2A); thus showing that the capsid and tegument have separated together into the insoluble fraction. gB is present in the soluble fraction and absent from the insoluble fraction (fig 5.2B). This showed that the envelope has been successfully dissolved from the rest of the virus. It also shows that the inclusion of an ionic detergent has not denatured the virion envelope proteins. When the fractions are probed for gpUL141 (fig 5.2C), the protein was predominantly present in the soluble fraction with a small amount detected in the insoluble fraction. This result was also consistent with that gpUL141 being present in the envelope membrane. The C-terminal tail of gpUL141 is predicted topologically to be inside the virion envelope. The fact that gpUL141 was also detected in the insoluble fraction suggests that a component of the protein may interact with the tegument, to a greater degree than gB. Nevertheless, gpUL141 was predominantly located in the HCMV envelope, consistent with it being a transmembrane glycoprotein.

## 5.3 GLYCOSYLATION OF VIRION gpUL141

For gpUL141 to be incorporated in the virus particle it must be trafficked from the ER to the cytoplasmic assembly site. Endo H selectively cleaves high-mannose asparagines-linked oligosaccharides typically associated with core oligosaccharide added to proteins the ER, but not processed complex oligosaccharides. Remodelling of oligosaccharides occurs during protein trafficking through the Golgi apparatus, with high-mannose oligosaccharides being trimmed and converted to complex oligosaccharides. Cell-associated gpUL141 was sensitive to Endo H digestion, which is consistent with immunofluorescence studies showing gpUL141 being ER resident. To be incorporated into virions, however, gpUL141 must exit the ER. To assess whether gpUL141 is processed through the Golgi apparatus, the glycosylation status of gpUL141 from cells and virus particles was examined. Strain Merlin HCMV was purified by isopycnic gradient ultracentrifugation then digested overnight with Endo H or with PNGase. PNGase deaminates asparagine to release all high-mannose and complex oligosaccharides from glycoproteins.

gB in strain Merlin virions and infected-cell extract display the same pattern of glycosylation (fig 5.3A), which is consistent with previously published results (Marshall et al. 1996; Strive et al. 2002a). gB is partially sensitive to Endo H digestion but further sugar residues are released when digested by PNGase. This is consistent with gB in both cells and virus particles being a hybrid molecule consisting of both high mannose and complex oligosaccharide side chains. To achieve partial protection against PNGase, gB presumably has been exposed to enzymes in the Golgi apparatus.

gpUL141 in strain Merlin-infected cell extract migrated by SDS-PAGE to produce a protein doublet with molecular mass estimated to be 40 and 37 kDa (fig 5.3B). Following digestion by Endo H or by PNGase, gpUL141 is deglycosylated to a 35kDa band. gpUL141 in infected cell extracts was sensitive to Endo H, which is consistent with gpUL141 being as ER resident protein. gpUL141 present in purified Merlin virions appeared to co-migrate with gpUL141 in cell extracts. PNGase digestion of gpUL141 from purified virions yielded a single 34kDa product. Endo H digestion of gpUL141 from virions produced two major products with apparent molecular masses of 38 and 36 kDa, while PNGase digestion of cellular gpUL141 produced a single band at 34kDa. PNGase treatment of virions and cell extracts generated a similar size product; consistent with there being no obvious modification of the protein backbone during incorporation of gpUL141 into the virus particle. The slower migrating band in the virion is completely protected by Endo H, while the faster migrating for is partially susceptible to digestion. This is consistent with two populations of gpUL141 being packaged. The fact they appear to reduce to a single size on PNGase treatment indicated that they were different glyocoforms. One of the glycoforms was processed to a completely Endo H-resistant form, while the other was only partially protected; like gB corresponding to a hybrid glycoprotein. While the majority of gpUL141 in infected cells remained Endo H sensitive and ER-localised, a proportion appeared to transit through the Golgi apparatus to be selective incorporated into HCMV virions.

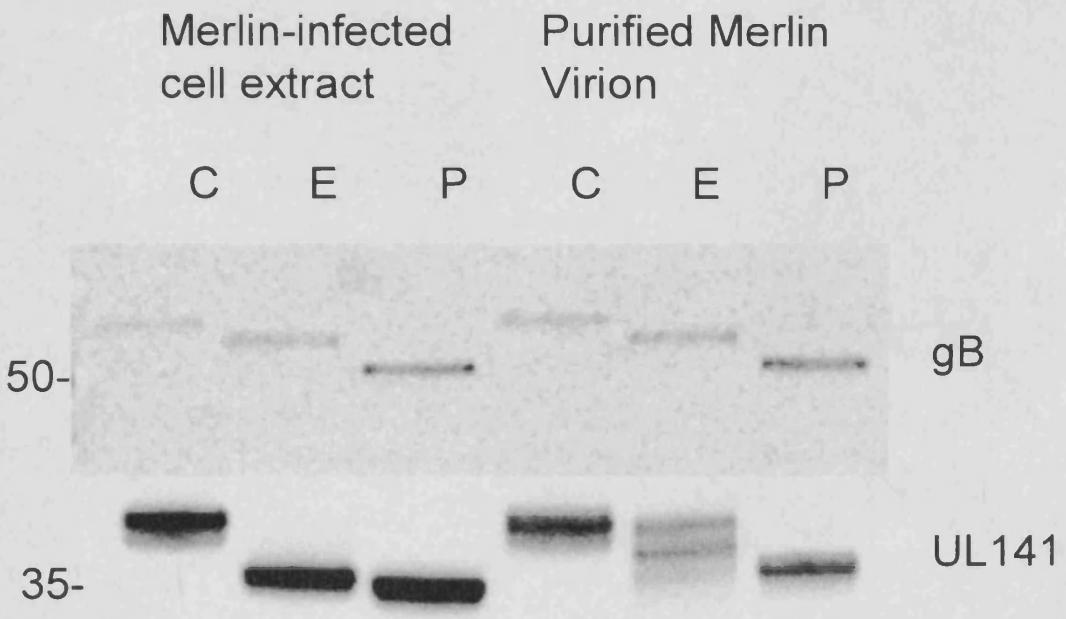


**Figure 5.3. Glycosylation of UL141 in cells and virus particles.**
Cell extract of HFFF infected with strain Merlin HCMV and purified strain Merlin HCMV virus particles were digested overnight with Endoglycosylase H (E), PNGase (P) or mock digested (C). The digested cell extracts and virus particles were then blotted with 2F12 mAb specific for the envelope glycoprotein gB and the gpUL141-specific M550 mAbs

### 5.3.1 Timecourse of gpUL141 glycosylation

gpUL141 in strain Merlin virions has a different pattern of glycosylation from gpUL141 in the ER. HCMV has an exceptionally slow replication cycle in fibroblasts. Typically, *de novo* virus production is first detected at 72h p.i., yet peak levels are not reached until 120 h p.i.. In this laboratory, NK assays are typically performed at 72 h p.i., and thus that was the preferred time point to monitor gpUL141 expression. At 72h p.i., the function of gpUL141 was likely to be biased towards CD155 retention rather than virus production. Since the complex glycosylation pattern was associated with virion production, I sought to follow gpUL141 expression temporarily across a full cycle of productive infection. HFFF were infected with Merlin HCMV at a high MOI and cell extracts were collected at 24 hour intervals. The cell extracts were then digested overnight with Endo H or PNGase (fig 5.4). All samples were blotted for actin to control for protein levels (fig 5.4A). gB was blotted to control for virus infection and digestion by Endo H and PNGase (fig 5.44B). gB is first detected at 3 days post infection with the same pattern of glycosylation observed above. gpUL141 is first detected at day 2 and the protein accumulates during the timecourse (fig 5.4C). gpUL141 is first detected as is a single 40 kDa species (2 days p.i.), yet over the course of infection a faster migrating species becomes more abundant. By 5 days p.i. the two forms of gpUL141 are expressed in similar abundance. The Endo H and PNGase digestion follow the same pattern. At early timepoints, Endo H and PNGase digestion both produce a single product at about 34kDa while at later time points deglycosylation of gpUL141 produces a doublet with the apparent sizes 32 and 34 kDa. As this doublet is present in the undigested and PNGase

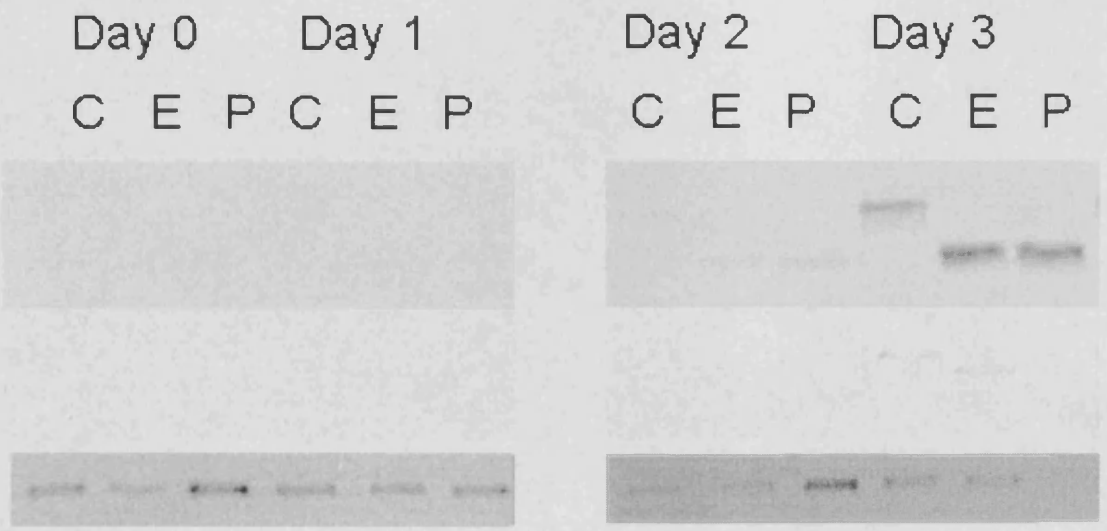


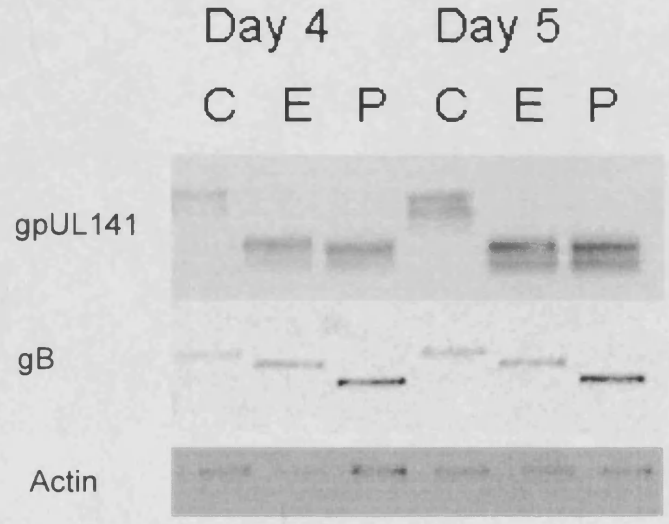


**Figure 5.4. UL141 glycosylation during the course of HCMV infection.**
HFFF were infected with strain Merlin HCMV at a moi of 5. Samples were taken at 0, 1, 2, 3, 4 and 5 days post infection. The cells extracts were mock digested (C) or digested with Endoglycosidase H (E) or PNGase (P). The digested extracts were blotted for gB, UL141 and actin.

digested samples it due to a modification (possibly proteolytic processing) in the protein backbone of gpUL141 rather than a change in glycosylation.

### 5.3.2 Comparison of the glycosylation of gpUL141 from cells and virus particles

In the previous section small differences in the migration of gpUL141 was observed between samples. It was unclear whether these differences were actual differences in molecular weight or a result of uneven migration on nonadjacent tracks on the polyacrylamide gel. To minimise gel effects and to enable more direct comparison of the digested forms of gpUL141, a western blot was performed with the samples grouped by glycosidase digestion method (fig 5.5). The undigested products of the three samples all migrate as a doublet consisting of 40 and 37 kDa products, albeit in different abundance. However, the pattern of Endo H digestion is different in each of the three samples. gpUL141 from both HCMV-infected cell extracts (day 3 and 5) are sensitive to Endo H digestion. Digestion of gpUL141 in the 3 day p.i. cell extract produced a single band with an apparent molecular weight of 34 kDa. A doublet, with the apparent molecular weights of 34 and 32 kDa, was observed following digestion of 5 day p.i. cell extract. gpUL141 in virions exhibits a degree of resistance to Endo H, the 40 and 36 kDa species corresponds to the doublet observed in the undigested fraction. However, the apparent increase in the 36kDa form and appearance of low abundance faster migrating species indicated some sensitivity to Endo H. PNGase digestion produces a single 34 kDa band in both the day three post infection cell extract and the purified virion, while PNGase digestion of day five cell extract produces a 34 and 33 kDa doublet.

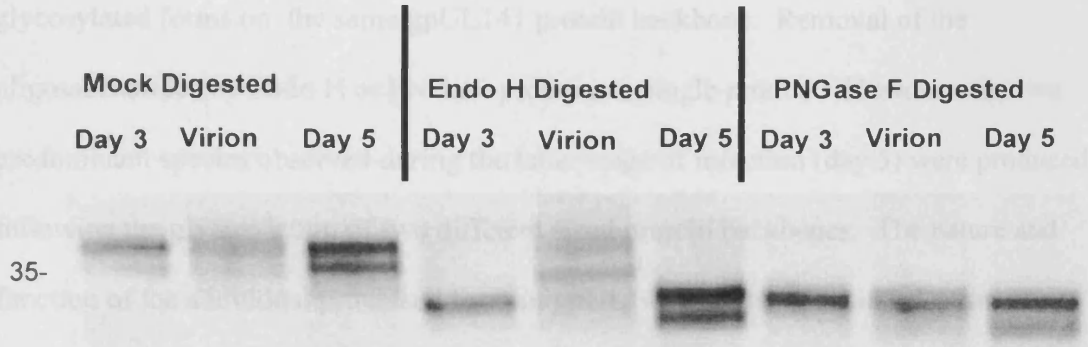


**Figure 5.5. Comparison of glycosylation of early and late time point gpUL141 and virion gpUL141.**
Cell extracts from fibroblasts infected with a high moi of strain Merlin HCMV were taken at three days post infection and five days post infection. Purified strain Merlin virions and the cell extracts were digested overnight with Endo H, PNGase or mock digested. The digested samples were then blotted for gpUL141.

Taken together these results indicated that the two species observed during the early stages of HCMV infection in fibroblasts were probably the result of two different glycosylated forms on the same gpUL141 protein backbone. Removal of the oligosaccharides by Endo H or PNGase produces a single product. However, the two predominant species observed during the latter stage of infection (day 5) were produced following the glycosylation of two different sized protein backbones. The nature and function of the additional processed form of gpUL141 produced late in infection is currently not known, it was not packaged into virions. Additional low abundance bands visible on with undigested sample (day 5), would also be consistent with it also being expressed as two glycoforms. gpUL141 incorporated into the virion has a different glycosylation pattern than the most abundant form of gpUL141 from HCMV-infected cells; the virion-associated gpUL141 being resistant to Endo H digestion. This shows that the virion-associated form of gpUL141 does not accumulate within the cell; rather it must be processed then rapidly incorporated into the virion.

## 5.4 NEUTRALISATION OF HCMV INFECTION WITH ANTI-GPUL141 ANTIBODIES

UL141 is located on the envelope of HCMV virus particles. The possibility exists that gpUL141 could have a role in virus infection, possibly exploiting its interaction with CD155. As a component of the virion envelope, gpUL141 also become a potential target for the humoral immune system. To investigate whether gpUL141 is accessible on the surface of virion for antibody binding, a neutralisation assay was performed.

As controls, HCMV seropositive (HS3) and seronegative (HS11) human polyclonal antibodies were used to set parameters. Since gB is recognised to contain a number of neutralising epitopes, a mAb to gB potentially provided a positive control. I was fortunate to have access to two gpUL141-specific mAbs (m550.2 and m550.3) and a strain Merlin reported virus encoding a UL32GFP fusion protein. Both gpUL141-specific mAbs were generated against a soluble form of gpUL141 which only consists of the extracellular domain. HCMV was mixed with doubling dilutions of serum or monoclonal antibodies then the mixture was added to confluent fibroblasts in triplicate. Additionally, virus without any antibodies was added to fibroblasts to control for initial virus levels. After 2 days the cells were examined and the number of green fluorescent cells were counted. HCMV positive human sera neutralised the infection, while HCMV negative human serum did not. 50% neutralisation occurred at a dilution greater than 1:640 for positive serum HS3 (fig 5.6). MAbs specific for gB neutralised the infection with 50% neutralisation occurring at a dilution between 1:80 and 1:160. MAbs specific

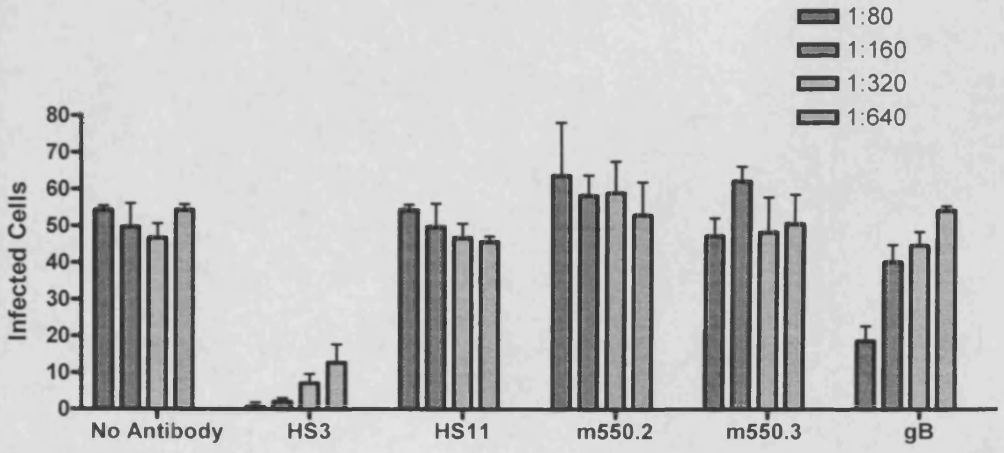


**Figure 5.6. Neutralisation of HCMV infection by human sera and HCMV specific monoclonal antibodies.**
Neutralisation of HCMV infection of HCMV positive human serum (HS3), HCMV negative human serum (HS11), two gpUL141 specific mAbs (m550.2 and m550.3) and gB specific mAb. GFP positive cells were counted. Data shown is the mean of three replicates with the standard deviation.

for UL141 did not neutralise at any dilution used (fig 5.6). It is possible that the UL141-specific antibodies are binding to the virion but not enough to induce neutralisation. These results show that UL141-specific antibodies do not neutralise HCMV infection. This could mean that UL141 is not on the outside of the envelope and, therefore is not accessible to the antibodies. Alternatively, the UL141 antibodies may be binding to UL141 but are unable to neutralise the infection.

## 5.5 FLOW CYTOMETRY ANALYSIS OF HCMV VIRIONS

In a further attempt to detect gpUL141 on the surface of Merlin virus particles flow cytometry was used. Brussaard and colleagues (2000) have described the ability to detect fluorescence-labelled HCMV virions by flow cytometry. However, the use of flow cytometry to stain for HCMV virion glycoproteins appears to be novel approach.

Initially, I needed to establish that HCMV virions could be detected by flow cytometry. Recombinant HCMV virions encoding a UL32GFP fusion protein, UL32GFP-RCMV, were purified using ultracentrifugation then inactivated by gamma-irradiation (data not shown). Unstained purified UL32GFP-RCMV virions were then analysed by flow cytometry. Individual virus particle were observed by side and forward scatter (fig 5.7A). The virus particles were also detected by GFP fluorescence, while untagged HCMV virions were negative for GFP fluorescence (fig 5.7B).

Having established that individual virus particles could be detected by flow cytometry, I then attempted to detect envelope glycoproteins by staining with specific antibodies. In

addition to the gpUL141-specific mAb, antibodies specific to the envelope glycoprotein gB and the tegument protein pp65 were also used. The virions were stained with gB as a positive control of the staining procedure and pp65 staining was included to ensure that the virion particles where intact. Purified and gamma-irradiated UL32GFP-RCMV virus particles and AD169 virus particles were stained for gB, pp65 and gpUL141 then analysed by flow cytometry (fig 5.7B). Although initial preliminary results were encouraging (not shown), it became apparent that a high level of non-specific and auto fluorescence was responsible for the signal. Both Merlin and AD169 purified virions also stained positive for gpUL141. As AD169 lacks the UL141 ORF, it must be concluded that this result is non-specific binding of the antibody to the virion.

The detection of envelope glycoproteins by flow cytometry could potentially be a powerful technique for the study of HCMV virions. The development of this technique was limited by time and available reagents. There are still several limitations to overcome before this technique could be used.

The major issue that needs to be addressed is the high level of non-specific fluorescence. The size of a virus particle limits the amount of antigen available; it is clearly much smaller than a eukaryotic cell. High concentrations of antibody may therefore be required to produce a detectable signal. However, high antibody concentrations contribute to the high levels of background fluorescence. The development and use of

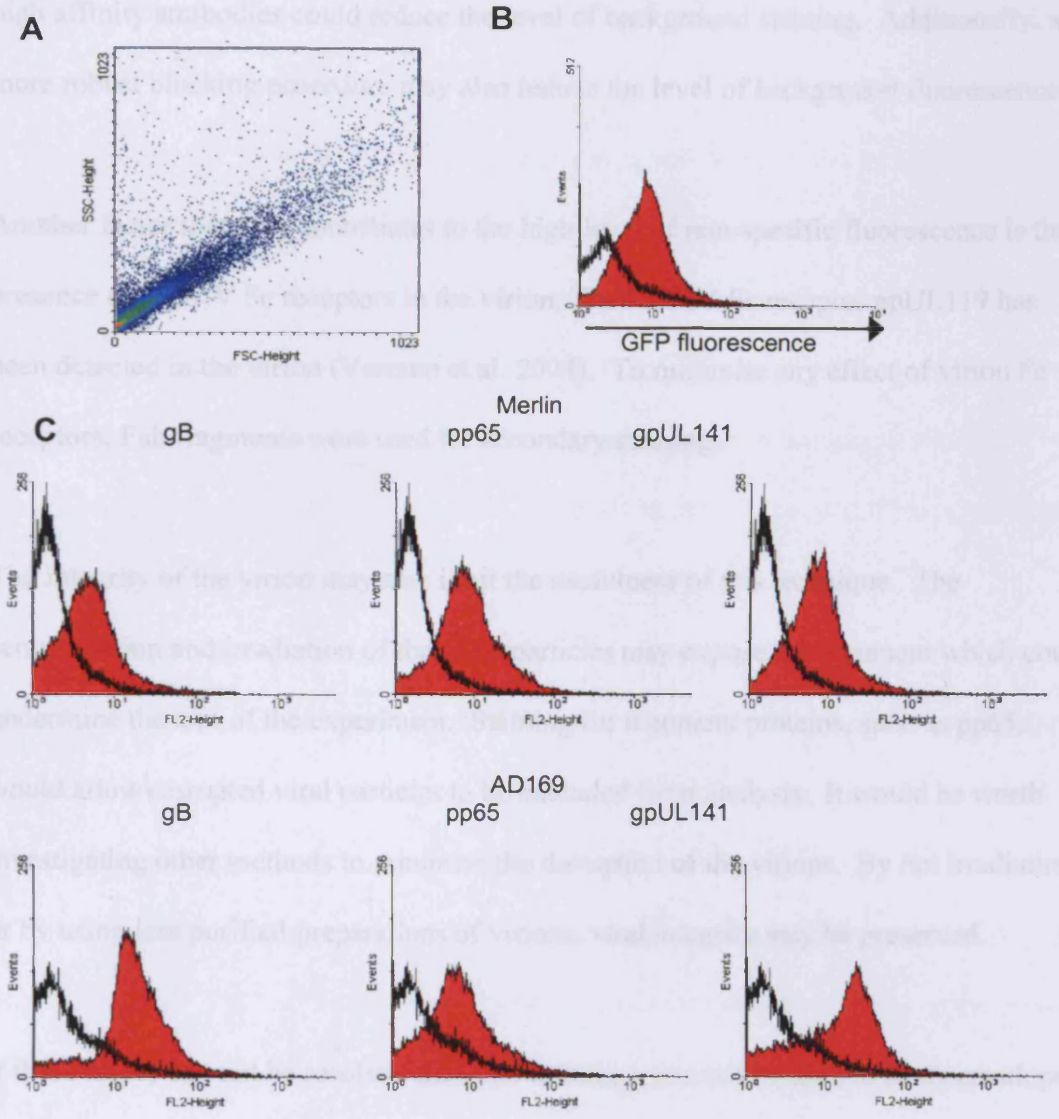


**Figure 5.7. Flow cytometry analysis of purified HCMV virions**
(A) Forward scatter and side scatter profile of HCMVUL32GFP. (B) GFP fluorescence of purified HCMVUL32GFP virions (red), black line is untagged HCMV virions. (C) Purified strain Merlin and strain AD169 virions were stained with monoclonal antibodies specific for gB, pp65 and gpUL141 or with mouse IgG1 as isotype control (black lines) then stained with anti-mouse Alexa Fluor AF488. The stained virions were then analysed by flow cytometry.

high affinity antibodies could reduce the level of background staining. Additionally, a more robust blocking procedure may also reduce the level of background fluorescence.

Another factor that may contributes to the high level of non-specific fluorescence is the presence of HCMV Fc receptors in the virion; The HCMV Fc receptor gpUL119 has been detected in the virion (Varnum et al. 2004). To minimise any effect of virion Fc receptors, Fab fragments were used for secondary staining.

The integrity of the virion may also limit the usefulness of this technique. The centrifugation and irradiation of the virus particles may expose the tegument which could undermine the aim of the experiment. Staining for tegument proteins, such as pp65, would allow disrupted viral particles to be excluded from analysis. It would be worth investigating other methods to minimise the disruption of the virions. By not irradiating or by using less purified preparations of virions, viral integrity may be preserved.

If these issues can not be resolved then this technique can not be used to study envelope glycoproteins. However, it may be useful for titration of viruses. Individual virus particles can be detected and counted (fig 5.7A) which enables the ratio of particle to plaque forming units to be determined in conjunction with cell culture methods. Once the ratio is established, rapid titration of virus would be possible by counting virus particles by flow cytometry.

### 5.5.1 FACS-based virus adhesion assay

A possible role for virion gpUL141 could be to bind cell surface CD155 and thereby promote attachment. While it did not prove possible to detect antibody bound to virus particles to cells by flow cytometry, the presence of the UL32GFP fusion protein was. By utilising fluorescent virus particles, it would therefore be possible to measure directly the amount of virus bound to a cell. The initial strategy was to investigate HCMV binding to HFFF compared with the same cell with knocked-down CD155 expression. To this end, HFFFs were infected with five different Mission Lentiviral shRNA transduction particles (Sigma-Aldrich, Poole, UK). Each replication deficient lentivirus encodes a shRNA, consisting of a 21 base sense sequence, a 6 base loop then a 21 base anti-sense sequence, which is designed to target CD155 using a proprietary algorithm (sigma) (fig 5.8A for clones names and shRNA sequences). Following infection of HFFFs at a moi of 5, genomic integration was selected for by the addition of G418 to the growth medium. CD155 knockdown was observed in 1/5 stable cells lines established by lentivirus transduction (fig 5.8B). The growth rate of this knock down cell line was significantly slower than those expressing normal levels of CD155. Frozen stocks of this cell line were established, however, the knock down of CD155 expression was lost from resuscitated cells. During recovery from frozen stocks there would have been strong selective pressure against the downregulation of CD155.

An alternative strategy was devised to measure if gpUL141 on the virion enhanced virus-cell binding. Fibroblasts were infected with RAdCD155mCh (or mock infected) for three days before HCMVUL32GFP was added at 4°C for three hours (fig 5.9A). Unattached virus was washed off then adherent virus and cells were fixed

A

| Clone ID | Sequence |
|---|---|
| TRCN0000062908 | CCGGGAGGTATCCATCTCTGGCTATCTCGAGATAGCCA GAGATGGATACCTCTTTTTG |
| TRCN0000062909 | CCGGCTAATGGGCATGTCTCCTATTCTCGAGAATAGGA GACATGCCCATTAGTTTTTG |
| TRCN0000062910 | CCGGCCCAGCTATTCGGAGTCCAAACTCGAGTTTGGACT CCGAATAGCTGGGTTTTTG |
| TRCN0000062911 | CCGGCAGAGCCCACAGGCTATAATTCTCGAGAATTATA GCCTGTGGGCTCTGTTTTTG |
| TRCN0000062912 | CCGGCGGCAAGAATGTGACCTGCAACTCGAGTTGCAGG TCACATTCTTGCCGTTTTTG |

B

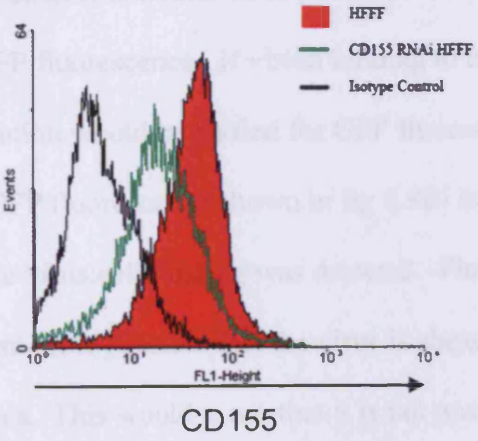


**Figure 5.8. CD155 Knock-down in lentiviral transduced HFFF**
(A) Five lentiviral vectors encoding shRNA designed to target CD155 coding region were obtained from Sigma-Aldrich (Poole, UK). Official clone names and shRNA sequences shown.
(B) Stable cell lines were produced by infecting HFFFs with a lentiviral vector at a moi of 5 then selecting for genomic integration under G418 selection. CD155 knock-down was determined by flow cytometry using the D171 mAb specific for CD155 (Abcam). Of the 5 cell lines tested, only TRCN0000062909 produced CD155 knock-down (green line).

with paraformaldehyde, trypsanised then analysed by flow cytometry. GFP fluorescence was measured as an indicator of virus attachment to the cells. Mock-infected cells plus GFP Merlin and RAdCD155mCh infected cells plus GFP Merlin displayed a small increase in GFP fluorescence (fig 5.9Bi). When GFP and mCherry fluorescence was graphed, RAdCD155mCh infected cells plus PBS displayed two populations (fig 5.9Cii); a mCherry positive, GFP negative population of RAd infected cells and a second mCherry negative, GFP negative population of uninfected cells. However, RAdCD155mCh infected cells plus GFP Merlin displayed a third population (fig 5.9Ciii). This GFP positive population is unbound virus particles. The mCherry population of cells are negative for GFP fluorescence. If virion binding to cells was detected then the mCherry positive population would be shifted for GFP fluorescence. Taken together this shows that the shift in GFP fluorescence shown in fig 5.9Bi is caused by unbound virus particles and not because virus:cell binding was detected. Flow cytometry may not be suited for this experiment. It is possible that the virus is sheared from the cells during the processing of the samples. This would mean that it is not possible to detect virion:cell binding by flow cytometry.

Following flow cytometry, attempts were made to observe virions attaching to cells by direct microscopy. However, the GFP tagged virions were at the limit of detection which prevented observation of the virions and cells. Both techniques could possibly be improved by using excess virions. This would increase the level of fluorescent signal enhancing the ability to detect any virion:cell interaction.

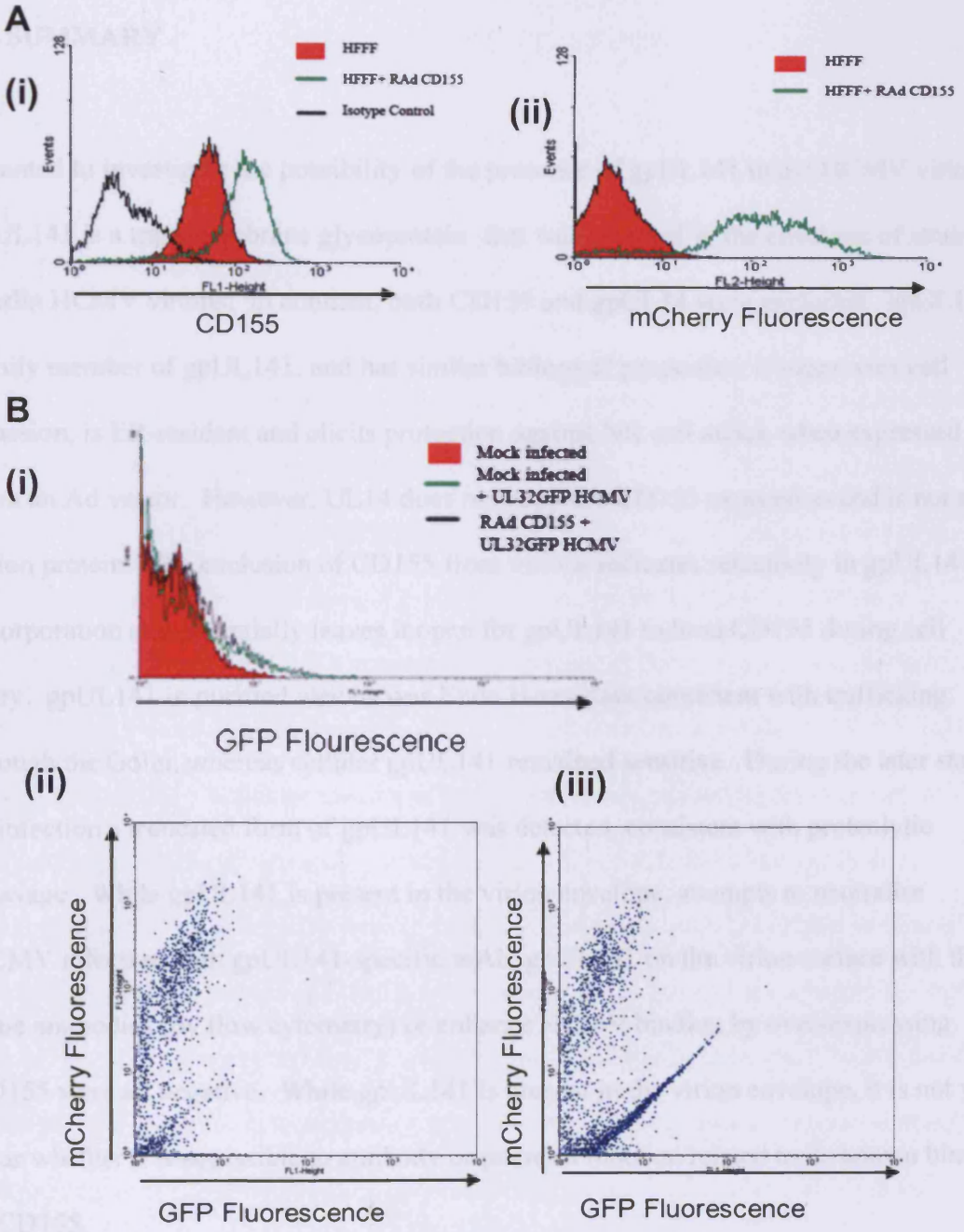


**Figure 5.9. Effect of relative levels of CD155 on virion binding**
(A) RAdCD155mCh infected HFFF were stained with anti-CD155 and AF 488 then analysed by flow cytometry. (i) CD155 expression levels and (ii) mCherry fluorescence. (B) ) RAdCD155mCh infected HFFF were incubated at 4°C with HCMVUL32GFP or PBS. After washing unbound virus cells were analysed by FACS. (i) GFP fluorescence (ii) dotplot showing mCherry fluorescence against GFP fluorescence for RAdCD155mCh infected fibroblasts incubated with PBS. (ii) dotplot showing mCherry fluorescence against GFP fluorescence for RAdCD155mCh infected fibroblasts incubated with HCMVUL32GFP.

## 5.6 SUMMARY

I wanted to investigate the possibility of the presence of gpUL141 in the HCMV virion. gpUL141 is a transmembrane glycoprotein that was detected in the envelope of strain Merlin HCMV virions; in contrast, both CD155 and gpUL14 were excluded. gpUL14, a family member of gpUL141, and has similar biological properties: it suppresses cell adhesion, is ER-resident and elicits protection against NK cell attack when expressed from an Ad vector. However, UL14 does not suppress CD155 expression and is not a virion protein. The exclusion of CD155 from virions indicates selectivity in gpUL141's incorporation and potentially leaves it open for gpUL141 to bind CD155 during cell entry. gpUL141 in purified virions was Endo H-resistant consistent with trafficking through the Golgi, whereas cellular gpUL141 remained sensitive. During the later stages of infection a truncated form of gpUL141 was detected, consistent with proteolytic cleavage. While gpUL141 is present in the virion envelope, attempts to neutralise HCMV infection with gpUL141-specific mAb, gpUL141 on the virion surface with the same antibodies (by flow cytometry) or enhance HCMV binding by over-expressing CD155 were all negative. While gpUL141 is present in the virion envelope, it is not yet clear whether it is accessible to antibody or posses a function related to its known binding to CD155.

# 6 DISCUSSION

## 6.1 UL141 ALTERS CELL ADHERENCE

HCMV encodes a powerful NK evasion gene that is present in clinical isolates but lost from the commonly used laboratory strains AD169 and Towne. UL141 suppresses NK cell activation during productive infection by downregulating cell surface expression of CD155, a ligand for the activating NK activating receptors DNAM-1, CD96 and SIGLEC. However, CD155 is a constitutively expressed protein that has important cellular functions that appear superficially to be quite distinct from its role in NK cell recognition: CD155 has important roles in promoting cell migration, growth cell:cell and cell:matrix interactions. In most quiescent cells, CD155 would be subject to post-translational downregulation following binding of nectin 3 or be consumed in functional protein:protein interactions. CD155 becomes exposed on the surface when cells break free of their natural contacts when undergoing proliferation or migration, both enhanced following malignant transformation. Certain virus infection can also produces changes comparable with transformation (growth stimulation, cell cycle progression), break cell:cell contacts and HCMV appears to promote monocytic migration. Consequently, the normal biological properties of CD155 do relate to its role in NK recognition, its exposure on the cell surface is perceived by NK cells as a 'danger' signal. This study sought to determine for the first time how downregulation of CD155 impacted on the physiology of the infected cell.

UL141 expression reduced the ability of 293 cells and HFFFs to adhere to the growth substrate (fig 3.2 and 3.5). In both cell lines CD155 was downregulated from the cell surface following the expression UL141 in isolation (fig 3.1 and 3.5). CD155 enhances adhesion by binding to its ligands nectin-3 and the ECM component vitronectin (Ikeda et al. 2003; Lange et al. 2001). Following ligand interaction, the internalisation of CD155 promotes the formation of focal complexes (Minami et al. 2007a). Additionally, CD155 co-localises with, and enhances the signalling of $\alpha_V\beta_3$ integrin with also enhances adhesion of cells. The downregulation of cell surface CD155 by gpUL141 would disrupt the adhesion functions of CD155. Additionally, CD155 has an important role in the initiation of cell-cell contact and the formation of AJs via an interaction with nectin-3. The formation of cell-cell contacts likely stabilises newly adhered cells by providing additional contacts. This is another potential mechanism by which UL141 affects cell adhesion by downregulating cell surface CD155.

The downregulation of adhesion molecules is a common theme in HCMV infection. The virus downregulates a wide range of adhesion molecules including integrins, NCAM (neural cell adhesion molecule, CD56) and the Ig superfamily member Thy-1 (CD90) (Blaheta et al. 2004; Leis et al. 2004; Warren et al. 1994b). HCMV disrupts the formation of focal complexes and downregulates four cellular proteins (focal adhesion kinase, Hic-5, paxillin, and alpha-actinin) involved in the formation and maintenance of focal complexes (Stanton et al. 2007). When HCMV-infected fibroblasts were tested in the adhesion assay, there was a large reduction in cell adhesion. Deletion of UL141 from the virus genome did not result in a detectable increase in the level infected cell adherence. Any UL141-dependant effect on adhesion is masked is masked during

productive infection in fibroblasts by other effects. Interestingly, CD155 is integral to the formation of focal complexes (Minami et al. 2007a) so there may be a redundancy of function in HCMV infection. As long term passaged laboratory strains of HCMV, such as AD169, lack the UL/b' region which contains UL141 (Cha et al. 1996) it indicates that there are additional focal adhesion-disrupting functions encoded by HCMV. While UL141 does not reduce adherence during HCMV infection in fibroblasts it may have a role *in vivo*. HCMV infects a wide range of cells *in vivo* and it is possible that the UL141-dependant downregulation of CD155 may affect the adherence of certain cell types. It would be of interest to study the effects of UL141 expression on a wide range of cell types in order to elucidate an *in vivo* function.

Elevated levels of CD155 expression in cancerous cells correlates with enhanced migration (Ikeda et al. 2004; Minami et al. 2007b; Sloan et al. 2004) An *in vitro* scratch assay was used to assess the impact of UL141 on cell movement (fig 3.8). While $UL141^{+}$ cells took the same time to close the gap, the control cells did so at a more constant rate. Cells expressing gpUL141 displayed four distinct phases: a period of expansion, a lag phase, a phase of rapid closure, then finally the rate of closure matched that of the control cells.

Within seconds of wounding, the leading edges of the 293-UL141GFP monolayer detached from the substrate yet remain attached to the rest of the monolayer. The floating cells then re-settle either back onto either the monolayer or into the gap near their original location. This peeling of the monolayer may simply be due to downregulation of CD155 causing reduced adherence.

Following the detachment of the leading edges of the monolayer there then follows a phase where the gpUL141-expressing cells do not close the gap. It is possible that this phase is caused by the reattachment of the leading edges. Alternatively, it may be that the gpUL141-expressing cells are in a state of contact inhibition. The internalisation of cell surface CD155 is a powerful mechanism for the inhibition of movement following contact (Minami et al. 2007b). Intracellular signalling by cell surface CD155 leads to the reorganisation of the cytoskeleton promoting movement. Following contact, CD155 is downregulated and the intracellular signals are ablated. Therefore without CD155 on the surface, the UL141 expressing cells would constantly be in a state of contact inhibition, believing that they are in contact with other cells. As CD155 internalisation is not the only contact inhibition mechanism the cells eventually begin to move.

Once the cells begin to close the gap there is a period of increased movement compared to the control cells. This may be a result of the detached regions of the monolayer reattaching. Reattachment of cells would equate to a reduction in the size of the void. Conversely, the reduced adherence caused by the downregulation of CD155 could enhance cell movement.

In the final phase of wound closure, both UL141-expressing and control cells close the gap at a similar rate which lasts until both leading edges make contact. For the 293-UL141 cells this is markedly slower than the previous phase. If the previous phase was a result of the resettling of the detached monolayer then this phase marks the point where the reattachment is no longer a factor in the movement of the leading edge.

It cannot be excluded that the UL141-dependant effects described are a result of an interaction with another cell adhesion molecule and not CD155. However, Tomasec and colleagues (2005) performed an extensive survey on the effects of UL141 expression on a panel of adhesion molecules and they identified CD155 as the only cell adhesion molecule downregulated by UL141 expressed in isolation. In attempt to mimic the phenotype of gpUL141 expressing cells CD155 was successfully downregulated by RNA interference induced by lentiviral vector. The downregulation was not tolerated in stable cell lines. The potential exists to remake and reselect the cell line for each experiment. However, if this strategy is pursued then there is no advantage in using a transducing vector. Transient delivery of the interfering RNA, for example by electroporation, would perhaps be more successful in reproducibly knocking down CD155 expression. Alternatively, RAd vectors provide efficient transient expression and are compatible with RNA interference. Three shRNA designed to target CD155 were introduced into the AdZ vector (McSharry and Wilkinson, personal communication) but these constructs did not sufficiently suppress CD155 expression. If this technology can be made to work then it would be a powerful tool to dissect the function of UL141.

When monocytes migrate through a monolayer of endothelial cells, CD226 disrupts AJs and binds to CD155 on the endothelial cells; antibodies against either molecule will arrest migration (Reymond et al. 2004). HCMV is recognised to infect both monocytes and endothelial cells; indeed it is possible that monocyte may potentially acquire the virus during diapedesis through a layer of chronically infected endothelial cells. The expression and effect of UL141, and additional HCMV-encoded function that impact on

cell adhesion, on the integrity of endothelium lining blood vessels warrants investigation. It will also be important to study the effect of gpUL141 expression in endothelial cells on trans-endothelial cell migration. In this context, if HCMV UL141 efficiently downregulates CD155 in endothelial cells theoretically diapedesis should be inhibited. In monocytes, CD155 may also be required to interact with nectin-3 from the AJs to enhance monocyte migration. The HCMV transcriptional cascade is regulated by myeloid cell differentiation. In monocytes HCMV gene expression has been reported to be restricted essentially to IE genes, thus UL141 should not be expressed. Following differentiation into macrophages, activation of UL141 expression and the concomitant downregulation of CD155 may contribute to suppressed cell migration in the target organ. While these questions can be addressed in *in vitro* models of transendothelial cell migration, there is currently a technical issue delivering fibroblast-adapted HCMV strains to these cell types. A wild type Merlin BAC, repaired in RL13 and UL128, which has intact tropism for endothelial cells is currently being created (Stanton, personal communication). When this BAC is available it would be interesting to look at transendothelial cell migration with virus (± UL141) in monocytes and endothelial cells

UL141 is the only other member of the UL14 family, presumably due to gene duplication during HCMV evolution, with the two genes diverging. Interestingly, rhesus CMV contains homologues of both genes with the rhesus UL141 homologue also being capable of downregulating CD155 (Aicheler, personal communication). The conservation of these genes is remarkable in that it appears not to be true of other HCMV NK modulators (UL16, UL18, UL142). Like gpUL141, gpUL14 is an ER resident glycoprotein, however it does not downregulate CD155 or the nectin family members nectin-2 or nectin-3 (Mel

Armstrong, PhD thesis). When expressed from an Ad vector gpUL14 can provide protection from NK cell recognition, however, UL14 has yet to be demonstrated to function in the context of virus infection (Prod'homme, Armstrong, Tomasec & Wilkinson, personal communication). In order to compare the two homologues, 293 cells stably expressing UL14 was also included in adhesion assays. Cells expressing a gpUL14GFP fusion protein had a similar level of adhesion reduction as cells expressing UL141GFP. This result would be consistent with a model in which gpUL14 also downregulates surface expression of an endogenous cellular adhesion molecule, possibly also by retention in the ER. In view of the potential for this function to be a ligand for an NK activating receptor, there is clear merit in identifying this protein. The cellular target for UL14 could be sought by systematic screen of all known cellular adhesion, or by using biochemical/proteomic approaches.

## 6.2 CO-LOCALISATION OF gpUL141 AND CD155 IN THE ENDOPLASMIC RETICULUM

CD155 is retained within the cell in an immature 69kDa Endo H sensitive form in HCMV-infected cells (Tomasec et al. 2005). While this immature form was readily observed by western blot, the only available mAb compatible with immunofluorescence could not detect immature intracellular CD155. Expression of UL141 was associated with a loss of CD155 staining. To address this issue, plasmids encoding fluorescent fusion proteins of CD155 and UL141 were generated. When transfected individually, CD155 was expressed on the cell surface while UL141 was expressed as an intracellular protein with large bodies of high concentration observed. These inclusion bodies varied in both size and shape (fig 4.5 and 4.6). gpUL141 has been described as forming dimers and high molecular complexes with itself (Mel Armstrong, PhD thesis); therefore, these bodies are likely large multimeric UL141 complexes. It is not clear whether CD155 has a role in formation of these complexes, as the endogenous cellular protein is present in all experiments. While CD155 RNA knock down experiments could provide further insight, even this approach would be associated with a level of residual expression.

The fluorescent fusion of CD155 is downregulated from the cell surface when UL141 is expressed. However, because of the fluorescent tag connected to CD155 it was possible to directly image the immature form within the cell (fig 4.5 and 4.6). When expressed in the presence of gpUL141, CD155 is intracellular with the same distribution as gpUL141. CD155 co-localises closely with gpUL141 including in the inclusion bodies. CD155 has not previously been detected in the inclusion bodies as the antibodies could not penetrate.

However by using fluorescent fusion proteins it was possible to demonstrate that CD155 is included in these bodies. By taking serial sections along the z axis, I also demonstrated that the inclusion bodies are composed of a homogenous mixture of CD155YFP and gpUL141CFP (fig 4.7). The size and number of the inclusion bodies is highly variable; cells may have several smaller bodies or occasionally they will have fewer large bodies. It appears that the size of the bodies is dependant on the relative expression levels of the two proteins.

The downregulation of CD155 by UL141 is not absolute; a small level of cell surface CD155 can be detected by flow cytometry (fig 4.6) (Tomasec et al. 2005). This is verified by the use of the fluorescent fusion proteins. When fluorescent CD155 and UL141 are co-expressed, there is often faint CD155 fluorescence visible on the cell surface. This is breakthrough expression as the cell surface CD155 is not localised with gpUL141.

Tomasec and colleagues hypothesised that because of the Endo H sensitivity of CD155 that the interaction between CD155 and gpUL141 occurred in the ER (Tomasec et al. 2005). However they did not produce any specific evidence to support this hypothesis. This hypothesis was confirmed by staining cells co-transfected with gpUL141 and CD155 with the ER resident protein calnexin (fig 4.8). The interaction with CD155 and gpUL141 occurred exclusively within the ER. Both the granular intracellular staining and the inclusion bodies co-localises closely with calnexin. Indeed, the co-localisation is so precise that it is likely that calnexin is involved in the interaction between CD155 and gpUL141. Calnexin operates as a chaperon in the ER, ensuring the correct folding and

glycosylation of glycoproteins (reviewed in Helenius and Aebi 2004). Considering the immature glycosylation of CD155 in the presence of gpUL141 (Tomasec et al. 2005), it is likely that gpUL141 is disrupting the calnexin-dependant glycosylation of CD155. However, by being involved in the gpUL141:CD155 interaction calnexin loses credence as an ER marker. It may be transported from the ER with the gpUL141:CD155 complex. It would be worth while repeating this experiment with other ER markers to confirm the ER localisation. Also, it would be of interest to study the co-localisation of other ER chaperones, such as calreticulin, to see if their distribution is changed by UL141 expression.

By infecting cells expressing fluorescent CD155 with the UL141 deletion HCMV or the parental virus it was possible to observe CD155 during infection. CD155 was down regulated in Merlin strain virus infected cells, but not in the UL141 deletion virus infected cells. CD155 cell surface downregulation correlated with internal CD155 fluorescence, in agreement with the results discussed above. Large inclusion bodies were not observed, however some cells display smaller bodies. This supports the conclusion above that the bodies are dependant on expression level. The large bodies observed during transient transfection are likely a result of the overexpression of both proteins. While during HCMV infection, UL141 expression is much lower therefore the inclusion bodies are smaller.

While I show close association between CD155 and gpUL141, direct interaction has not been shown. It is of importance to indentify if gpUL141 binds directly with CD155 or if there are intermediary molecules involved in the interaction. Immunoprecipitation was

attempted but was fruitless; co-immunoprecipitation of CD155 is recognised to be problematic. Another technique which could potentially determine if direct binding occurs is to mix epitope-labelled soluble gpUL141 and soluble CD155, then attempt to pull down CD155 using mAbs to the epitope-tagged soluble gpUL141. Unfortunately, there were technical problems purifying the soluble gpUL141 which prevented the experiment from being performed.

It was discovered late in the course of this study that the recombinant HCMVΔUL141 loses the ability to downregulate nectin-2, as well as CD155 (Tomasec and Prod'homme, personal communication). However UL141, when expressed on its own only downregulates CD155 and not nectin-2 (Tomasec et al. 2005). This implies that UL141 is working in concert with another HCMV gene to downregulate nectin-2. Most non-essential genes, including UL14, have been eliminated in the search for the partner (Tomasec and Sugrue, personal communication). Regardless of the identity of the binding partner, the distribution and interaction of CD155 and gpUL141 is likely to be more complex *in vivo* than the situation produced by the introduced expression of UL141 and CD155 fluorescent fusion proteins. Once the other HCMV component is identified, further studies will be required to determine the relative distribution and interactions between CD155, gpUL141, nectin-2 and the other HCMV protein. These studies would have to utilise fluorescent fusion proteins because, as previously discussed, there are problems attempting to perform immunofluorescence with CD155 and gpUL141.

## 6.3 gpUL141 IS A COMPONENT OF THE HCMV VIRION ENVELOPE

The envelope of HCMV is a derived from host membrane. Transmembrane HCMV glycoproteins are expressed on the envelope; the most studied are the major glycoprotein complexes gB, gH:gL:gO and gM:gN (discussed in section 1.2.4). However, a small number of other envelope glycoproteins have been identified including UL22A, UL33, UL41A, UL119 and UL128-UL131A (Varnum et al. 2004; Wang and Shenk 2005b). As UL141 is a transmembrane glycoprotein, it has the potential to be incorporated into the virus particle. gpUL141 was detected in purified strain HCMV virions. Cellular contamination was ruled out as the virions were negative for intracellular proteins. The identification of gpUL141 in the virion is a novel observation; previously gpUL141 was thought to only be an intracellular protein.

Interestingly, CD155 was absent from the virion. As demonstrated in chapter 4, CD155 and gpUL141 closely co-localise when expressed together. There is little free gpUL141 that does not co-localise with CD155 in the transfected fibroblasts. However, late in infection increasing gpUL141 may no longer be saturated by binding CD155 giving rise to free gpUL141. The absence of CD155 from the virion also provides further evidence that the incorporation of gpUL141 is selective and not attributable to non-specific contamination.

Virion particles are highly structured with the positioning of most proteins appearing to be highly regulated and related to their functional role during infection. gpUL141 is a transmembrane protein, and the envelope is the only membrane in the virion. It was

therefore perhaps to be expected that gpUL141 was present in the envelope fraction (fig 5.2). A small level of gpUL141 was detected in the capsid and tegument fraction. It is most unlikely that gpUL141 is also a component of the tegument, rather the data would be consistent with gpUL141 being envelope-located but with the internal domain of the protein having an interactions with the tegument, which results in the increased association of gpUL141 with the tegument during the separation process. Interactions between the tegument and envelope is a common feature of HCMV proteins, such as the tegument protein pp28 which interacts with the envelope (Silva et al. 2003). Irmiere and Gibson (1983) have demonstrated that parts of the envelope can still be attached to the tegument following extensive de-envelopment. As gB was only present in the envelope fraction, it suggests that there was good separation of the envelope from the tegument and capsid.

One technique which could potentially confirm the location of gpUL141 in the virion is electron microscopy. By probing purified virions with gold-labelled antibodies it may be possible to visualise gpUL141. However, because the label is on the end of the antibody it means that the label is adjacent to, not on, the epitope. Therefore, the location may not be revealed.

The topological orientation of HCMV envelope proteins is essential for their functions. The major glycoproteins are arranged so that their glycosylated domains are facing out from the virus enabling interactions with cellular molecules during attachment. Conversely, certain molecules may be arranged to enable interactions with the tegument. These interactions are important for the secondary envelopment of the virion prior to

egress from the cell. To define the topological orientation of gpUL141 in the virion flow cytometry and neutralisation assays were performed using UL141 mAbs. These antibodies were generated against a soluble form of UL141 which consists of the Ig-like domain but does not have the transmembrane or cytoplasmic domain (Tomasec et al. 2005). Unfortunately, neither technique provided definite results. In both assays binding of the UL141 antibody to virus particles were not detected. This could mean that the Ig-like domain of gpUL141 is contained within the virion, although this would represent a topological challenge during envelopment. It is more likely that the Ig-like domain of gpUL141 is located on the envelope surface. Antibodies may be unable to access complementary epitopes in this context because of steric hindrance, possible by other HCMV or host-encoded envelope proteins blocking antibody binding. It is also possible that the mAbs do not recognise the mature, fully glycosylated form of the protein in the virion, present in disulphide-bridged complexes when unreduced. Alternatively, the mAbs may be binding virions but producing a signal below the threshold level detectable by flow cytometry, with the mAbs binding without neutralising.

As mentioned above I attempted to detect gpUL141 on the virion by flow cytometry (fig 5.7). This built on the techniques by Brussaard and colleagues (2000) who showed that they could detect purified fluorescent-labelled virions from a wide range of virus families. They could detect picornaviruses, baculoviruses retroviruses and fluorescent labelled HCMV virus particles. Having confirmed that fluorescent-tagged HCMV virions could be detected by flow cytometry, I attempted to detect purified virions stained with antibodies. However, I was limited by time and reagents. Several technical limitations limited the detection of specific fluorescence. Virion size limits the amount of

antigen they can contain. Extremely high concentrations of antibody were utilised before a positive signal could be detected; however, these condition inevitably led to a high level of non-specific staining. Unless the high background staining can be minimised then this technique is of limited usefulness. The use of high affinity antibodies should reduce the non-specific staining. If the non-specific fluorescence could be reduced then this could be a powerful technique for the studying of envelope glycoproteins. At the moment flow cytometry of virions may be useful for counting virus particles. If the ratio of measured virus particles to plaque formation units was established then it would then be possible to count virus particles by flow cytometry and compare it with the infectivity.

gpUL141 is sensitive to Endo H in HCMV infected cells (Tomasec et al. 2005). gpUL141 in the virion, however, displays resistance to Endo H digestion (fig 5.3). Two glycoforms of gpUL141 are incorporated into virion; one that is completely resistant to Endo H digestion and one that is partially resistant. The development of Endo H resistance is characteristic of processing through the Golgi apparatus, therefore gpUL141 must be processed to an Endo H resistant form in the Golgi apparatus before incorporation in the virion. The specific glycoforms present in the virion do not accumulate in the cell during infection; the Endo H resistant forms are only detected in the virion and not at early or late timepoints during HCMV infection. Tomasec and colleagues characterised UL141 as being expressed in cells as a doublet consisting of two differently sized glycoforms (Tomasec et al. 2005). This is correct early in infection (fig 5.5); however, at latter times in infection the observed doublet consists of differently sized protein backbones. At late times during infection, complete deglycosylation of cellular gpUL141 by PNGase produces two separate products. The generation of this

alternate, 32 kDa protein backbone form of gpUL141 is not currently known. As the UL141 ORF does not have an obvious alternative start site (Davison et al. 2003; Dolan et al. 2004), the generation of this faster-migrating form is presumably a consequence of post-translational modification. The function of this modification (if any) is also unknown. It is not required for the downregulation of CD155 as it occurs at early times during infection when this form is not present. Also the alternate form is not detected in the virion, only glycoforms of the smaller 32kDa are incorporated into the virion. It is possible UL141 may have additional roles late in HCMV infection.

The role of gpUL141 in the virion is currently unknown. The possibility that virion gpUL141 downregulates CD155 immediately upon virus entry can only be expected to work in a local context; the amount of CD155 on a virion is not sufficient to impact globally on CD155 on the newly infected cell. Indeed, CD155 downregulation cannot be detected until the late phase of infection (Tomasec et al. 2005). Perhaps the most intriguing possible function for virion gpUL141 is an involvement in virus entry. Recently, Soroceanu and colleagues (2008) identified the PDGF receptor (PDGFR) as an important receptor for HCMV. Blocking of PDGFR function or knock down of the protein made cells non-permissive for HCMV infection. The envelope glycoprotein gB interacts directly with PDGFR inducing receptor phosphorylation and the activation of the phosphoinositide 3-kinase (PI3K) and Atk. HCMV-induced upregulation of the PI3K pathway provides strong anti-apoptosis signals and is important for the initiation of viral DNA replication (Johnson et al. 2001). CD155 is known to co-localise on the cell surface with, and enhances the signalling from, the PDGF receptor (Kakunaga et al. 2004). CD155 enhances PDGF-induced signalling through the Ras-Raf-MEK-ERK

pathway (Kakunaga et al. 2004) but there is no data yet on the effects of CD155 on the PDGF-dependant PI3K and Atk signalling pathway. However, the close family members of CD155, nectin-2 and nectin-3 have both been shown to enhance PDGF-induced activation of the PI3K-Atk pathway (Kanzaki et al. 2008). This opens the possibility that CD155 may also affect the PI3K-Atk pathway as nectins and CD155 share similar cytoplasmic signalling pathways (Sato et al. 2005).

$\alpha_V\beta_3$ integrin has been shown to bind the envelope glycoproteins gB and gH and act as a co-receptor for HCMV (Wang et al. 2005). Originally $\alpha_V\beta_3$ integrin was thought to function as a co-receptor, signalling in concert with the epidermal growth factor receptor (Wang et al. 2005), although a later study does shown that EGFR is not essential for HCMV entry (Isaacson et al. 2007). Remarkably, as with PDGF receptor, CD155 is known to enhance signalling by $\alpha_V\beta_3$ integrin (Ikeda et al. 2004; Minami et al. 2007a). This gives virion gpUL141 another potential mechanism for enhancing intracellular signalling during HCMV attachment and entry. In addition to cytoskeletal reorganisation integrin signalling can enhance signalling from both EGFR and PDGFR (Streuli and Akhtar 2009).

Another possibility is that gpUL141 does not enhance CD155 signalling but rather that gpUL141 promotes the physical attachment of the virion during entry. UL141 is non-essential for replication and is often lost during *in vitro* passage of HCMV clinical isolates (Davison, Dargan personal communication), however, that does not preclude it from having a role in virus attachment and/or entry. A mutation in the UL128 locus (UL128, UL130 or UL131A) is rapidly selected whenever HCMV clinical isolates are

propagated in fibroblasts (Dolan et al. 2004), yet the gH:gO:gL:UL128-131A complex is essential for the productive infection of endothelial cells (Ryckman et al. 2008a; Ryckman et al. 2008b). Although UL141 is not essential *in vitro,* it may be required to expand virus tropism *in vivo.* It is possible that *in vitro*, the cells are supplied with sufficient growth factors and anti-apoptotic signals from the serum in the media, while, *in vivo* addition anti-apoptotic signals are required to productively infect cells.

It is important to determine if gpUL141 enhances PDGFR signalling during HCMV entry. One way to determine this is to probe the phosphorylation state of intracellular signalling molecules following attachment and entry by HCMVΔUL141 or strain Merlin HCMV. The phosphorylation state of molecules from the Ras-Raf-MEK-ERK pathway and the PI3K-Atk pathway should be probed. If gpUL141 enhance PDGFR signalling then an increase in phosphorylation would be detected in Merlin strain HCMV infected cells compared to HCMVΔUL141 infected cells.

If it transpires that gpUL141 is involved in virus entry then the next stage would be to determine its role *in vivo.* To answer this, the first step should be to test the infectivity and growth of the HCMVΔUL141 and parental virus in a wide range of cell types to see if the presence of UL141 expands tropism or enhances productive infection in specific cell types.

Interest in UL141 has focused on its role in suppressing cell surface expression of the powerful NK cell activating ligand CD155. In this study, I show the first indication that UL141 has additional roles during HCMV infection. In addition to showing that UL141

expression reducing cellular adhesion, the identification of UL141 as a component of the virion envelope may suggest that it is involved in cell entry. Further studies will be required to elucidate the function of gpUL141 in the virion.

# 7 REFERENCES


Abate, D. A. et al. 2004. Major human cytomegalovirus structural protein pp65 (ppUL83) prevents interferon response factor 3 activation in the interferon response. *J Virol* 78(20), pp. 10995-11006.

Adair, R. et al. 2002. The products of human cytomegalovirus genes UL23, UL24, UL43 and US22 are tegument components. *J Gen Virol* 83(Pt 6), pp. 1315-1324.

Adler, B. et al. 2006. Role of human cytomegalovirus UL131A in cell type-specific virus entry and release. *J Gen Virol* 87(Pt 9), pp. 2451-2460.

Ahn, J. H. et al. 1998a. Disruption of PML subnuclear domains by the acidic IE1 protein of human cytomegalovirus is mediated through interaction with PML and may modulate a RING finger-dependent cryptic transactivator function of PML. *Mol Cell Biol* 18(8), pp. 4899-4913.

Ahn, J. H. et al. 1998b. Evaluation and mapping of the DNA binding and oligomerization domains of the IE2 regulatory protein of human cytomegalovirus using yeast one and two hybrid interaction assays. *Gene* 210(1), pp. 25-36.

Ahn, J. H. and Hayward, G. S. 1997. The major immediate-early proteins IE1 and IE2 of human cytomegalovirus colocalize with and disrupt PML-associated nuclear bodies at very early times in infected permissive cells. *J Virol* 71(6), pp. 4599-4613.

Ahn, K. et al. 1996. Human cytomegalovirus inhibits antigen presentation by a sequential multistep process. *Proc Natl Acad Sci U S A* 93(20), pp. 10990-10995.

Ahn, K. et al. 1997. The ER-luminal domain of the HCMV glycoprotein US6 inhibits peptide translocation by TAP. *Immunity* 6(5), pp. 613-621.

Akrigg, A. et al. 1985. The structure of the major immediate early gene of human cytomegalovirus strain AD169. *Virus Res* 2(2), pp. 107-121.

Akter, P. et al. 2003a. Two novel spliced genes in human cytomegalovirus. *J Gen Virol* 84(Pt 5), pp. 1117-1122.

Akter, P. et al. 2003b. Two novel spliced genes in human cytomegalovirus. *J Gen Virol* 84(5), pp. 1117-1122.

Allal, C. et al. 2004. Human cytomegalovirus carries a cell-derived phospholipase A2 required for infectivity. *J Virol* 78(14), pp. 7717-7726.

Amano, H. et al. 2008. Interaction and localization of Necl-5 and PDGF receptor beta at the leading edges of moving NIH3T3 cells: Implications for directional cell movement. *Genes Cells* 13(3), pp. 269-284.

Aoki, J. et al. 1997. Mouse homolog of poliovirus receptor-related gene 2 product, mPRR2, mediates homophilic cell aggregation. *Exp Cell Res* 235(2), pp. 374-384.

Arnon, T. I. et al. 2005. Inhibition of the NKp30 activating receptor by pp65 of human cytomegalovirus. *Nat Immunol* 6(5), pp. 515-523.

Atalay, R. et al. 2002. Identification and expression of human cytomegalovirus transcription units coding for two distinct Fcgamma receptor homologs. *J Virol* 76(17), pp. 8596-8608.

Azzeh, M. et al. 2006. Structural changes in human cytomegalovirus cytoplasmic assembly sites in the absence of UL97 kinase activity. *Virology* 354(1), pp. 69-79.

Bacon, L. et al. 2004. Two Human ULBP/RAET1 Molecules with Transmembrane Regions Are Ligands for NKG2D. *J Immunol* 173(2), pp. 1078-1084.

Baldick, C. J., Jr. et al. 1997. Human cytomegalovirus tegument protein pp71 (ppUL82) enhances the infectivity of viral DNA and accelerates the infectious cycle. *J Virol* 71(6), pp. 4400-4408.

Baldick, C. J., Jr. and Shenk, T. 1996. Proteins associated with purified human cytomegalovirus particles. *J Virol* 70(9), pp. 6097-6105.

Baldwin, B. R. et al. 2000. Cloning and epitope mapping of a functional partial fusion receptor for human cytomegalovirus gH. *J Gen Virol* 81(1), pp. 27-35.

Ballestrem, C. et al. 2001. Marching at the front and dragging behind: differential alphaVbeta3-integrin turnover regulates focal adhesion behavior. *J Cell Biol* 155(7), pp. 1319-1332.

Baum, E. Z. et al. 1993. Expression and analysis of the human cytomegalovirus UL80-encoded protease: identification of autoproteolytic sites. *J Virol* 67(1), pp. 497-506.

Baury, B. et al. 2001. Organization of the rat Tage4 gene and herpesvirus entry activity of the encoded protein. *Gene* 265(1-2), pp. 185-194.

Baury, B. et al. 2003. Identification of secreted CD155 isoforms. *Biochem Biophys Res Commun* 309(1), pp. 175-182.

Baxter, M. K. and Gibson, W. 2001. Cytomegalovirus basic phosphoprotein (pUL32) binds to capsids in vitro through its amino one-third. *J Virol* 75(15), pp. 6865-6873.

Bechtel, J. T. and Shenk, T. 2002. Human Cytomegalovirus UL47 Tegument Protein Functions after Entry and before Immediate-Early Gene Expression. *J. Virol.* 76(3), pp. 1043-1050.

Beck, S. and Barrell, B. G. 1988. Human cytomegalovirus encodes a glycoprotein homologous to MHC class-I antigens. *Nature* 331(6153), pp. 269-272.

Beersma, M. F. et al. 1993. Human cytomegalovirus down-regulates HLA class I expression by reducing the stability of class I H chains. *J Immunol* 151(9), pp. 4455-4464.

Bego, M. et al. 2005. Characterization of an Antisense Transcript Spanning the UL81-82 Locus of Human Cytomegalovirus. *J. Virol.* 79(17), pp. 11022-11034.

Benko, D. M. et al. 1988. Virion basic phosphoprotein from human cytomegalovirus contains O-linked N-acetylglucosamine. *Proc Natl Acad Sci U S A* 85(8), pp. 2573-2577.

Bernhardt, G. et al. 1994. Molecular characterization of the cellular receptor for poliovirus. *Virology* 199(1), pp. 105-113.

Bhella, D. et al. 2000. Cryomicroscopy of human cytomegalovirus virions reveals more densely packed genomic DNA than in herpes simplex virus type 1. *J Mol Biol* 295(2), pp. 155-161.

Biegalke, B. J. et al. 2004. Characterization of the human cytomegalovirus UL34 gene. *J Virol* 78(17), pp. 9579-9583.

Billstrom, M. A. et al. 1998. Intracellular signaling by the chemokine receptor US28 during human cytomegalovirus infection. *J Virol* 72(7), pp. 5535-5544.

Biron, C. A. et al. 1989. Severe herpesvirus infections in an adolescent without natural killer cells. *N Engl J Med* 320(26), pp. 1731-1735.

Blaheta, R. A. et al. 2004. Human cytomegalovirus infection of tumor cells downregulates NCAM (CD56): a novel mechanism for virus-induced tumor invasiveness. *Neoplasia* 6(4), pp. 323-331.

Bodaghi, B. et al. 1998. Chemokine sequestration by viral chemoreceptors as a novel viral escape strategy: withdrawal of chemokines from the environment of cytomegalovirus-infected cells. *J Exp Med* 188(5), pp. 855-866.

Bogner, E. et al. 1998. The gene product of human cytomegalovirus open reading frame UL56 binds the pac motif and has specific nuclease activity. *J Virol* 72(3), pp. 2259-2264.

Boles, K. S. et al. 2005. The tumor suppressor TSLC1/NECL-2 triggers NK-cell and CD8+ T-cell responses through the cell-surface receptor CRTAM. *Blood* 106(3), pp. 779-786.

Bolovan-Fritts, C. A. et al. 1999. Peripheral blood CD14(+) cells from healthy subjects carry a circular conformation of latent cytomegalovirus genome. *Blood* 93(1), pp. 394-398.

Booy, F. P. et al. 1991. Liquid-crystalline, phage-like packing of encapsidated DNA in herpes simplex virus. *Cell* 64(5), pp. 1007-1015.

Borysiewicz, L. K. et al. 1988. Human cytomegalovirus-specific cytotoxic T cells. Relative frequency of stage-specific CTL recognizing the 72-kD immediate early protein and glycoprotein B expressed by recombinant vaccinia viruses. *J Exp Med* 168(3), pp. 919-931.

Boshart, M. et al. 1985. A very strong enhancer is located upstream of an immediate early gene of human cytomegalovirus. *Cell* 41(2), pp. 521-530.

Bottino, C. et al. 2003. Identification of PVR (CD155) and Nectin-2 (CD112) as cell surface ligands for the human DNAM-1 (CD226) activating molecule. *J Exp Med* 198(4), pp. 557-567.

Boyle, K. A. and Compton, T. 1998. Receptor-binding properties of a soluble form of human cytomegalovirus glycoprotein B. *J Virol* 72(3), pp. 1826-1833.

Bradley, A. J. et al. 2008. Genotypic analysis of two hypervariable human cytomegalovirus genes. *J Med Virol* 80(9), pp. 1615-1623.

Bradley, A. J. et al. 2009. High-throughput sequence analysis of variants of human cytomegalovirus strains Towne and AD169. *J Gen Virol*, pp. vir.0.013250-013250.

Brandenburg, B. et al. 2007. Imaging Poliovirus Entry in Live Cells. *PLoS Biol* 5(7), p. e183.

Braud, V. M. et al. 1998. HLA-E binds to natural killer cell receptors CD94/NKG2A, B and C. *Nature* 391(6669), pp. 795-799.

Britt, W. J. and Auger, D. 1986. Synthesis and processing of the envelope gp55-116 complex of human cytomegalovirus. *J Virol* 58(1), pp. 185-191.

Browne, E. P. and Shenk, T. 2003. Human cytomegalovirus UL83-coded pp65 virion protein inhibits antiviral gene expression in infected cells. *Proc Natl Acad Sci U S A* 100(20), pp. 11439-11444.

Browne, H. et al. 1990. A complex between the MHC class I homologue encoded by human cytomegalovirus and beta 2 microglobulin. *Nature* 347(6295), pp. 770-772.

Brussaard, C. P. et al. 2000. Flow cytometric detection of viruses. *J Virol Methods* 85(1-2), pp. 175-182.

Bukowski, J. F. et al. 1984. Pathogenesis of murine cytomegalovirus infection in natural killer cell-depleted mice. *J Virol* 52(1), pp. 119-128.

Burns, G. F. et al. 1985. TLiSA1, a human T lineage-specific activation antigen involved in the differentiation of cytotoxic T lymphocytes and anomalous killer cells from their precursors. *J Exp Med* 161(5), pp. 1063-1078.

Butcher, S. J. et al. 1998. Structure of the human cytomegalovirus B capsid by electron cryomicroscopy and image reconstruction. *J Struct Biol* 124(1), pp. 70-76.

Camozzi, D. et al. 2008. Remodelling of the nuclear lamina during human cytomegalovirus infection: role of the viral proteins pUL50 and pUL53. *J Gen Virol* 89(Pt 3), pp. 731-740.

Cantrell, S. R. and Bresnahan, W. A. 2006. Human Cytomegalovirus (HCMV) UL82 Gene Product (pp71) Relieves hDaxx-Mediated Repression of HCMV Replication. *J. Virol.* 80(12), pp. 6188-6191.

Carlsten, M. et al. 2007. DNAX accessory molecule-1 mediated recognition of freshly isolated ovarian carcinoma by resting natural killer cells. *Cancer Res* 67(3), pp. 1317-1325.

Castriconi, R. et al. 2004. Natural killer cell-mediated killing of freshly isolated neuroblastoma cells: critical role of DNAX accessory molecule-1-poliovirus receptor interaction. *Cancer Res* 64(24), pp. 9180-9184.

Cha, T. A. et al. 1996. Human cytomegalovirus clinical isolates carry at least 19 genes not found in laboratory strains. *J Virol* 70(1), pp. 78-83.

Chang, W. L. et al. 2009. Human cytomegalovirus suppresses type I interferon secretion by plasmacytoid dendritic cells through its interleukin 10 homolog. *Virology.*

Chapman, T. L. et al. 1999. The inhibitory receptor LIR-1 uses a common binding interaction to recognize class I MHC molecules and the viral homolog UL18. *Immunity* 11(5), pp. 603-613.

Chee, M. et al. 1989. Identification of the major capsid protein gene of human cytomegalovirus. *J. Virol.* 63(3), pp. 1345-1353.

Chee, M. S. et al. 1990a. Analysis of the protein-coding content of the sequence of human cytomegalovirus strain AD169. *Curr Top Microbiol Immunol* 154, pp. 125-169.

Chee, M. S. et al. 1990b. Human cytomegalovirus encodes three G protein-coupled receptor homologues. *Nature* 344(6268), pp. 774-777.

Chen, D. H. et al. 1999. Three-dimensional visualization of tegument/capsid interactions in the intact human cytomegalovirus. *Virology* 260(1), pp. 10-16.

Cherrington, J. M. et al. 1991. Human cytomegalovirus ie2 negatively regulates alpha gene expression via a short target sequence near the transcription start site. *J Virol* 65(2), pp. 887-896.

Chevillotte, M. et al. 2009. Major tegument protein pp65 of human cytomegalovirus is required for the incorporation of pUL69 and pUL97 into the virus particle and for viral growth in macrophages. *J Virol* 83(6), pp. 2480-2490.

Child, S. J. et al. 2004. Evasion of cellular antiviral responses by human cytomegalovirus TRS1 and IRS1. *J Virol* 78(1), pp. 197-205.

Cobbold, M. et al. 2005. Adoptive transfer of cytomegalovirus-specific CTL to stem cell transplant patients after selection by HLA-peptide tetramers. *J. Exp. Med.* 202(3), pp. 379-386.

Colberg-Poley, A. M. 1996. Functional roles of immediate early proteins encoded by the human cytomegalovirus UL36-38, UL115-119, TRS1/IRS1 and US3 loci. *Intervirology* 39(5-6), pp. 350-360.

Compton, T. et al. 1993. Initiation of human cytomegalovirus infection requires initial interaction with cell surface heparan sulfate. *Virology* 193(2), pp. 834-841.

Cosman, D. et al. 1997. A novel immunoglobulin superfamily receptor for cellular and viral MHC class I molecules. *Immunity* 7(2), pp. 273-282.

Cosman, D. et al. 2001. ULBPs, novel MHC class I-related molecules, bind to CMV glycoprotein UL16 and stimulate NK cytotoxicity through the NKG2D receptor. *Immunity* 14(2), pp. 123-133.

Coyne, C. B. et al. 2007. Poliovirus entry into human brain microvascular cells requires receptor-induced activation of SHP-2. *Embo J* 26(17), pp. 4016-4028.

Craighead, J. E. et al. 1972. Nonviral microbodies with viral antigenicity produced in cytomegalovirus-infected cells. *J Virol* 10(4), pp. 766-775.

Cranage, M. P. et al. 1986. Identification of the human cytomegalovirus glycoprotein B gene and induction of neutralizing antibodies via its expression in recombinant vaccinia virus. *Embo J* 5(11), pp. 3057-3063.

Dardalhon, V. et al. 2005. CD226 is specifically expressed on the surface of Th1 cells and regulates their expansion and effector functions. *J Immunol* 175(3), pp. 1558-1565.

Dargan, D. J. et al. 1997. The published DNA sequence of human cytomegalovirus strain AD169 lacks 929 base pairs affecting genes UL42 and UL43. *J Virol* 71(12), pp. 9833-9836.

Das, S. et al. 2007. Three-dimensional structure of the human cytomegalovirus cytoplasmic virion assembly complex includes a reoriented secretory apparatus. *J Virol* 81(21), pp. 11861-11869.

Davison, A. J. et al. 2003. The human cytomegalovirus genome revisited: comparison with the chimpanzee cytomegalovirus genome. *J Gen Virol* 84(Pt 1), pp. 17-28.

Dittmer, A. and Bogner, E. 2005. Analysis of the quaternary structure of the putative HCMV portal protein PUL104. *Biochemistry* 44(2), pp. 759-765.

Dittmer, A. et al. 2005. Interaction of the putative human cytomegalovirus portal protein pUL104 with the large terminase subunit pUL56 and its inhibition by benzimidazole-D-ribonucleosides. *J Virol* 79(23), pp. 14660-14667.

Dolan, A. et al. 2004. Genetic content of wild-type human cytomegalovirus. *J Gen Virol* 85(Pt 5), pp. 1301-1312.

Dubin, G. et al. 1991. Herpes simplex virus type 1 Fc receptor protects infected cells from antibody-dependent cellular cytotoxicity. *J Virol* 65(12), pp. 7046-7050.

Dunn, C. et al. 2003. Human cytomegalovirus glycoprotein UL16 causes intracellular sequestration of NKG2D ligands, protecting against natural killer cell cytotoxicity. *J Exp Med* 197(11), pp. 1427-1439.

Elek, S. D. and Stern, H. 1974. DEVELOPMENT OF A VACCINE AGAINST MENTAL RETARDATION CAUSED BY CYTOMEGALOVIRUS INFECTION IN UTERO. *The Lancet* 303(7845), p. 1.

Ellsmore, V. et al. 2003. Detection of human cytomegalovirus DNA replication in non-permissive Vero and 293 cells. *J Gen Virol* 84(Pt 3), pp. 639-645.

Erickson, B. M. et al. 2006. Tightly regulated induction of the adhesion molecule necl-5/CD155 during rat liver regeneration and acute liver injury. *Hepatology* 43(2), pp. 325-334.

Fahnestock, M. L. et al. 1995. The MHC class I homolog encoded by human cytomegalovirus binds endogenous peptides. *Immunity* 3(5), pp. 583-590.

Farrar, G. H. and Oram, J. D. 1984. Characterization of the Human Cytomegalovirus Envelope Glycoproteins. *J Gen Virol* 65(11), pp. 1991-2001.

Feire, A. L. et al. 2004. Cellular integrins function as entry receptors for human cytomegalovirus via a highly conserved disintegrin-like domain. *Proc Natl Acad Sci U S A* 101(43), pp. 15470-15475.

Fraile-Ramos, A. et al. 2001. The human cytomegalovirus US28 protein is located in endocytic vesicles and undergoes constitutive endocytosis and recycling. *Mol Biol Cell* 12(6), pp. 1737-1749.

Frank, I. and Friedman, H. M. 1989. A novel function of the herpes simplex virus type 1 Fc receptor: participation in bipolar bridging of antiviral immunoglobulin G. *J Virol* 63(11), pp. 4479-4488.

Fuchs, A. et al. 2004. Cutting edge: CD96 (tactile) promotes NK cell-target cell adhesion by interacting with the poliovirus receptor (CD155). *J Immunol* 172(7), pp. 3994-3998.

Fuchs, A. and Colonna, M. 2006. The role of NK cell recognition of nectin and nectin-like proteins in tumor immunosurveillance. *Semin Cancer Biol* 16(5), pp. 359-366.

Fujito, T. et al. 2005. Inhibition of cell movement and proliferation by cell-cell contact-induced interaction of Necl-5 with nectin-3. *J. Cell Biol.* 171(1), pp. 165-173.

Fukuhara, T. et al. 2004. Activation of Cdc42 by trans interactions of the cell adhesion molecules nectins through c-Src and Cdc42-GEF FRG. *J Cell Biol* 166(3), pp. 393-405.

Fukuyama, T. et al. 2005. Involvement of the c-Src-Crk-C3G-Rap1 signaling in the nectin-induced activation of Cdc42 and formation of adherens junctions. *J Biol Chem* 280(1), pp. 815-825.

Gamadia, L. E. et al. 2003. Primary immune responses to human CMV: a critical role for IFN-gamma-producing CD4+ T cells in protection against CMV disease. *Blood* 101(7), pp. 2686-2692.

Gao, J. L. and Murphy, P. M. 1994. Human cytomegalovirus open reading frame US28 encodes a functional beta chemokine receptor. *J Biol Chem* 269(46), pp. 28539-28542.

Geraghty, R. J. et al. 1998. Entry of alphaherpesviruses mediated by poliovirus receptor-related protein 1 and poliovirus receptor. *Science* 280(5369), pp. 1618-1620.

Gerna, G. et al. 2004. Pathogenesis of human cytomegalovirus infection and cellular targets. *Hum Immunol* 65(5), pp. 381-386.

Gerna, G. et al. 2005. Dendritic-cell infection by human cytomegalovirus is restricted to strains carrying functional UL131-128 genes and mediates efficient viral antigen presentation to CD8+ T cells. *J Gen Virol* 86(2), pp. 275-284.

Gibson, W. 1983. Protein counterparts of human and simian cytomegaloviruses. *Virology* 128(2), p. 391.

Gibson, W. et al. 1996a. Cytomegalovirus "missing" capsid protein identified as heat-aggregable product of human cytomegalovirus UL46. *J Virol* 70(11), pp. 7454-7461.

Gibson, W. et al. 1996b. Human cytomegalovirus (HCMV) smallest capsid protein identified as product of short open reading frame located between HCMV UL48 and UL49. *J Virol* 70(8), pp. 5680-5683.

Gibson, W. et al. 1990. Identification of precursor to cytomegalovirus capsid assembly protein and evidence that processing results in loss of its carboxy-terminal end. *J Virol* 64(3), pp. 1241-1249.

Gicklhorn, D. et al. 2003. Differential effects of glycoprotein B epitope-specific antibodies on human cytomegalovirus-induced cell-cell fusion. *J Gen Virol* 84(Pt 7), pp. 1859-1862.

Goldmacher, V. S. et al. 1999. A cytomegalovirus-encoded mitochondria-localized inhibitor of apoptosis structurally unrelated to Bcl-2. *Proc Natl Acad Sci U S A* 96(22), pp. 12536-12541.

Goodrum, F. et al. 2007. Human cytomegalovirus sequences expressed in latently infected individuals promote a latent infection in vitro. *Blood* 110(3), pp. 937-945.

Greenaway, P. J. and Wilkinson, G. W. 1987. Nucleotide sequence of the most abundantly transcribed early gene of human cytomegalovirus strain AD169. *Virus Res* 7(1), pp. 17-31.

Greijer, A. E. et al. 2000. Human cytomegalovirus virions differentially incorporate viral and host cell RNA during the assembly process. *J Virol* 74(19), pp. 9078-9082.

Gretch, D. R. et al. 1988. Identification and characterization of three distinct families of glycoprotein complexes in the envelopes of human cytomegalovirus. *J Virol* 62(3), pp. 875-881.

Grey, F. and Nelson, J. 2008. Identification and function of human cytomegalovirus microRNAs. *J Clin Virol* 41(3), pp. 186-191.

Griffin, C. et al. 2005. Characterization of a highly glycosylated form of the human cytomegalovirus HLA class I homologue gpUL18. *J Gen Virol* 86(Pt 11), pp. 2999-3008.

Groh, V. et al. 1996. Cell stress-regulated human major histocompatibility complex class I gene expressed in gastrointestinal epithelium. *Proc Natl Acad Sci U S A* 93(22), pp. 12445-12450.

Grundy, J. E. et al. 1987. Beta 2 microglobulin enhances the infectivity of cytomegalovirus and when bound to the virus enables class I HLA molecules to be used as a virus receptor. *J Gen Virol* 68 (Pt 3), pp. 793-803.

Guma, M. et al. 2004. Imprint of human cytomegalovirus infection on the NK cell receptor repertoire. *Blood* 104(12), pp. 3664-3671.

Hahn, G. et al. 1998. Cytomegalovirus remains latent in a common precursor of dendritic and myeloid cells. *Proc Natl Acad Sci U S A* 95(7), pp. 3937-3942.

Hakki, M. et al. 2006. Binding and Nuclear Relocalization of Protein Kinase R by Human Cytomegalovirus TRS1. *J. Virol.* 80(23), pp. 11817-11826.

Hakki, M. et al. 2003. Immune reconstitution to cytomegalovirus after allogeneic hematopoietic stem cell transplantation: impact of host factors, drug therapy, and subclinical reactivation. *Blood* 102(8), pp. 3060-3067.

Harari, A. et al. 2004a. Skewed representation of functionally distinct populations of virus-specific CD4 T cells in HIV-1-infected subjects with progressive disease: changes after antiretroviral therapy. *Blood* 103(3), pp. 966-972.

Harari, A. et al. 2002. Analysis of HIV-1- and CMV-specific memory CD4 T-cell responses during primary and chronic infection. *Blood* 100(4), pp. 1381-1387.

Harari, A. et al. 2004b. Cytomegalovirus (CMV)-specific cellular immune responses. *Hum Immunol* 65(5), pp. 500-506.

Hegde, N. R. and Johnson, D. C. 2003. Human cytomegalovirus US2 causes similar effects on both major histocompatibility complex class I and II proteins in epithelial and glial cells. *J Virol* 77(17), pp. 9287-9294.

Hegde, N. R. et al. 2002. Inhibition of HLA-DR Assembly, Transport, and Loading by Human Cytomegalovirus Glycoprotein US3: a Novel Mechanism for Evading Major Histocompatibility Complex Class II Antigen Presentation. *J. Virol.* 76(21), pp. 10929-10941.

Heieren, M. H. et al. 1988. Human cytomegalovirus infection of kidney glomerular visceral epithelial and tubular epithelial cells in culture. *Transplantation* 46(3), pp. 426-432.

Helenius, A. and Aebi, M. 2004. Roles of N-linked glycans in the endoplasmic reticulum. *Annu Rev Biochem* 73, pp. 1019-1049.

Hengel, H. et al. 1996. Human cytomegalovirus inhibits peptide translocation into the endoplasmic reticulum for MHC class I assembly. *J Gen Virol* 77 (Pt 9), pp. 2287-2296.

Hewitt, E. W. et al. 2001. The human cytomegalovirus gene product US6 inhibits ATP binding by TAP. *Embo J* 20(3), pp. 387-396.

Hogle, J. M. 2002. Poliovirus cell entry: common structural themes in viral cell entry pathways. *Annu Rev Microbiol* 56, pp. 677-702.

Hokland, M. et al. 1988. Natural killer function following allogeneic bone marrow transplantation. Very early reemergence but strong dependence of cytomegalovirus infection. *Transplantation* 45(6), pp. 1080-1084.

Hollenbach, A. D. et al. 2002. Daxx and histone deacetylase II associate with chromatin through an interaction with core histones and the chromatin-associated protein Dek. *J Cell Sci* 115(16), pp. 3319-3330.

Homman-Loudiyi, M. et al. 2003. Envelopment of human cytomegalovirus occurs by budding into Golgi-derived vacuole compartments positive for gB, Rab 3, trans-golgi network 46, and mannosidase II. *J Virol* 77(5), pp. 3191-3203.

Huber, M. T. and Compton, T. 1997. Characterization of a novel third member of the human cytomegalovirus glycoprotein H-glycoprotein L complex. *J Virol* 71(7), pp. 5391-5398.

Huber, M. T. and Compton, T. 1998. The human cytomegalovirus UL74 gene encodes the third component of the glycoprotein H-glycoprotein L-containing envelope complex. *J Virol* 72(10), pp. 8191-8197.

Huber, M. T. and Compton, T. 1999. Intracellular Formation and Processing of the Heterotrimeric gH-gL-gO (gCIII) Glycoprotein Envelope Complex of Human Cytomegalovirus. *J. Virol.* 73(5), pp. 3886-3892.

Hudecz, F. et al. 1985. Preparation of highly purified human cytomegalovirus envelope antigen. *Vaccine* 3(3), pp. 300-304.

Huh, Y. H. et al. 2008. Binding STAT2 by the Acidic Domain of Human Cytomegalovirus IE1 Promotes Viral Growth and Is Negatively Regulated by SUMO. *J. Virol.* 82(21), pp. 10444-10454.

Ikeda, W. et al. 2003. Tage4/Nectin-like molecule-5 heterophilically trans-interacts with cell adhesion molecule Nectin-3 and enhances cell migration. *J Biol Chem* 278(30), pp. 28167-28172.

Ikeda, W. et al. 2004. Nectin-like molecule-5/Tage4 enhances cell migration in an integrin-dependent, Nectin-3-independent manner. *J Biol Chem* 279(17), pp. 18015-18025.

Ikeda, W. et al. 1999. Afadin: A key molecule essential for structural organization of cell-cell junctions of polarized epithelia during embryogenesis. *J Cell Biol* 146(5), pp. 1117-1132.

Irmiere, A. and Gibson, W. 1983. Isolation and characterization of a noninfectious virion-like particle released from cells infected with human strains of cytomegalovirus. *Virology* 130(1), pp. 118-133.

Irmiere, A. and Gibson, W. 1985a. Isolation of human cytomegalovirus intranuclear capsids, characterization of their protein constituents, and demonstration that the B-capsid assembly protein is also abundant in noninfectious enveloped particles. *J. Virol.* 56(1), pp. 277-283.

Irmiere, A. and Gibson, W. 1985b. Isolation of human cytomegalovirus intranuclear capsids, characterization of their protein constituents, and demonstration that the B-capsid assembly protein is also abundant in noninfectious enveloped particles. *J Virol* 56(1), pp. 277-283.

Isaacson, M. K. et al. 2007. Epidermal Growth Factor Receptor Is Not Required for Human Cytomegalovirus Entry or Signaling. *J. Virol.* 81(12), pp. 6241-6247.

Ishov, A. M. et al. 1997. Human cytomegalovirus immediate early interaction with host nuclear structures: definition of an immediate transcript environment. *J Cell Biol* 138(1), pp. 5-16.

Isomura, H. et al. 2008. Noncanonical TATA sequence in the UL44 late promoter of human cytomegalovirus is required for the accumulation of late viral transcripts. *J Virol* 82(4), pp. 1638-1646.

Isomura, H. et al. 2007. The late promoter of the human cytomegalovirus viral DNA polymerase processivity factor has an impact on delayed early and late viral gene products but not on viral DNA synthesis. *J Virol* 81(12), pp. 6197-6206.

Iwayama, S. et al. 1994. Intracellular localization and DNA-binding activity of a class of viral early phosphoproteins in human fibroblasts infected with human cytomegalovirus (Towne strain). *J Gen Virol* 75 (Pt 12), pp. 3309-3318.

Jenkins, D. E. et al. 1994. Human cytomegalovirus late protein encoded by ie2: a trans-activator as well as a repressor of gene expression. *J Gen Virol* 75 (Pt 9), pp. 2337-2348.

Jian, J. L. et al. 2006. Identification and characterization of the CD226 gene promoter. *J Biol Chem* 281(39), pp. 28731-28736.

Jiang, X. J. et al. 2008. UL74 of human cytomegalovirus contributes to virus release by promoting secondary envelopment of virions. *J Virol* 82(6), pp. 2802-2812.

Johnson, R. A. et al. 2001. Human Cytomegalovirus Up-Regulates the Phosphatidylinositol 3-Kinase (PI3-K) Pathway: Inhibition of PI3-K Activity Inhibits Viral Replication and Virus-Induced Signaling. *J. Virol.* 75(13), pp. 6022-6032.

Jones, T. R. and Sun, L. 1997. Human cytomegalovirus US2 destabilizes major histocompatibility complex class I heavy chains. *J Virol* 71(4), pp. 2970-2979.

Jones, T. R. et al. 1996. Human cytomegalovirus US3 impairs transport and maturation of major histocompatibility complex class I heavy chains. *Proc Natl Acad Sci U S A* 93(21), pp. 11327-11333.

Jonjic, S. et al. 2008. Dissection of the antiviral NK cell response by MCMV mutants. *Methods Mol Biol* 415, pp. 127-149.

Kajita, M. et al. 2007. Regulation of platelet-derived growth factor-induced Ras signaling by poliovirus receptor Necl-5 and negative growth regulator Sprouty2. *Genes Cells* 12(3), pp. 345-357.

Kakunaga, S. et al. 2005. Nectin-like molecule-1/TSLL1/SynCAM3: a neural tissue-specific immunoglobulin-like cell-cell adhesion molecule localizing at non-junctional contact sites of presynaptic nerve terminals, axons and glia cell processes. *J Cell Sci* 118(Pt 6), pp. 1267-1277.

Kakunaga, S. et al. 2004. Enhancement of Serum- and Platelet-derived Growth Factor-induced Cell Proliferation by Necl-5/Tage4/Poliovirus Receptor/CD155 through the Ras-Raf-MEK-ERK Signaling. *J. Biol. Chem.* 279(35), pp. 36419-36425.

Kanzaki, N. et al. 2008. Involvement of the nectin-afadin complex in PDGF-induced cell survival. *J Cell Sci* 121(Pt 12), pp. 2008-2017.

Kari, B. and Gehrz, R. 1992. A human cytomegalovirus glycoprotein complex designated gC-II is a major heparin-binding component of the envelope. *J. Virol.* 66(3), pp. 1761-1764.

Kari, B. et al. 1990. Structure and composition of a family of human cytomegalovirus glycoprotein complexes designated gC-I (gB). *J Gen Virol* 71 (Pt 11), pp. 2673-2680.

Karlin, S. et al. 1994. Molecular evolution of herpesviruses: genomic and protein sequence comparisons. *J Virol* 68(3), pp. 1886-1902.

Katz, F. E. et al. 1985. Identification of a membrane glycoprotein associated with haemopoietic progenitor cells. *Leuk Res* 9(2), pp. 191-198.

Kawakatsu, T. et al. 2005. Vav2 as a Rac-GDP/GTP exchange factor responsible for the nectin-induced, c-Src- and Cdc42-mediated activation of Rac. *J Biol Chem* 280(6), pp. 4940-4947.

Kaye, J. F. et al. 1992. Glycoprotein H of human cytomegalovirus (HCMV) forms a stable complex with the HCMV UL115 gene product. *J Gen Virol* 73 (Pt 10), pp. 2693-2698.

Keay, S. and Baldwin, B. 1991. Anti-idiotype antibodies that mimic gp86 of human cytomegalovirus inhibit viral fusion but not attachment. *J Virol* 65(9), pp. 5124-5128.

Kelly, C. et al. 1995. Disruption of PML-associated nuclear bodies during human cytomegalovirus infection. *J Gen Virol* 76 (Pt 11), pp. 2887-2893.

Kern, F. et al. 2000. Analysis of CD8 T cell reactivity to cytomegalovirus using protein-spanning pools of overlapping pentadecapeptides. *Eur J Immunol* 30(6), pp. 1676-1682.

Kerry, J. A. et al. 1997. Translational regulation of the human cytomegalovirus pp28 (UL99) late gene. *J Virol* 71(2), pp. 981-987.

Kledal, T. N. et al. 1998. Selective recognition of the membrane-bound CX3C chemokine, fractalkine, by the human cytomegalovirus-encoded broad-spectrum receptor US28. *FEBS Lett* 441(2), pp. 209-214.

Koike, S. et al. 1990. The poliovirus receptor protein is produced both as membrane-bound and secreted forms. *Embo J* 9(10), pp. 3217-3224.

Kondo, E. et al. 2004. Identification of novel CTL epitopes of CMV-pp65 presented by a variety of HLA alleles. *Blood* 103(2), pp. 630-638.

Kondo, K. et al. 1996. Human cytomegalovirus latent gene expression in granulocyte-macrophage progenitors in culture and in seropositive individuals. *Proc Natl Acad Sci U S A* 93(20), pp. 11137-11142.

Kotenko, S. V. et al. 2000. Human cytomegalovirus harbors its own unique IL-10 homolog (cmvIL-10). *Proc Natl Acad Sci U S A* 97(4), pp. 1695-1700.

Kubin, M. et al. 2001. ULBP1, 2, 3: novel MHC class I-related molecules that bind to human cytomegalovirus glycoprotein UL16, activate NK cells. *Eur J Immunol* 31(5), pp. 1428-1437.

Kuhn, D. E. et al. 1995. The cytomegalovirus US28 protein binds multiple CC chemokines with high affinity. *Biochem Biophys Res Commun* 211(1), pp. 325-330.

Kuramitsu, K. et al. 2008. Novel role of nectin: implication in the co-localization of JAM-A and claudin-1 at the same cell-cell adhesion membrane domain. *Genes Cells* 13(8), pp. 797-805.

Lafemina, R. L. et al. 1989. Expression of the acidic nuclear immediate-early protein (IE1) of human cytomegalovirus in stable cell lines and its preferential association with metaphase chromosomes. *Virology* 172(2), pp. 584-600.

Lang, D. and Stamminger, T. 1993. The 86-kilodalton IE-2 protein of human cytomegalovirus is a sequence-specific DNA-binding protein that interacts directly with the negative autoregulatory response element located near the cap site of the IE-1/2 enhancer-promoter. *J Virol* 67(1), pp. 323-331.

Lange, R. et al. 2001. The poliovirus receptor CD155 mediates cell-to-matrix contacts by specifically binding to vitronectin. *Virology* 285(2), pp. 218-227.

LaPierre, L. A. and Biegalke, B. J. 2001. Identification of a novel transcriptional repressor encoded by human cytomegalovirus. *J Virol* 75(13), pp. 6062-6069.

Lee, A. W. et al. 2006. Human Cytomegalovirus Alters Localization of MHC Class II and Dendrite Morphology in Mature Langerhans Cells. *J Immunol* 177(6), pp. 3960-3971.

Leis, M. et al. 2004. Downregulation of the cellular adhesion molecule Thy-1 (CD90) by cytomegalovirus infection of human fibroblasts. *J Gen Virol* 85(7), pp. 1995-2000.

Leong, C. C. et al. 1998. Modulation of natural killer cell cytotoxicity in human cytomegalovirus infection: the role of endogenous class I major histocompatibility complex and a viral class I homolog. *J Exp Med* 187(10), pp. 1681-1687.

Li, L. et al. 1997. Glycoprotein H-related complexes of human cytomegalovirus: identification of a third protein in the gCIII complex. *J Virol* 71(4), pp. 3090-3097.

Lilleri, D. et al. 2007. Development of human cytomegalovirus-specific T cell immunity during primary infection of pregnant women and its correlation with virus transmission to the fetus. *J Infect Dis* 195(7), pp. 1062-1070.

Lilleri, D. et al. 2009. Human cytomegalovirus-specific CD4+ and CD8+ T cell responses in primary infection of the immunocompetent and the immunocompromised host. *Clin Immunol* 131(3), pp. 395-403.

Lilley, B. N. and Ploegh, H. L. 2004. A membrane protein required for dislocation of misfolded proteins from the ER. *Nature* 429(6994), pp. 834-840.

Lilley, B. N. et al. 2001. Human cytomegalovirus open reading frame TRL11/IRL11 encodes an immunoglobulin G Fc-binding protein. *J Virol* 75(22), pp. 11218-11221.

Liu, B. et al. 1991. A cis-acting element in the major immediate-early (IE) promoter of human cytomegalovirus is required for negative regulation by IE2. *J Virol* 65(2), pp. 897-903.

Liu, B. and Stinski, M. F. 1992. Human cytomegalovirus contains a tegument protein that enhances transcription from promoters with upstream ATF and AP-1 cis-acting elements. *J Virol* 66(7), pp. 4434-4444.

Liu, Y. et al. 2009. The tegument protein UL94 of human cytomegalovirus as a binding partner for tegument protein pp28 identified by intracellular imaging. *Virology* 388(1), pp. 68-77.

Lockridge, K. M. et al. 2000. Primate cytomegaloviruses encode and express an IL-10-like protein. *Virology* 268(2), pp. 272-280.

Lukashchuk, V. et al. 2008. Human Cytomegalovirus Protein pp71 Displaces the Chromatin-Associated Factor ATRX from Nuclear Domain 10 at Early Stages of Infection. *J. Virol.* 82(24), pp. 12543-12554.

Lunetta, J. M. and Wiedeman, J. A. 2000. Latency-associated sense transcripts are expressed during in vitro human cytomegalovirus productive infection. *Virology* 278(2), pp. 467-476.

Luo, M. H. et al. 2008. Neonatal Neural Progenitor Cells and Their Neuronal and Glial Cell Derivatives Are Fully Permissive for Human Cytomegalovirus Infection. *J. Virol.* 82(20), pp. 9994-10007.

Ma, Y. P. et al. 2006. Sequence variability of the human cytomegalovirus UL141 Open Reading Frame in clinical strains. *Arch Virol* 151(4), pp. 827-835.

Mach, M. et al. 2000. Complex formation by human cytomegalovirus glycoproteins M (gpUL100) and N (gpUL73). *J Virol* 74(24), pp. 11881-11892.

Mach, M. et al. 2005. Complex formation by glycoproteins M and N of human cytomegalovirus: structural and functional aspects. *J Virol* 79(4), pp. 2160-2170.

Maier, M. K. et al. 2007. The adhesion receptor CD155 determines the magnitude of humoral immune responses against orally ingested antigens. *Eur J Immunol* 37(8), pp. 2214-2225.

Mandai, K. et al. 1997. Afadin: A novel actin filament-binding protein with one PDZ domain localized at cadherin-based cell-to-cell adherens junction. *J Cell Biol* 139(2), pp. 517-528.

Manley, T. J. et al. 2004. Immune evasion proteins of human cytomegalovirus do not prevent a diverse CD8+ cytotoxic T-cell response in natural infection. *Blood* 104(4), pp. 1075-1082.

Marshall, G. S. et al. 1996. Processing of human cytomegalovirus glycoprotein B in recombinant adenovirus-infected cells. *J Gen Virol* 77(7), pp. 1549-1557.

Marshall, G. S. et al. 1992. Antibodies to recombinant-derived glycoprotein B after natural human cytomegalovirus infection correlate with neutralizing activity. *J Infect Dis* 165(2), pp. 381-384.

Martinez, W. M. and Spear, P. G. 2001. Structural features of nectin-2 (HveB) required for herpes simplex virus entry. *J Virol* 75(22), pp. 11185-11195.

Masson, D. et al. 2001. Overexpression of the CD155 gene in human colorectal carcinoma. *Gut* 49(2), pp. 236-240.

Maurel, P. et al. 2007. Nectin-like proteins mediate axon Schwann cell interactions along the internode and are essential for myelination. *J Cell Biol* 178(5), pp. 861-874.

McLean, K. A. et al. 2004. Similar activation of signal transduction pathways by the herpesvirus-encoded chemokine receptors US28 and ORF74. *Virology* 325(2), pp. 241-251.

McSharry, B. P. et al. 2003. The most abundantly transcribed human cytomegalovirus gene (beta 2.7) is non-essential for growth in vitro. *J Gen Virol* 84(Pt 9), pp. 2511-2516.

McVoy, M. A. et al. 1998. Sequences within the herpesvirus-conserved pac1 and pac2 motifs are required for cleavage and packaging of the murine cytomegalovirus genome. *J Virol* 72(1), pp. 48-56.

Mendelsohn, C. L. et al. 1989. Cellular receptor for poliovirus: molecular cloning, nucleotide sequence, and expression of a new member of the immunoglobulin superfamily. *Cell* 56(5), pp. 855-865.

Mendelson, M. et al. 1996. Detection of endogenous human cytomegalovirus in CD34+ bone marrow progenitors. *J Gen Virol* 77 (Pt 12), pp. 3099-3102.

Metcalf, D. 1989. The molecular control of cell division, differentiation commitment and maturation in haemopoietic cells. *Nature* 339(6219), pp. 27-30.

Miller, D. M. et al. 1998. Human cytomegalovirus inhibits major histocompatibility complex class II expression by disruption of the Jak/Stat pathway. *J Exp Med* 187(5), pp. 675-683.

Milne, R. S. et al. 1998. Human cytomegalovirus glycoprotein H/glycoprotein L complex modulates fusion-from-without. *J Gen Virol* 79(4), pp. 855-865.

Minami, Y. et al. 2007a. Necl-5/poliovirus receptor interacts in cis with integrin alphaVbeta3 and regulates its clustering and focal complex formation. *J Biol Chem* 282(25), pp. 18481-18496.

Minami, Y. et al. 2007b. Involvement of up-regulated Necl-5/Tage4/PVR/CD155 in the loss of contact inhibition in transformed NIH3T3 cells. *Biochem Biophys Res Commun* 352(4), pp. 856-860.

Misaghi, S. et al. 2004. Structural and Functional Analysis of Human Cytomegalovirus US3 Protein. *J. Virol.* 78(1), pp. 413-423.

Mocarski, E. S. et al. 1997. Reassessing the organization of the UL42-UL43 region of the human cytomegalovirus strain AD169 genome. *Virology* 239(1), pp. 169-175.

Mocarski, E. S. et al. 2007. Cytomegaloviruses.*Field's Virology*. 5th ed. Philadelphia, PA: Lippincott Williams and Wilkins.

Morimoto, K. et al. 2008. Interaction of cancer cells with platelets mediated by Necl-5/poliovirus receptor enhances cancer cell metastasis to the lungs. *Oncogene* 27(3), pp. 264-273.

Mueller, S. et al. 2002. Interaction of the poliovirus receptor CD155 with the dynein light chain Tctex-1 and its implication for poliovirus pathogenesis. *J Biol Chem* 277(10), pp. 7897-7904.

Munger, J. et al. 2006. UL26-Deficient Human Cytomegalovirus Produces Virions with Hypophosphorylated pp28 Tegument Protein That Is Unstable within Newly Infected Cells. *J. Virol.* 80(7), pp. 3541-3548.

Murphy, J. C. et al. 2002. Control of cytomegalovirus lytic gene expression by histone acetylation. *Embo J* 21(5), pp. 1112-1120.

Nachtwey, J. and Spencer, J. V. 2008. HCMV IL-10 suppresses cytokine expression in monocytes through inhibition of nuclear factor-kappaB. *Viral Immunol* 21(4), pp. 477-482.

Nagamatsu, Y. et al. 2008. Roles of Necl-5/poliovirus receptor and Rho-associated kinase (ROCK) in the regulation of transformation of integrin alpha(V)beta(3)-based focal complexes into focal adhesions. *J Biol Chem* 283(21), pp. 14532-14541.

Nguyen, N. L. et al. 2008. Nuclear localization sequences in cytomegalovirus capsid assembly proteins (UL80 proteins) are required for virus production: inactivating NLS1, NLS2, or both affects replication to strikingly different extents. *J Virol* 82(11), pp. 5381-5389.

Nigro, G. et al. 2005. Passive immunization during pregnancy for congenital cytomegalovirus infection. *N Engl J Med* 353(13), pp. 1350-1362.

Noriega, V. M. and Tortorella, D. 2009. Human cytomegalovirus-encoded immune modulators partner to downregulate major histocompatibility complex class I molecules. *J Virol* 83(3), pp. 1359-1367.

Novotny, J. et al. 2001. In silico structural and functional analysis of the human cytomegalovirus (HHV5) genome. *J Mol Biol* 310(5), pp. 1151-1166.

Nowlin, D. M. et al. 1991. Expression of a human cytomegalovirus receptor correlates with infectibility of cells. *J Virol* 65(6), pp. 3114-3121.

Oda, T. et al. 2004. Ligand stimulation of CD155alpha inhibits cell adhesion and enhances cell migration in fibroblasts. *Biochem Biophys Res Commun* 319(4), pp. 1253-1264.

Ohka, S. et al. 2004. Receptor (CD155)-dependent endocytosis of poliovirus and retrograde axonal transport of the endosome. *J Virol* 78(13), pp. 7186-7198.

Oram, J. D. et al. 1982. Use of recombinant plasmids to investigate the structure of the human cytomegalovirus genome. *J Gen Virol* 59(Pt 1), pp. 111-129.

Pari, G. S. 2008. Nuts and bolts of human cytomegalovirus lytic DNA replication. *Curr Top Microbiol Immunol* 325, pp. 153-166.

Park, B. et al. 2004. Human cytomegalovirus inhibits tapasin-dependent peptide loading and optimization of the MHC class I peptide cargo for immune evasion. *Immunity* 20(1), pp. 71-85.

Paterson, D. A. et al. 2002. A Role for Human Cytomegalovirus Glycoprotein O (gO) in Cell Fusion and a New Hypervariable Locus. *Virology* 293(2), p. 281.

Patrone, M. et al. 2007. Cytomegalovirus UL131-128 Products Promote gB Conformational Transition and gB-gH Interaction during Entry into Endothelial Cells. *J. Virol.* 81(20), pp. 11479-11488.

Patterson, C. E. and Shenk, T. 1999. Human cytomegalovirus UL36 protein is dispensable for viral replication in cultured cells. *J Virol* 73(9), pp. 7126-7131.

Peggs, K. et al. 2002. Characterization of human cytomegalovirus peptide-specific CD8+ T-cell repertoire diversity following in vitro restimulation by antigen-pulsed dendritic cells. *Blood* 99(1), pp. 213-223.

Pellissier, F. et al. 2007. The adhesion molecule Necl-3/SynCAM-2 localizes to myelinated axons, binds to oligodendrocytes and promotes cell adhesion. *BMC Neuroscience* 8(1), p. 90.

Pende, D. et al. 2005a. PVR (CD155) and Nectin-2 (CD112) as ligands of the human DNAM-1 (CD226) activating receptor: involvement in tumor cell lysis. *Mol Immunol* 42(4), pp. 463-469.

Pende, D. et al. 2005b. Analysis of the receptor-ligand interactions in the natural killer-mediated lysis of freshly isolated myeloid or lymphoblastic leukemias: evidence for the involvement of the Poliovirus receptor (CD155) and Nectin-2 (CD112). *Blood* 105(5), pp. 2066-2073.

Penfold, M. E. et al. 1999. Cytomegalovirus encodes a potent alpha chemokine. *Proc Natl Acad Sci U S A* 96(17), pp. 9839-9844.

Penfold, M. E. and Mocarski, E. S. 1997. Formation of cytomegalovirus DNA replication compartments defined by localization of viral proteins and DNA synthesis. *Virology* 239(1), pp. 46-61.

Pizzorno, M. C. et al. 1988. trans-activation and autoregulation of gene expression by the immediate-early region 2 gene products of human cytomegalovirus. *J Virol* 62(4), pp. 1167-1179.

Prichard, M. N. et al. 1998. Identification of persistent RNA-DNA hybrid structures within the origin of replication of human cytomegalovirus. *J Virol* 72(9), pp. 6997-7004.

Prod'homme, V. et al. 2007. The human cytomegalovirus MHC class I homolog UL18 inhibits LIR-1+ but activates LIR-1- NK cells. *J Immunol* 178(7), pp. 4473-4481.

Ralston, K. J. et al. 2004. The LFA-1-associated molecule PTA-1 (CD226) on T cells forms a dynamic molecular complex with protein 4.1G and human discs large. *J Biol Chem* 279(32), pp. 33816-33828.

Ravens, I. et al. 2003. Characterization and identification of Tage4 as the murine orthologue of human poliovirus receptor/CD155. *Biochem Biophys Res Commun* 312(4), pp. 1364-1371.

Redpath, S. et al. 1999. Murine cytomegalovirus infection down-regulates MHC class II expression on macrophages by induction of IL-10. *J Immunol* 162(11), pp. 6701-6707.

Reeves, M. B. et al. 2007. Complex I Binding by a Virally Encoded RNA Regulates Mitochondria-Induced Cell Death. *Science* 316(5829), pp. 1345-1348.

Reeves, M. B. et al. 2005a. An in vitro model for the regulation of human cytomegalovirus latency and reactivation in dendritic cells by chromatin remodelling. *J Gen Virol* 86(Pt 11), pp. 2949-2954.

Reeves, M. B. et al. 2005b. Latency, chromatin remodeling, and reactivation of human cytomegalovirus in the dendritic cells of healthy carriers. *Proc Natl Acad Sci U S A* 102(11), pp. 4140-4145.

Reusser, P. et al. 1991. Cytotoxic T-lymphocyte response to cytomegalovirus after human allogeneic bone marrow transplantation: pattern of recovery and correlation with cytomegalovirus infection and disease. *Blood* 78(5), pp. 1373-1380.

Revello, M. G. et al. 1998. Human cytomegalovirus in blood of immunocompetent persons during primary infection: prognostic implications for pregnancy. *J Infect Dis* 177(5), pp. 1170-1175.

Reyburn, H. T. et al. 1997. The class I MHC homologue of human cytomegalovirus inhibits attack by natural killer cells. *Nature* 386(6624), pp. 514-517.

Reymond, N. et al. 2001. Nectin4/PRR4, a new afadin-associated member of the nectin family that trans-interacts with nectin1/PRR1 through V domain interaction. *J Biol Chem* 276(46), pp. 43205-43215.

Reymond, N. et al. 2004. DNAM-1 and PVR regulate monocyte migration through endothelial junctions. *J Exp Med* 199(10), pp. 1331-1341.

Roberts, P. L. 2008. Virus inactivation by solvent/detergent treatment using Triton X-100 in a high purity factor VIII. *Biologicals* 36(5), p. 330.

Rodems, S. M. et al. 1998. Separate DNA elements containing ATF/CREB and IE86 binding sites differentially regulate the human cytomegalovirus UL112-113 promoter at early and late times in the infection. *J Virol* 72(4), pp. 2697-2707.

Romanowski, M. J. et al. 1997. pIRS1 and pTRS1 are present in human cytomegalovirus virions. *J Virol* 71(7), pp. 5703-5705.

Rowe, W. P. et al. 1956. Cytopathogenic agent resembling human salivary gland virus recovered from tissue cultures of human adenoids. *Proc Soc Exp Biol Med* 92(2), pp. 418-424.

Ryckman, B. J. et al. 2008a. HCMV gH/gL/UL128â€"131 interferes with virus entry into epithelial cells: Evidence for cell type-specific receptors. *Proceedings of the National Academy of Sciences* 105(37), pp. 14118-14123.

Ryckman, B. J. et al. 2008b. Characterization of the Human Cytomegalovirus gH/gL/UL128-131 Complex That Mediates Entry into Epithelial and Endothelial Cells. *J. Virol.* 82(1), pp. 60-70.

Sakamoto, Y. et al. 2006. Interaction of integrin alpha(v)beta3 with nectin. Implication in cross-talk between cell-matrix and cell-cell junctions. *J Biol Chem* 281(28), pp. 19631-19644.

Sakamoto, Y. et al. 2008. Involvement of nectin in inactivation of integrin alpha(v)beta(3) after the establishment of cell-cell adhesion. *J Biol Chem* 283(1), pp. 496-505.

Sanchez, V. et al. 1998. Localization of Human Cytomegalovirus Structural Proteins to the Nuclear Matrix of Infected Human Fibroblasts. *J. Virol.* 72(4), pp. 3321-3329.

Sanchez, V. et al. 2000a. Accumulation of Virion Tegument and Envelope Proteins in a Stable Cytoplasmic Compartment during Human Cytomegalovirus Replication: Characterization of a Potential Site of Virus Assembly. *J. Virol.* 74(2), pp. 975-986.

Sanchez, V. et al. 2000b. Human cytomegalovirus pp28 (UL99) localizes to a cytoplasmic compartment which overlaps the endoplasmic reticulum-golgi-intermediate compartment. *J Virol* 74(8), pp. 3842-3851.

Sarcinella, E. et al. 2004. Detection of RNA in purified cytomegalovirus virions. *Virus Res* 104(2), pp. 129-137.

Sato, T. et al. 2005. Common signaling pathway is used by the trans-interaction of Necl-5/Tage4/PVR/CD155 and nectin, and of nectin and nectin during the formation of cell-cell adhesion. *Cancer Science* 96(9), pp. 578-589.

Sato, T. et al. 2004. Involvement of heterophilic trans-interaction of Necl-5/Tage4/PVR/CD155 with nectin-3 in formation of nectin- and cadherin-based adherens junctions. *Genes Cells* 9(9), pp. 791-799.

Satoh-Horikawa, K. et al. 2000. Nectin-3, a new member of immunoglobulin-like cell adhesion molecules that shows homophilic and heterophilic cell-cell adhesion activities. *J Biol Chem* 275(14), pp. 10291-10299.

Schuessler, A. et al. 2008. Charge cluster-to-alanine scanning of UL128 for fine tuning of the endothelial cell tropism of human cytomegalovirus. *J Virol* 82(22), pp. 11239-11246.

Scott, J. L. et al. 1989. Characterization of a novel membrane glycoprotein involved in platelet activation. *J Biol Chem* 264(23), pp. 13475-13482.

Seth, S. et al. 2007. The murine pan T cell marker CD96 is an adhesion receptor for CD155 and nectin-1. *Biochem Biophys Res Commun* 364(4), pp. 959-965.

Shamu, C. E. et al. 2001. Polyubiquitination is required for US11-dependent movement of MHC class I heavy chain from endoplasmic reticulum into cytosol. *Mol Biol Cell* 12(8), pp. 2546-2555.

Shamu, C. E. et al. 1999. The pathway of US11-dependent degradation of MHC class I heavy chains involves a ubiquitin-conjugated intermediate. *J Cell Biol* 147(1), pp. 45-58.

Shibuya, A. et al. 1996. DNAM-1, a novel adhesion molecule involved in the cytolytic function of T lymphocytes. *Immunity* 4(6), pp. 573-581.

Shibuya, A. et al. 1998. Protein kinase C is involved in the regulation of both signaling and adhesion mediated by DNAX accessory molecule-1 receptor. *J Immunol* 161(4), pp. 1671-1676.

Shibuya, K. et al. 2003. CD226 (DNAM-1) is involved in lymphocyte function-associated antigen 1 costimulatory signal for naive T cell differentiation and proliferation. *J Exp Med* 198(12), pp. 1829-1839.

Shimamura, M. et al. 2006. Human cytomegalovirus infection elicits a glycoprotein M (gM)/gN-specific virus-neutralizing antibody response. *J Virol* 80(9), pp. 4591-4600.

Shingai, T. et al. 2003. Implications of nectin-like molecule-2/IGSF4/RA175/SgIGSF/TSLC1/SynCAM1 in cell-cell adhesion and transmembrane protein localization in epithelial cells. *J Biol Chem* 278(37), pp. 35421-35427.

Shirakawa, J. et al. 2006. LFA-1-dependent lipid raft recruitment of DNAM-1 (CD226) in CD4+ T cell. *Int Immunol* 18(6), pp. 951-957.

Silva, M. C. et al. 2003. Human Cytomegalovirus UL99-Encoded pp28 Is Required for the Cytoplasmic Envelopment of Tegument-Associated Capsids. *J. Virol.* 77(19), pp. 10594-10605.

Sinclair, J. and Sissons, P. 2006. Latency and reactivation of human cytomegalovirus. *J Gen Virol* 87(7), pp. 1763-1779.

Sinzger, C. et al. 2008. Cytomegalovirus cell tropism. *Curr Top Microbiol Immunol* 325, pp. 63-83.

Sinzger, C. et al. 1995. Fibroblasts, epithelial cells, endothelial cells and smooth muscle cells are major targets of human cytomegalovirus infection in lung and gastrointestinal tissues. *J Gen Virol* 76 (Pt 4), pp. 741-750.

Sinzger, C. et al. 2000. Tropism of human cytomegalovirus for endothelial cells is determined by a post-entry step dependent on efficient translocation to the nucleus. *J Gen Virol* 81(Pt 12), pp. 3021-3035.

Skaletskaya, A. et al. 2001. A cytomegalovirus-encoded inhibitor of apoptosis that suppresses caspase-8 activation. *Proc Natl Acad Sci U S A* 98(14), pp. 7829-7834.

Sloan, K. E. et al. 2004. CD155/PVR plays a key role in cell motility during tumor cell invasion and migration. *BMC Cancer* 4, p. 73.

Sloan, K. E. et al. 2005. CD155/PVR enhances glioma cell dispersal by regulating adhesion signaling and focal adhesion dynamics. *Cancer Res* 65(23), pp. 10930-10937.

Smith-Garvin, J. E. et al. 2009. T cell activation. *Annu Rev Immunol* 27, pp. 591-619.

Soderberg-Naucler, C. et al. 1997. Reactivation of latent human cytomegalovirus by allogeneic stimulation of blood cells from healthy donors. *Cell* 91(1), pp. 119-126.

Solecki, D. et al. 2000. Identification of a nuclear respiratory factor-1 binding site within the core promoter of the human polio virus receptor/CD155 gene. *J Biol Chem* 275(17), pp. 12453-12462.

Solecki, D. et al. 1999. Identification and characterization of the cis-acting elements of the human CD155 gene core promoter. *J Biol Chem* 274(3), pp. 1791-1800.

Solecki, D. J. et al. 2002. Expression of the human poliovirus receptor/CD155 gene is activated by sonic hedgehog. *J Biol Chem* 277(28), pp. 25697-25702.

Soroceanu, L. et al. 2008. Platelet-derived growth factor-[agr] receptor activation is required for human cytomegalovirus infection. *Nature* 455(7211), p. 391.

Spaete, R. R. and Mocarski, E. S. 1985a. The alpha sequence of the cytomegalovirus genome functions as a cleavage/packaging signal for herpes simplex virus defective genomes. *J Virol* 54(3), pp. 817-824.

Spaete, R. R. and Mocarski, E. S. 1985b. Regulation of cytomegalovirus gene expression: alpha and beta promoters are trans activated by viral functions in permissive human fibroblasts. *J Virol* 56(1), pp. 135-143.

Spaete, R. R. et al. 1993. Coexpression of truncated human cytomegalovirus gH with the UL115 gene product or the truncated human fibroblast growth factor receptor results in transport of gH to the cell surface. *Virology* 193(2), pp. 853-861.

Spaete, R. R. et al. 1988. Human cytomegalovirus strain Towne glycoprotein B is processed by proteolytic cleavage. *Virology* 167(1), pp. 207-225.

Spear, G. T. et al. 1995. Host cell-derived complement control proteins CD55 and CD59 are incorporated into the virions of two unrelated enveloped viruses. Human T cell leukemia/lymphoma virus type I (HTLV-I) and human cytomegalovirus (HCMV). *J Immunol* 155(9), pp. 4376-4381.

Spencer, J. V. et al. 2002. Potent Immunosuppressive Activities of Cytomegalovirus-Encoded Interleukin-10. *J. Virol.* 76(3), pp. 1285-1292.

Spiegel, I. et al. 2007. A central role for Necl4 (SynCAM4) in Schwann cell-axon interaction and myelination. *Nat Neurosci* 10(7), pp. 861-869.

Spiller, O. B. et al. 1996. Altered expression of host-encoded complement regulators on human cytomegalovirus-infected cells. *Eur J Immunol* 26(7), pp. 1532-1538.

Stannard, L. M. 1989. Beta 2 microglobulin binds to the tegument of cytomegalovirus: an immunogold study. *J Gen Virol* 70 (Pt 8), pp. 2179-2184.

Stanton, R. J. et al. 2008. Re-engineering adenovirus vector systems to enable high-throughput analyses of gene function. *Biotechniques* 45(6), pp. 659-662, 664-658.

Stanton, R. J. et al. 2007. Cytomegalovirus Destruction of Focal Adhesions Revealed in a High-Throughput Western Blot Analysis of Cellular Protein Expression. *J. Virol.* 81(15), pp. 7860-7872.

Stenberg, R. M. et al. 1985. Multiple spliced and unspliced transcripts from human cytomegalovirus immediate-early region 2 and evidence for a common initiation site within immediate-early region 1. *J. Virol.* 56(3), pp. 665-675.

Stinski, M. F. 1976. Human cytomegalovirus: glycoproteins associated with virions and dense bodies. *J Virol* 19(2), pp. 594-609.

Stone, S. F. et al. 2006. Cytomegalovirus (CMV)-specific CD8+ T cells in individuals with HIV infection: correlation with protection from CMV disease. *J Antimicrob Chemother* 57(4), pp. 585-588.

Story, C. M. et al. 1999. The cytosolic tail of class I MHC heavy chain is required for its dislocation by the human cytomegalovirus US2 and US11 gene products. *Proc Natl Acad Sci U S A* 96(15), pp. 8516-8521.

Streblow, D. N. et al. 1999. The human cytomegalovirus chemokine receptor US28 mediates vascular smooth muscle cell migration. *Cell* 99(5), pp. 511-520.

Streuli, C. H. and Akhtar, N. 2009. Signal co-operation between integrins and other receptor systems. *Biochem J* 418(3), pp. 491-506.

Strive, T. et al. 2002a. Proteolytic Processing of Human Cytomegalovirus Glycoprotein B Is Dispensable for Viral Growth in Culture. *J. Virol.* 76(3), pp. 1252-1264.

Strive, T. et al. 2002b. Proteolytic processing of human cytomegalovirus glycoprotein B is dispensable for viral growth in culture. *J Virol* 76(3), pp. 1252-1264.

Suzuki, Y. 2006. Ancient positive selection on CD155 as a possible cause for susceptibility to poliovirus infection in simians. *Gene* 373, pp. 16-22.

Sylwester, A. W. et al. 2005. Broadly targeted human cytomegalovirus-specific CD4+ and CD8+ T cells dominate the memory compartments of exposed subjects. *J. Exp. Med.* 202(5), pp. 673-685.

Tachibana, K. et al. 2000. Two cell adhesion molecules, nectin and cadherin, interact through their cytoplasmic domain-associated proteins. *J Cell Biol* 150(5), pp. 1161-1176.

Tahara-Hanaoka, S. et al. 2006. Tumor rejection by the poliovirus receptor family ligands of the DNAM-1 (CD226) receptor. *Blood* 107(4), pp. 1491-1496.

Tahara-Hanaoka, S. et al. 2004. Functional characterization of DNAM-1 (CD226) interaction with its ligands PVR (CD155) and nectin-2 (PRR-2/CD112). *Int Immunol* 16(4), pp. 533-538.

Takahashi, K. et al. 1999. Nectin/PRR: an immunoglobulin-like cell adhesion molecule recruited to cadherin-based adherens junctions through interaction with Afadin, a PDZ domain-containing protein. *J Cell Biol* 145(3), pp. 539-549.

Takahashi, M. et al. 2008. Sequential activation of Rap1 and Rac1 small G proteins by PDGF locally at leading edges of NIH3T3 cells. *Genes Cells* 13(6), pp. 549-569.

Takai, Y. et al. 2008a. The immunoglobulin-like cell adhesion molecule nectin and its associated protein afadin. *Annu Rev Cell Dev Biol* 24, pp. 309-342.

Takai, Y. et al. 2008b. Nectins and nectin-like molecules: roles in contact inhibition of cell movement and proliferation. *Nat Rev Mol Cell Biol* 9(8), pp. 603-615.

Tamarit, A. et al. 2004. Assessment of human cytomegalovirus specific T cell immunity in human immunodeficiency virus infected patients in different disease stages following HAART and in long-term non-progressors. *J Med Virol* 74(3), pp. 382-389.

Tao, D. et al. 2005. CD226 expression deficiency causes high sensitivity to apoptosis in NK T cells from patients with systemic lupus erythematosus. *J Immunol* 174(3), pp. 1281-1290.

Tavalai, N. et al. 2008. Nuclear Domain 10 Components Promyelocytic Leukemia Protein and hDaxx Independently Contribute to an Intrinsic Antiviral Defense against Human Cytomegalovirus Infection. *J. Virol.* 82(1), pp. 126-137.

Taylor-Wiedeman, J. et al. 1991. Monocytes are a major site of persistence of human cytomegalovirus in peripheral blood mononuclear cells. *J Gen Virol* 72(9), pp. 2059-2064.

Terhune, S. S. et al. 2004. RNAs are packaged into human cytomegalovirus virions in proportion to their intracellular concentration. *J Virol* 78(19), pp. 10390-10398.

Theiler, R. N. and Compton, T. 2001. Characterization of the Signal Peptide Processing and Membrane Association of Human Cytomegalovirus Glycoprotein O. *J. Biol. Chem.* 276(42), pp. 39226-39231.

Thomsen, D. R. et al. 1984. Promoter-regulatory region of the major immediate early gene of human cytomegalovirus. *Proc Natl Acad Sci U S A* 81(3), pp. 659-663.

Tomasec, P. et al. 2000. Surface expression of HLA-E, an inhibitor of natural killer cells, enhanced by human cytomegalovirus gpUL40. *Science* 287(5455), p. 1031.

Tomasec, P. et al. 2005. Downregulation of natural killer cell-activating ligand CD155 by human cytomegalovirus UL141. *Nat Immunol* 6(2), pp. 181-188.

Tomazin, R. et al. 1999. Cytomegalovirus US2 destroys two components of the MHC class II pathway, preventing recognition by CD4+ T cells. *Nat Med* 5(9), pp. 1039-1043.

Trus, B. L. et al. 1999. Capsid structure of simian cytomegalovirus from cryoelectron microscopy: evidence for tegument attachment sites. *J Virol* 73(3), pp. 2181-2192.

Tsukasaki, Y. et al. 2007. Role of multiple bonds between the single cell adhesion molecules, nectin and cadherin, revealed by high sensitive force measurements. *J Mol Biol* 367(4), pp. 996-1006.

Tu, W. et al. 2006. T-cell immunity to subclinical cytomegalovirus infection reduces cardiac allograft disease. *Circulation* 114(15), pp. 1608-1615.

Varnum, S. M. et al. 2004. Identification of proteins in human cytomegalovirus (HCMV) particles: the HCMV proteome. *J Virol* 78(20), pp. 10960-10966.

Vasioukhin, V. et al. 2000. Directed Actin Polymerization Is the Driving Force for Epithelial Cell-Cell Adhesion. *Cell* 100(2), p. 209.

Venkataraman, G. M. et al. 2007. Promoter region architecture and transcriptional regulation of the genes for the MHC class I-related chain A and B ligands of NKG2D. *J Immunol* 178(2), pp. 961-969.

Vivier, E. et al. 2008. Functions of natural killer cells. *Nat Immunol* 9(5), p. 503.

Walter, E. A. et al. 1995. Reconstitution of cellular immunity against cytomegalovirus in recipients of allogeneic bone marrow by transfer of T-cell clones from the donor. *N Engl J Med* 333(16), pp. 1038-1044.

Wang, D. et al. 2004a. Human cytomegalovirus encodes a highly specific RANTES decoy receptor. *Proc Natl Acad Sci U S A* 101(47), pp. 16642-16647.

Wang, D. and Shenk, T. 2005a. Human cytomegalovirus UL131 open reading frame is required for epithelial cell tropism. *J Virol* 79(16), pp. 10330-10338.

Wang, D. and Shenk, T. 2005b. Human cytomegalovirus virion protein complex required for epithelial and endothelial cell tropism. *Proceedings of the National Academy of Sciences of the United States of America* 102(50), pp. 18153-18158.

Wang, D. et al. 2007. Human cytomegalovirus uses two distinct pathways to enter retinal pigmented epithelial cells. *Proc Natl Acad Sci U S A* 104(50), pp. 20037-20042.

Wang, E. C. et al. 2002. UL40-mediated NK evasion during productive infection with human cytomegalovirus. *Proc Natl Acad Sci U S A* 99(11), pp. 7570-7575.

Wang, P. L. et al. 1992. Identification and molecular cloning of tactile. A novel human T cell activation antigen that is a member of the Ig gene superfamily. *J Immunol* 148(8), pp. 2600-2608.

Wang, S.-K. et al. 2004b. Human Cytomegalovirus UL76 Encodes a Novel Virion-Associated Protein That Is Able To Inhibit Viral Replication. *J. Virol.* 78(18), pp. 9750-9762.

Wang, S. K. et al. 2004c. Human cytomegalovirus UL76 encodes a novel virion-associated protein that is able to inhibit viral replication. *J Virol* 78(18), pp. 9750-9762.

Wang, W. et al. 2008. The infection of human primary cells and cell lines by human cytomegalovirus: new tropism and new reservoirs for HCMV. *Virus Res* 131(2), pp. 160-169.

Wang, X. et al. 2005. Integrin alphavbeta3 is a coreceptor for human cytomegalovirus. *Nat Med* 11(5), pp. 515-521.

Warner, M. S. et al. 1998. A cell surface protein with herpesvirus entry activity (HveB) confers susceptibility to infection by mutants of herpes simplex virus type 1, herpes simplex virus type 2, and pseudorabies virus. *Virology* 246(1), pp. 179-189.

Warren, A. P. et al. 1994a. Human cytomegalovirus-infected cells have unstable assembly of major histocompatibility complex class I complexes and are resistant to lysis by cytotoxic T lymphocytes. *J Virol* 68(5), pp. 2822-2829.

Warren, A. P. et al. 1994b. Down-regulation of integrin {alpha}1/beta1 expression and association with cell rounding in human cytomegalovirus-infected fibroblasts. *J Gen Virol* 75(12), pp. 3319-3325.

Warren, A. P. et al. 1994c. Down-regulation of integrin alpha 1/beta 1 expression and association with cell rounding in human cytomegalovirus-infected fibroblasts. *J Gen Virol* 75 (Pt 12), pp. 3319-3325.

Welte, S. A. et al. 2003. Selective intracellular retention of virally induced NKG2D ligands by the human cytomegalovirus UL16 glycoprotein. *Eur J Immunol* 33(1), pp. 194-203.

Weststrate, M. W. et al. 1980. Human cytomegalovirus DNA: physical maps for restriction endonucleases BglII, hindIII and XbaI. *J Gen Virol* 49(1), pp. 1-21.

White, E. A. et al. 2007. The IE2 60-kilodalton and 40-kilodalton proteins are dispensable for human cytomegalovirus replication but are required for efficient delayed early and late gene expression and production of infectious virus. *J Virol* 81(6), pp. 2573-2583.

Wiertz, E. J. et al. 1996. The human cytomegalovirus US11 gene product dislocates MHC class I heavy chains from the endoplasmic reticulum to the cytosol. *Cell* 84(5), pp. 769-779.

Wilkinson, G. W. et al. 1984. Transcription of the immediate early genes of human cytomegalovirus strain AD169. *Virus Res* 1(2), pp. 101-106.

Wilkinson, G. W. et al. 1998. Disruption of PML-associated nuclear bodies mediated by the human cytomegalovirus major immediate early gene product. *J Gen Virol* 79 (Pt 5), pp. 1233-1245.

Wilkinson, G. W. G. et al. 2008. Modulation of natural killer cells by human cytomegalovirus. *Journal of Clinical Virology* 41(3), p. 206.

Wills, M. R. et al. 2005. Human Cytomegalovirus Encodes an MHC Class I-Like Molecule (UL142) That Functions to Inhibit NK Cell Lysis. *J Immunol* 175(11), pp. 7457-7465.

Wing, B. A. et al. 1998. Identification of positive and negative regulatory regions involved in regulating expression of the human cytomegalovirus UL94 late promoter: role of IE2-86 and cellular p53 in mediating negative regulatory function. *J Virol* 72(3), pp. 1814-1825.

Wing, B. A. et al. 1996. The human cytomegalovirus UL94 open reading frame encodes a conserved herpesvirus capsid/tegument-associated virion protein that is expressed with true late kinetics. *J Virol* 70(6), pp. 3339-3345.

Winkler, M. et al. 1994. UL69 of human cytomegalovirus, an open reading frame with homology to ICP27 of herpes simplex virus, encodes a transactivator of gene expression. *J. Virol.* 68(6), pp. 3943-3954.

Winkler, M. and Stamminger, T. 1996. A specific subform of the human cytomegalovirus transactivator protein pUL69 is contained within the tegument of virus particles. *J Virol* 70(12), pp. 8984-8987.

Wolf, D. G. et al. 2001. Distinct and separate roles for herpesvirus-conserved UL97 kinase in cytomegalovirus DNA synthesis and encapsidation. *Proc Natl Acad Sci U S A* 98(4), pp. 1895-1900.

Woodhall, D. L. et al. 2006. Human Daxx-mediated repression of human cytomegalovirus gene expression correlates with a repressive chromatin structure around the major immediate early promoter. *J Biol Chem* 281(49), pp. 37652-37660.

Wright, D. A. et al. 1988. Four phosphoproteins with common amino termini are encoded by human cytomegalovirus AD169. *J Virol* 62(1), pp. 331-340.

Wright, J. F. et al. 1995. Host cellular annexin II is associated with cytomegalovirus particles isolated from cultured human fibroblasts. *J Virol* 69(8), pp. 4784-4791.

Xu, B. et al. 1989. Characterization of IgG Fc receptors induced by human cytomegalovirus. *J Gen Virol* 70 (Pt 4), pp. 893-900.

Yu, X. et al. 2005. Three-dimensional localization of the smallest capsid protein in the human cytomegalovirus capsid. *J Virol* 79(2), pp. 1327-1332.

Zanghellini, F. et al. 1999. Asymptomatic primary cytomegalovirus infection: virologic and immunologic features. *J Infect Dis* 180(3), pp. 702-707.

Zhu, H. et al. 1995. Human cytomegalovirus IE1 and IE2 proteins block apoptosis. *J Virol* 69(12), pp. 7960-7970.

Zini, N. et al. 1999. The novel structural protein of human cytomegalovirus, pUL25, is localized in the viral tegument. *J Virol* 73(7), pp. 6073-6075.